To the Graduate Council:

We are submitting herewith a thesis written by NANDITA BANDYOPADHYAY entitled "Evaluation of the Effect of Various Emission Sources on Ozone Formation in Memphis, Tennessee". We have examined the final copy of this thesis for form and content and recommend that it be accepted in partial fulfillment of the requirements for the degree of Master of Science, with a major in Environmental Engineering.

Wayne T. Davis, Major Professor

Terry L. Miller, Major Professor

I have read this thesis and
recommend its acceptance:

Accepted for the Council:

Associate Vice Chancellor
and Dean of the Graduate School

STATEMENT OF PERMISSION TO USE

In presenting this thesis in partial fulfillment of the requirements for a Master's degree at the University of Tennessee, Knoxville, I agree that the Library shall make it available to borrowers under rules of the Library. Brief quotations from this thesis are allowable without special permission, provided that accurate acknowledgement of the source is made.

Permission for extensive quotation from or reproduction of this thesis may be granted by either of my major professors, or in their absence, by the Head of Interlibrary Services when, in the opinion of either, the proposed use of the material is for scholarly purposes. Any copying or use of the material in this thesis for financial gain shall not be allowed without my written permission.

Signature Nandita Bandyopadhyay

Date 12/17/92

EVALUATION OF THE EFFECT OF VARIOUS EMISSION SOURCES ON OZONE FORMATION IN MEMPHIS, TENNESSEE

A Thesis

Presented for the

Master of Science

Degree

The University of Tennessee, Knoxville

Nandita Bandyopadhyay

May 1993

ACKNOWLEDGEMENTS

I would like to express my sincere thanks to my co-major professors Dr. Wayne T. Davis and Dr. Terry L. Miller for their continual assistant and insight throughout this project. I truly appreciate all the time and encouragement that they have given to me in preparing this thesis. I would also like to thank Dr. Bruce R. Robinson for serving on my thesis committee.

Special thanks are necessary for my officemates for their tolerance and sense of humor. I would especially like to thank Robert Burns and Harry Qin for their assistance, encouragement, and friendship throughout my stay here.

Finally, I would like to thank my family in India and my husband Arup Bandyopadhyay. Their willingness, and support made all of my work successful.

ABSTRACT

The Urban Airshed Model has been employed to predict the maximum impact of ozone formation in the atmosphere passing over Memphis, Tennessee during the period of 1986 to 1988. The wind direction was chosen from south-west to north-east. The model result was compared with the observed peak ozone concentration. The model result was within 7% of the observed ozone concentration.

The effects of various emission sources on ozone formation were evaluated. Mobile and area sources had the most significant contribution to ozone formation and those sources were also the most significant contributor to NO_x emissions. NO_x emissions from a local power plant were also high. This source showed less of a contribution to ozone formation at the ground level due to the stack height. In spite of large VOC emissions from biogenic sources, this source category also showed little contribution to ozone formation.

A sensitivity analysis was done by varying the VOCs emitted from mobile sources. Analysis showed that the ozone formation was NO_x limited. The peak ozone concentration did not change appreciably when VOC emissions from mobile sources were changed significantly. However, a reduction of NO_x emissions from mobile source caused a significant reduction in ozone formation based on the UAM modeling.

TABLE OF CONTENTS

Section			Page
1.0	INTRODUCTION		1
2.0	LITERATURE REVIEW		5
	2.1 Trends in Ozone		5
	2.2 Trends in Ozone Precursors		7
	2.3 Ozone Formation		8
		2.3.1 Photochemistry of Ozone Formation	8
		2.3.2 Use of Models	9
		2.3.3 Effect of Meteorology on Ozone Formation	12
		2.3.4 Ozone Transport	13
		2.3.5 Ozone Intrusions	14
	2.4 VOC Vs. NO_x Control		15
3.0	DEVELOPMENT OF MODELING INPUT		20
	3.1 Emissions from Point Sources		23
	3.2 Emissions from Area Sources		34
	3.3 Emissions from Mobile Sources		39
	3.4 Emissions from Biogenic Sources		52
	3.5 Speciation and Allocation		57
		3.5.1 Speciation of VOC	57
		3.5.2 Speciation of NO_x	67
		3.5.3 Speciation of Biogenic Emissions	72
	3.6 Preparation of Inputs for Model		72

3.6.1 AIRQUALITY..... 72
3.6.2 BOUNDARY..... 74
3.6.3 DIFFBREAK..... 77
3.6.4 EMISSIONS..... 80
3.6.5 METSCALARS..... 80
3.6.6 PTSOURCE..... 83
3.6.7 REGIONTOP..... 85
3.6.8 TEMPERATUR..... 85
3.6.9 TERRAIN..... 85
3.6.10 TOPCONC..... 88
3.6.11 WIND..... 90
4.0 ANALYSIS OF RESULTS..... 91
4.1 Base Case Evaluation..... 91
4.2 Sensitivity Analysis..... 95
4.2.1 Effect of a Large NO_x Point Source..... 95
4.2.2 Effect of Biogenic Sources..... 102
4.2.3 Effect of Area Sources..... 105
4.2.4 Effect of Mobile Sources..... 111
4.3 Discussion of Modeling Results..... 115
5.0 CONCLUSIONS..... 123
LIST OF REFERENCES..... 127
APPENDIX..... 132
VITA..... 143

LIST OF TABLES

Table		Page
3.1.	Ozone Precursor Emissions in the Study Area - 1988 Base Case (tons/day)	22
3.2.	Ten Highest Ozone Days (1986 - 1988)	24
3.1.1.	VOC Emission Data for Point Sources by County	26
3.1.2.	NO_x Emission Data for Point Sources by County	32
3.2.1.	Area Source VOC Emissions by Category and by County (tons/day)	35
3.2.2.	Area Source NO_x Emissions by Category and by County (tons/day)	37
3.2.3.	Area Source CO Emissions by Category and by County (tons/day)	38
3.3.1.	VOC Emission Factors for Urban Grids (g/vehicle mile/hr)	46
3.3.2.	VOC Emission Factors for Rural Grids (g/vehicle mile/hr)	47
3.3.3.	NO_x Emission Factors for Urban Grids (g/vehicle mile/hr)	48
3.3.4.	NO_x Emission Factors for Rural Grids (g/vehicle mile/hr)	49
3.3.5.	CO Emission Factors for Urban Grids (g/vehicle mile/hr)	50
3.3.6.	CO Emission Factors for Rural Grids (g/vehicle mile/hr)	51
3.4.1.	Site Information by County for PCBEIS Program	53
3.4.2.	Daily Maximum Temperature of Ten Highest Ozone Days	54
3.4.3.	Ranking of Days by Temperature	55

3.4.4.	Meteorological Data of 06/21/88 used for PCBEIS Program.....	56
3.4.5.	Output of PCBEIS Program for Shelby County.....	58
3.4.6.	Output of PCBEIS Program for Tipton County.....	59
3.4.7.	Output of PCBEIS Program for Desoto County.....	60
3.4.8.	Output of PCBEIS Program for Crittenden County.....	61
3.5.1.1.	Speciation Coefficients for Point Sources for Shelby County.....	63
3.5.1.2.	Speciation Coefficients for Point Sources for Crittenden County.....	65
3.5.1.3.	Speciation Coefficients for Point Sources for Tipton County.....	65
3.5.1.4.	Speciation Coefficients for Point Sources for Desoto County.....	65
3.5.1.5.	Data for Area Source VOC Emissions Speciation.....	68
3.5.1.6.	Table for Mass Ratio of VOC Emissions....	70
3.5.1.7.	Speciation Factors for Mobile Sources....	71
3.5.3.1.	Speciation Factors for Biogenic Emissions.....	73
3.6.1.1.	Initial Concentration of each Species used in the AIRQUALITY File.....	75
3.6.2.1.	Boundary Concentrations for Pollutants (ppm).....	78
3.6.2.2.	Boundary Concentrations for Ozone (ppb).....	79
3.6.3.1.	Mixing Height Data Used for Modeling.....	81
3.6.5.1.	Meteorological Data Used for Modeling....	84

3.6.8.1. Temperature Data Associated with the Highest Ozone Violation..... 86

3.6.10.1. Concentration of Ozone at top of the Region..... 89

4.2.1. The Relative Contribution of Each Source and the Location..... 96

4.3.1. The Relative Contribution of the TVA Power Plant to the Ozone Formation at Different Vertical Cells..... 117

4.3.2. Contribution of Mobile Source VOC Emissions to the Ozone Formation..... 119

4.3.3. Contribution of Mobile Source NO_x Emissions to the Ozone Formation..... 120

4.3.4. Comparisons of the Contribution of Mobile Source VOC and NO_x Emissions to the Ozone Formation..... 121

LIST OF FIGURES

Figures		Page
2.1.1.	Boxplot Comparisons of Trends in Annual Second Highest Daily Maximum 1-hour Ozone Concentration at 431 Monitoring Sites, 1980-1989. Source: EPA, 1991.....	6
2.4.1.	Typical Ozone Isopleths Used in EPA's EKMA Model. Source: Adapted from Dodge,1977.....	16
3.1.	Modeling Domain Showing the Location of Monitoring Stations.....	21
3.1.	Flow Chart for Overall Approach.....	25
3.2.1.	Population Data in Each Grid of the Counties that were Inventoried.....	40
3.2.2.	Allocation of Railroad Emissions in the Counties that were Inventoried.....	41
3.2.3.	Allocation of Airport Emissions in the Counties that were Inventoried.....	42
3.2.4.	Allocation of Water Body Emissions in the Counties that were Inventoried.....	43
3.2.5.	Allocation of Rural Emissions in the Counties that were Inventoried.....	44
3.5.1.1.	Flow Chart for Point Source VOC Emissions Speciation and Preparation of Input for UAM Preprocessor PTSRCE.....	66
3.5.1.2.	Flow Chart for Area Source VOC Emissions Speciation and Distribution.....	69
3.6.2.1.	Definition of Boundaries of the Modeling Domain.....	76
3.6.3.1.	Mixing Height Profile Used for Modeling.....	82
3.6.8.1.	Average Temperature Profile Used in Modeling.....	87
4.1.1.	Ozone Concentration Isopleth: Base Case Simulation.....	92

4.1.2. Comparison of Observed and Predicted Ozone Peak: Base Case Evaluation..... 94

4.2.1.1. Comparison of Ozone Concentration Profiles at Grids (25,26) and (27,30): with and without the TVA Power Plant Emissions..... 98

4.2.1.2. Comparison of Ozone Concentration Profiles at the TVA Power Plant Location (18,19) - with and without the TVA Power Plant Emissions..... 100

4.2.1.3. Differential Ozone Concentration Isopleth for TVA Power Plant Emissions (Scenario PTAMB - Scenario PAMB)..... 101

4.2.2.1. Comparison of Ozone Concentration Profiles at Grids (25,26) and (22,24): with and without the Biogenic Source Emissions... 104

4.2.2.2. Differential Ozone Concentration Isopleth for Biogenic Source Emissions (Scenario PTAMB - Scenario PTAM)..... 106

4.2.3.1. Comparison of Ozone Concentration Profiles at Grids (25,26) and (29,26): with and without the Area Source Emissions..... 108

4.2.3.2. Differential Ozone Concentration Isopleth for Area Source Emissions (Scenario PTAMB - Scenario PTMB)..... 110

4.2.4.1. Comparison of Ozone Concentration Profiles at Grids (25,26) and (27,27): with and without the Mobile Source Emissions..... 112

4.2.4.2. Differential Ozone Concentration Isopleth for Mobile Source Emissions (Scenario PTAMB - Scenario PTAB)..... 114

ABBREVIATIONS

ADT	Average Daily Traffic
AHCs	Anthropogenic Hydrocarbon Compounds
CAAA	Clean Air Act Ammendments
DOT	Department of Transportation
EIS	Emission Inventory System
EKMA	Emperical Kinetics Modeling Approach
EPA	Environmental Protection Agency
HCs	Hydrocarbons
LDT	Local Daylight Time
NAAQS	National Ambient Air Quality Standard
NEDS	National Inventory Data System
NMHC	Non-methane Hydrocarbon
NO	Nitric Oxide
NO_2	Nitrogen Dioxide
NO_x	Oxides of Nitrogen
OZIPP	A Photochemical Model Developed by SAI
O_3	Ozone
PCBEIS	Personal Computer Verson of the Biogenic Emissions Inventory System
UAM	Urban Airshed Model
VOC	Volatile Organic Compound

1.0 INTRODUCTION

Under the 1970 Clean Air Act Amendments (CAAA), a National Ambient Air Quality Standard (NAAQS) of 0.12 ppmv was established for ozone. In spite of past efforts to reduce peak ozone concentrations, there were still 96 nonattainment areas in U.S. as of 1991 (Paul, 1991). The NAAQS for ozone is defined as a one hour average concentration of 0.12 ppmv, not to be exceeded more than three times in any consecutive three year period.

Volatile organic compounds (VOCs), nitric oxide (NO), and nitrogen dioxide (NO_2) are the most important precursors for ozone formation. The main sources of VOCs are automobile exhaust and vegetation (mobile and biogenic sources), whereas the main sources of NO and NO_2 are power plants and automobile exhaust (point and mobile sources). Ozone concentrations may result from either local emissions of these precursors which react to form ozone or may be transported from the upwind direction.

There are three ozone nonattainment areas in Tennessee, of which the Memphis area is designated as 'marginal' by the Clean Air Act Amendments of 1990 (CAAA) and has a compliance date of 1993. The Memphis area violated the ozone NAAQS ten times during 1986-1988. The assessment of future compliance with the ozone standard can be enhanced by developing a comprehensive emission inventory of ozone

precursors followed by modeling of the formation of ozone. This requires an air quality model, which describes atmospheric transport, diffusion, and chemical reaction of the precursor pollutants (Seinfield, 1988).

In order to further understand the formation of ozone in the Memphis area, a modeling study was performed by the University of Tennessee, Department of Civil Engineering using EPA's Urban Airshed Model (UAM). The UAM is an air quality simulation model used to analyze the ozone air quality. The application of UAM requires a large database of ozone precursor emissions based on a gridded emissions inventory.

The UAM was run for the baseline year of 1988 for the Memphis area using a 1988 emission inventory and representative meteorological data based on the ten highest ozone violation days during 1986-1988. The ozone concentrations predicted by the model were analyzed and compared to actual observed concentration data in order to gain insight into the probable reasons for the violations of the ozone standard. The contribution of different sources to the ozone concentration have been analyzed and reported in Section 4.2.

The main objective of this thesis was to model the ozone formation for the base year of 1988 and to understand and analyze the effect of emissions from different types of

sources including point, mobile, area and biogenic sources.

An emission inventory for the Memphis area had been completed for the year of 1988 prior to the initiation of the work reported herein. This inventory included Shelby, and Tipton counties in Tennessee, Crittenden county in Arkansas, and Desoto county in Mississippi. In this work, a specific modeling domain was chosen which was located within the boundaries of the emission inventory. It consisted of a gridded, 20 X 20 matrix with 5 km X 5 km resolution. The gridded area for modeling was chosen in such a way, that the maximum ozone concentrations which occurred in 1986-88 were within the modeling domain. The emission data for VOC, NO_x, & CO were obtained from the emission inventory for point sources, area sources, mobile sources, and biogenic sources. Emissions of each of the precursors from each of the sources were allocated horizontally as well as vertically (in the case of elevated stacks) to individual grid cells in the modeling region and distributed temporally for each of the VOC species, NO_x, and CO. The emissions from each source were then summed to get a total emission for each species in each grid within the modeling domain. The meteorological inputs required in the modeling such as temperature, atmospheric pressure, water concentration, and solar intensity were obtained by analyzing the data for the ten highest ozone days in the period of 1986-88 to arrive at

a composite or average "ozone day".

The UAM modeling was conducted with the above inventory after which a sensitivity analysis was conducted to determine the contribution of specific source categories, and specific sources to ozone formation.

2.0 LITERATURE REVIEW

2.1 Trends in Ozone

The Committee on Tropospheric Ozone Formation and Measurement of the National Research Council (1991) described the trends in ozone concentrations in U.S. In order to assess the progress in reduction of ozone concentrations, it was necessary to measure and document the ozone concentrations. Ozone concentrations were reported to fluctuate from year to year. In order to analyze the ozone concentrations for assessing trends in ozone, EPA defined the composite average ozone concentration for any year as the nationwide average of second highest 1-hour daily maximum ozone concentration for that year. The boxplot in Figure 2.1.1 displays the 5th, 10th, 25th, 50th (Median), 75th and 95th percentiles of the data obtained from the trend report for 1989 (EPA, 1991), and also the composite average through the symbol 'x'. Figure 2.1.1 shows that the second highest ozone concentration averaged over 431 stations has remained relatively stable over the ten year period with a tendency to cycle between 0.12 to 0.14 ppm.

To measure the progress in ozone control, the number of days on which the 1-hour daily maximum of 120 ppb was exceeded were also measured for the period of 1980 to 1989. There was a 38% increase in the number of days between 1987

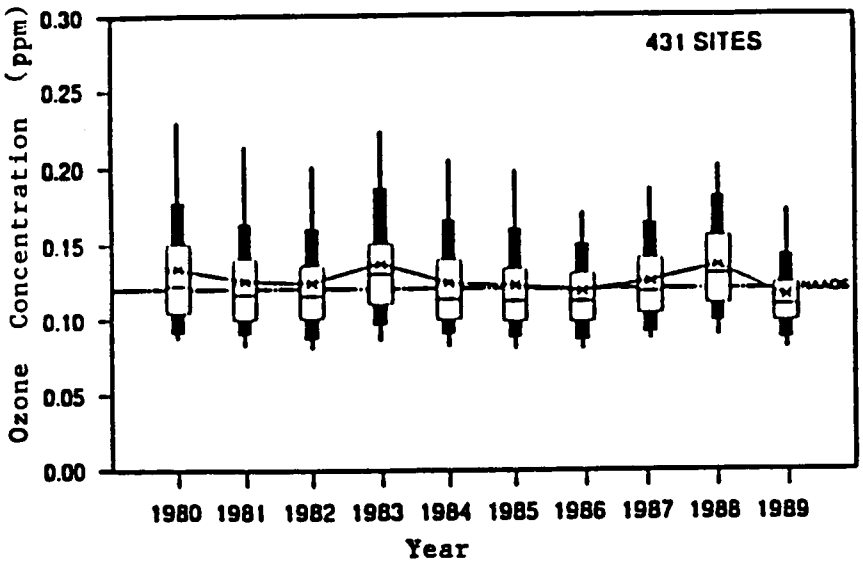


Figure 2.1.1. Boxplot Comparisons of Trends in Annual Second Highest Daily Maximum 1-hour Ozone Concentration at 431 Monitoring Sites, 1980-1989. Source: EPA, 1991.

and 1988, whereas there was an overall 53% decrease in the number of days between 1980 and 1989. Apart from that, there were also very high ozone concentrations in 1983 and 1988 as shown in Figure 2.1.1. The boxplot in Figure 2.1.1 shows that the 50th percentile (Median) of the data and the composite average ozone concentrations for 1983 and 1988 were greater as compared to those in the other years. On the other hand, lower ozone concentrations were observed in 1989. EPA (1991) suggested that the meteorological variations were the possible reasons for those fluctuations of maximum ozone concentrations.

Korsog and Wolff (1991) discussed the trend in ozone from 1973 to 1983 at eight major cities using a robust statistical method. The results of their analysis showed that there had been an overall decrease of only a few ppb in ozone concentrations on a yearly basis for most of the sites.

2.2 Trends in Ozone Precursors

Chock and Heuss (1987) discussed the trends in ozone precursors. The authors found that the estimates of nationwide emissions of VOC and NO_x were not very useful because these estimates were on an annual basis, not a ozone season basis, they were not related to any specific nonattainment area, and also they were uncertain.

The trend in ozone precursors (EPA, 1991) showed that between 1980 and 1989, annual VOC emissions decreased by 19%, whereas annual NO_x emissions decreased by 5%. Between 1987 and 1988, there was a large increase in ozone concentrations, but no large increases in precursor emissions were reported. Therefore, it was concluded (National Research Council, 1991) that there was no obvious relationship between precursor emissions and ozone concentrations. On the other hand, high ozone concentrations in 1988 could have been the result of the unusual meteorology (EPA, 1991).

2.3 Ozone Formation

2.3.1 Photochemistry of Ozone Formation

Formation of photochemical air pollution (ozone) is a result of complex chemical reactions between VOCs and NO_x in the presence of sunlight and high ambient temperature. These VOCs and NO_x are emitted in the atmosphere as a result of various anthropogenic (VOCs and NO_x) and biogenic (VOCs) emissions. Control of these emissions are required to achieve NAAQS of ozone. Uncontrolled biogenic emissions are known to be responsible for high concentration of ozone (photochemical smog) in areas where anthropogenic NO_x emissions are high (Lamb et al., 1987 ; Chamedies et al.,

1988) and these should be estimated more accurately to determine the control strategies. The authors also indicated that, when estimated on a continental scale, biogenic VOC emissions were found to be a large fraction of the total VOC emissions. However, Lamb et al. (1987) found that the estimation of biogenic emissions was uncertain as a result of errors in emission data, distribution of land use and vegetation type and variability in biomass density. This uncertainty in the inventory was estimated to be on the order of a factor of three.

2.3.2 Use of Models

Ozone formation is a result of a complex set of reactions involving VOCs and NO_x. Computer models are generally used in order to explain and predict the effects of anthropogenic and biogenic emissions and also of changes in these emissions on ozone formation. To calculate ozone concentrations, these models must contain a kinetic mechanism which describes a group of chemical reactions and rate constants representing the ozone formation process. Most of these kinetic mechanisms treat organic compounds in groups according to the type of bonds in the carbon atoms of the organic compounds. This mechanism is known as the Carbon-Bond Mechanism.

U. S. EPA recommends the use of either of two computer

models in order to gain insight into the effect of emission changes on ozone formation. The first one is the Empirical Kinetic Modeling Approach (EKMA). This model is a single trajectory model using the Carbon Bond-IV mechanism of ozone formation. This model assumes a parcel or column of air advects through an urban area based on the wind trajectory. The height of this column changes with the mixing height. The VOCs, NO_x and CO within the column react chemically resulting in ozone formation. A computer program called the Ozone Isopleth Plotting Package (OZIPP) is used to generate the ozone isopleth using this modeling approach.

Qin (1992) examined the sensitivity of ozone to biogenic and anthropogenic emissions in the Middle Tennessee area using the EKMA approach. Anthropogenic emissions were taken from the 1988 base year SIP inventory for the Middle Tennessee area and biogenic emissions were calculated by using U.S. EPA's PCBEIS program. Biogenic emissions accounted for 45% of the total VOC emissions in the study area, but only 9% of the total ozone loading in the presence of anthropogenic VOCs and NO_x emissions. The author concluded that ozone NAAQS in Middle Tennessee area could be attained by a 50% reduction in anthropogenic HC (AHC) emissions, a 50% reduction in NO_x emissions, or a 30% reduction in both AHCs and NO_x.

Another approach of modeling is to use the Urban

Airshed Model (UAM), developed by Systems Application, Inc. This modeling approach assumes a three dimensional grid-based modeling domain. The UAM uses the Carbon Bond-IV Mechanism. The model considers that the pollutants are transported and dispersed primarily by wind advection. A three-dimensional wind input is required by the model. Another mechanism of pollutant transport is turbulent diffusion. The UAM assumes that the turbulent diffusion of pollutants is proportional to the concentration gradient. This proportionality constant is called the turbulent diffusion coefficient.

To evaluate the validity and performance of the model, the model was used to simulate the ozone formation of some past episodes. The model predictions were then compared with the actual observations to evaluate the model performance. Anderson et al. (1977) used the UAM to simulate the ozone formation at various sites in the Denver area on 28th July, 1976. The authors showed a close comparison between the predicted and the observed ozone concentrations.

Zhou (1991) simulated ozone formation in the Middle Tennessee area using a 1988 base year inventory. The author used both the EKMA and the UAM models to compare the predicted and observed ozone concentrations. The simulation results were in good comparison with the observed data. The author also compared the predicted ozone concentrations from

both models. The predicted ozone profiles from both models are similar, but the EKMA model resulted in higher ozone values. The author explained further that the UAM considered the turbulent diffusion in addition to the transport of ozone and chemical reactions of chemical species. The EKMA considered only transport of ozone and chemical reactions of chemical species. The diffusion effect on ozone formation in the UAM was proposed as the reason behind the lower ozone concentration predicted by the UAM than that by the EKMA.

Schere (1988) discussed the need for urban and regional scale models to develop the emissions control strategies which could reduce ozone concentrations. To account for the long range transport, a regional scale model was needed, whereas for local emission precursor reactions, an urban scale model was sufficient.

Hess et al. (1992) evaluated the Carbon Bond-IV Mechanism using a new set of smog chamber data. It was found that the model was in good agreement with the experimental data, particularly at moderate temperatures (15 - 25 °C) and NMHC/NO_x ratios of 7-16.

2.3.3 Effect of Meteorology on Ozone Formation

Qin (1992) discussed that the effects of meteorology are of great concern in the formation of ozone. Decker et al. (1976) found that ozone violations occurred when a slow-

moving, high pressure system developed during summer and the air temperature was quite high due to the solar radiation. Ozone precursors accumulated rapidly due to the slow moving air and the rate of ozone formation increased.

2.3.4 Ozone Transport

Clarke and Ching (1983) observed the regional transport of ozone in the northeastern United States. The authors found that urban plumes containing relatively high ozone concentrations were transported from Ohio to the northeastern United States. The urban plume was made up of ground level (automobiles) NMHC and NO_x emissions along with industrial sources. This urban plume contained high olefinic VOC compounds from automobile emissions. Other ground level NO_x sources and these VOC sources gave rise to the ozone formation, typically 1-2 hours downwind.

Sexton and Westberg (1983) showed the occurrence of in-plume ozone buildup from large urban areas, petroleum refineries, automobile painting operations, and power plants. The authors found that the urban plume may contribute to ozone concentrations in the order of 80 ppb over background concentrations. They also found depletion of ozone immediately downwind of large NO_x point sources. This depletion was reportedly due to the low NMHC/NO_x ratios in the plume and also due to the ozone scavenging by nitric

oxide emitted from the plant.

2.3.5 Ozone Intrusions

Another potential source of ozone is from stratospheric ozone. Viezee et al. (1983) discussed the events of ozone intrusions from the stratosphere to the ground level. The authors concluded that the impacts of stratospheric ozone were unlikely. The authors suggested that higher concentrations of ozone at the ground level were more likely due to the surface transport and local photochemistry than to atmospheric intrusion.

Wakamatsu et al. (1989) discussed the mechanisms of ozone intrusions into the lower troposphere. Intensive field studies were made during 10-19 May, 1986 covering the northern Kyushu district, Japan. Two ozone peaks were observed on May 12 and May 16-17, 1986. The predominant wind direction was found to be northwest-north and the wind speed was high. Further, by analyzing the weather maps, they found that a low pressure system was formed and by analyzing the vertical cross-sectional wind and temperature data, it was found that cold air from the northwest intruded below the warm southeasterly air flow and a cold front was formed along with the low pressure system. Ozone-rich dry air from the stratosphere intruded into the upper troposphere and was retained by the stable layer. After that, on May 17, the

weather pattern changed and a high pressure system was formed. The ozone-rich air in the upper troposphere moved downward gradually under the high pressure system. The authors concluded that the ozone was transported into the upper troposphere near the cold front and under the low pressure system, and then moved to the subsequent ground level under the high pressure systems.

2.4 VOC Vs. NO_x Control

The Committee on Tropospheric Ozone Formation and Measurement of the National Research Council (1991) discussed the relative effectiveness of anthropogenic VOC, NO_x and Biogenic VOC on ozone formation. The ozone concentration is sensitive to the NMHC/NO_x ratio as shown in Figure 2.4.1, which contains ozone isopleths used in EPA's EKMA model. As illustrated in Figure 2.4.1, NO_x controls lead to higher reductions in ozone concentrations where the NMHC/NO_x ratio is high (NO_x limited zone), whereas VOC control is more effective in areas where the NMHC/NO_x ratio is low (VOC limited zone). For example, the NO_x should be reduced in order to reduce the ozone concentration from 360 ppb to 120 ppb when the NMHC/NO_x ratio is 15/1. On the Other hand, VOC should be reduced in order to reduce the ozone concentration from 360 ppb to 120 ppb when the NMHC/NO_x ratio is 4/1. However, the authors preferred the use of

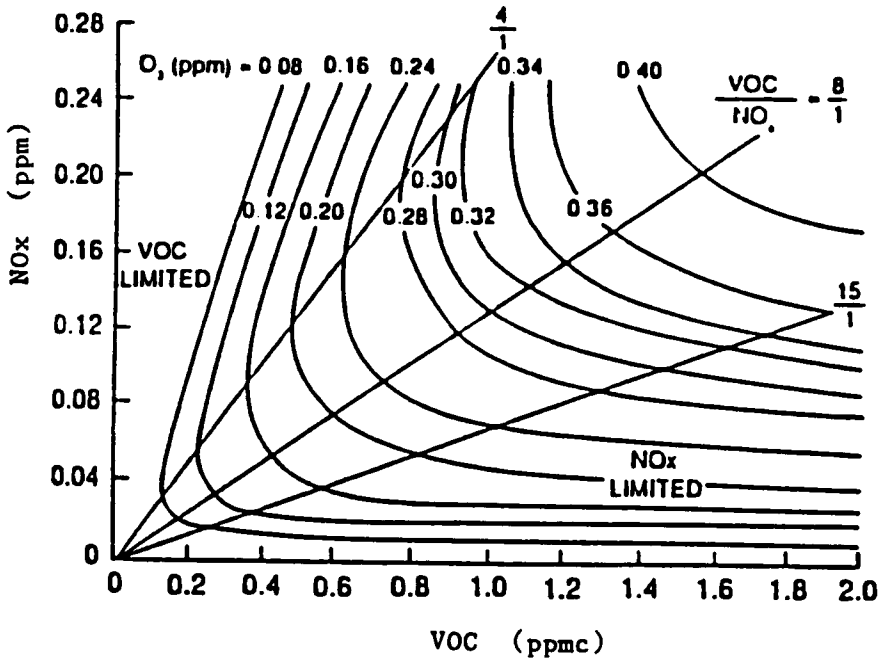


Figure 2.4.1. Typical Ozone Isopleths Used in EPA's EKMA Model. Source: Adapted from Dodge, 1977.

a grid-based model over a EKMA-based model, in order to understand the precursors' contributions to peak ozone concentrations.

Sillman et al. (1990) analyzed the sensitivity of ozone to nitrogen oxides and hydrocarbons in rural areas of the eastern United States. Anthropogenic emissions were taken from the National Acid Precipitation Assessment Program (NAPAP) inventory, for a typical summer weekday. The authors found that the ozone formation in rural areas strongly depended on the concentration of NO_x but was almost independent of the amount of hydrocarbons present.

McKeen et al. (1991) simulated ozone formation using a three-dimensional mesoscale model in the eastern United States using the NAPAP inventory for 1985. They concluded that the ozone formation was NO_x limited in rural areas. They also found that the ozone reduction was sensitive to NMHC emission reductions in the urban area, and ozone increased with NO_x emission reductions in the areas with strong urban characteristics. However, areas with urban influence comprised only 10% of the total study area. As a whole, ozone formation in the majority of the eastern United States was found to be limited by NO_x emissions rather than NMHC. They also conducted a sensitivity analysis by removing biogenic hydrocarbons. In the nonurban areas, the ozone value only decreased by 5-12%. However, in the areas with

strong urban influence the ozone reduction was largest. Anthropogenic VOCs and biogenic VOCs contributed similarly to ozone formation in urban areas. They concluded that at any location, the sensitivity of ozone concentrations to either anthropogenic or NO_x emission reduction was primarily dependent upon the extent of the urban influence.

Roselle et al. (1991) studied the sensitivity of regional ozone concentrations to biogenic hydrocarbon emissions in the northeastern United States using EPA's Regional Oxidant Model (ROM). The simulation study was conducted for three scenarios each for a 6-day period (July 12-18, 1980) during which peak hourly observed ozone concentrations exceeded 200 ppb. The biogenic hydrocarbon emissions comprised about 50% of total VOC emissions. The input for each simulation was identical except for the emissions data. The first scenario considered no biogenic emissions. The second scenario considered both anthropogenic and biogenic emissions. The third simulation included anthropogenic NO_x and all biogenic emissions but contained no anthropogenic NMHC emissions. The highest ozone concentration from the first scenario was predicted to be 154 ppb; 178 ppb from the second, and 122 ppb from the third. Analysis of the ozone concentration over the study area from these simulations showed that biogenic emissions have a significant effect on ozone formation. Further

analysis revealed that removal of biogenic emissions caused a reduction of the maximum ozone concentration by 10 - 20 ppb downwind of New York city.

3.0 DEVELOPMENT OF MODELING INPUT

Ozone formation in the atmosphere is a result of very complex physical and chemical processes. Therefore, computer models are used to predict the peak ozone formation. These models are validated by comparing observed and predicted peak ozone concentrations. Once validation has occurred these models can be used to evaluate future compliance. In determining control strategies which may be used for future compliance, it is important to analyze the ability of the models to predict the contribution of different sources including point, area, mobile and biogenic sources to ozone formation. This requires compilation of emissions, meteorological, air quality, and other chemical data obtained from actual episodes.

In this research, the modeling domain was selected within the boundaries of the 1988 emission inventory for the Memphis nonattainment area and was gridded as a 20 X 20 matrix with 5 km X 5 km resolution. Figure 3.1 shows the modeling domain with the county boundary and the location of the monitoring stations in the modeling domain. Emissions from point, area and mobile sources were calculated and distributed based on the 1988 emission inventory prepared by the University of Tennessee, Knoxville. Biogenic emissions were calculated using the USEPA's Personal Computer Version of the Biogenic Emissions System (PCBEIS). Table 3.1 shows

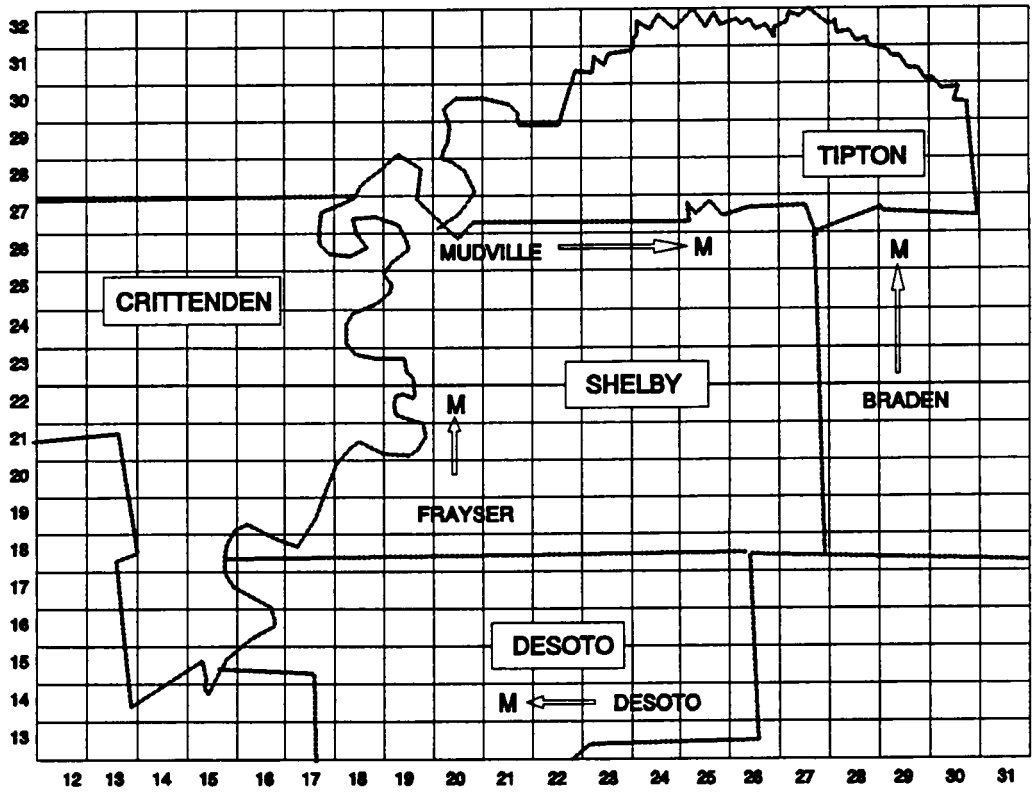


Figure 3.1. Modeling Domain Showing the Location of Monitoring Stations.

Table 3.1. Ozone Precursor Emissions in the Study Area - 1988 Base Case (tons/day).

SOURCE		POLLUTANT	
		VOC	NO_x
POINT	TVA (T)	0.14	75.60
	OTHER SOURCES (P)	55.71	14.90
MOBILE (M)		169.14	90.24
AREA (A)		92.74	83.61
BIOGENIC (B)		155.88	0.00
TOTAL		473.61	264.35

the emissions data for the modeling domain.

The meteorological inputs for the model were obtained by analyzing the data for the ten highest ozone days during 1986-88. Table 3.2 shows the ten highest ozone days between 1986 and 1988.

There were thirteen input files required in the UAM model. Those input files were prepared using the emissions and meteorological data. Then, the model was run for the 1988 base case. After that a sensitive analysis was conducted to determine the contribution to ozone formation of specific sources, and/or a combination of specific sources. The overall approach of this research is described in Figure 3.2.

3.1 Emissions from Point Sources

The emission inventory included all the point sources which emit more than 100 tons per year of ozone precursors. Point source data for the Tennessee areas (Shelby County, Tipton County) were obtained from the state EIS (Emission Inventory System) computerized data format, while data for Arkansas (Critenden County), and Mississippi (Desoto County) were obtained from EPA's standard NEDS (National Emissions Data System) computerized format. Table 3.1.1 and 3.1.2 show the emission data from the point sources in the modeling domain by county. The speciation of VOC is

Table 3.2. Ten Highest Ozone Days (1986 - 1988).

DAY	HIGHEST OZONE CONCENTRATION (ppb)	TIME OF OCCURRENCE (hr)	MONITORING STATION
05/13/86	0.130	14:00	MUDDVILLE
07/24/86	0.165	15:00	FRAYSER
08/05/86	0.159	14:00	MUDDVILLE
06/09/87	0.127	16:00	FRAYSER
06/24/87	0.146	16:00	FRAYSER
07/30/87	0.134	12:00	MUDDVILLE
06/15/88	0.144	13:00	FRAYSER
06/21/88	0.140	16:00	FRAYSER
06/22/88	0.125	15:00	FRAYSER
06/23/88	0.140	15:00	FRAYSER

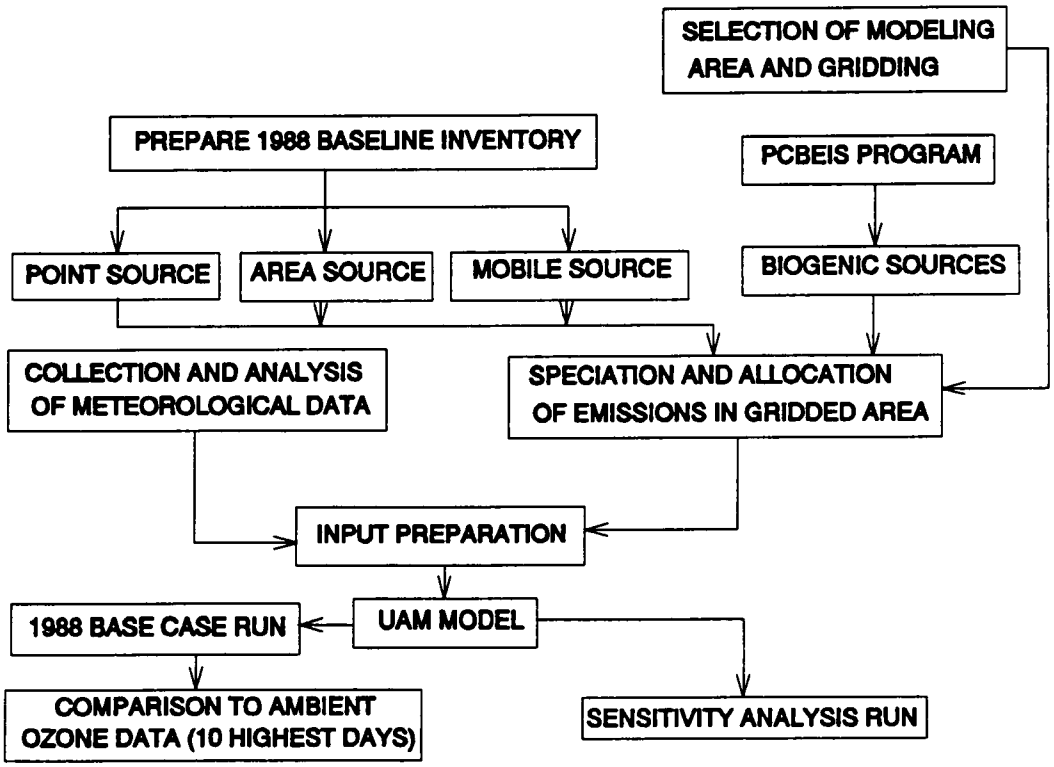


Figure 3.2. Flowchart of Overall Approach.

Table 3.1.1. VOC Emission Data for Point Sources by County.

COUNTY	POINT SOURCE	SCC CODE	GRID NO	EMISSION (KG/DAY)	HOUR
DESOTO	THOMPSON & FORMBY INC.	30101401	2417	1063.000	16
	AMERICAN NATIONAL CAN CO.	40201702	2417	348.900	24
	TYLER REFRIGERATION	40201702	2417	16.730	16
	MEMPHIS PROPELER SERVICE	30500201	2417	3.500	8
	AMERICAN SIGNATURE GRAPHICS	40500301	2417	1238.200	24
	KELLEY MANUFACTURING CO.	30500201	2417	147.400	8
	BURKEEN MANUFACTURING CO.	30500201	2417	12.600	8
	BOZOF DINETTES	30500201	2417	3.500	8
	TEXAS GAS TR. CORP.	30500201	1816	102.200	24
	FL AMERICAN ELECTRIC	30500201	2017	170.100	8
	DOVER ELEVATOR SYSTEMS	30500201	2418	192.600	8
	GUARDIAN FIBERGLASS INC.	30501402	2317	49.900	24
	AMERICAN HELMITIN CORP.	30500201	2517	18.100	8
	AMERICAN PLASTIC TOYS, INC.	30101801	2517	29.300	24
TIPTON	MUELLER BRASS CO.	30500205	2428	108.000	8
	ARTESIAN IND. MT.	40200601	2829	15.876	8
	ARTESIAN IND. MT.	49099999	2829	25.400	8

Table 3.1.1. (Cont.)

COUNTY	POINT SOURCE	SCC CODE	GRID NO	EMISSION (KG/DAY)	HOUR
TIPTON (CONTD.)	ARTESIAN IND. MT.	40200902	2829	21.80	8
	ARTESIAN IND. MT.	49099999	2829	25.40	8
	ARTESIAN IND. MT.	40200902	2829	83.50	8
	TEXAS GAS TR. CORP.	10200603	2829	134.50	24
CRITTENDEN	SUN PIPE LINE CO.	40600141	1821	9.98	24
	SUN PIPE LINE CO.	40400111	1821	32.40	24
	SUN PIPE LINE CO.	40400111	1821	32.40	24
	SUN PIPE LINE CO.	40400111	1821	32.40	24
	SUN PIPE LINE CO.	40400111	1821	32.40	24
	SUN PIPE LINE CO.	40400111	1821	9.98	24
	SUN PIPE LINE CO.	40400111	1821	32.40	24
	SUN PIPE LINE CO.	40400111	1821	32.40	24
	SUN PIPE LINE CO.	40400111	1821	32.40	24
	SUN PIPE LINE CO.	40400111	1821	32.40	24
	SUN PIPE LINE CO.	40400108	1821	2.50	24

Table 3.1.1. (Cont.)

COUNTY	POINT SOURCE	SCC CODE	GRID NO	EMISSION (KG/DAY)	HOUR
CRITTENDEN (Cont.)	SUN PIPE LINE CO.	40300115	1821	2.5	24
	SUN PIPE LINE CO.	40300115	1821	2.5	24
	SUN PIPE LINE CO.	40301115	1821	2.5	24
	SUN PIPE LINE CO.	40301119	1821	2.5	24
	SUN PIPE LINE CO.	40400108	1821	2.5	24
	SUN PIPE LINE CO.	40400111	1821	84.7	24
	SUN PIPE LINE CO.	40400111	1821	2.5	24
SHELBY	MAXWELL COMM. CORP.	40500513	2018	2442.5	24
	KIMBERLY-CLARK CORP.	30701399	2018	1246.2	4
	UNITED TECH. CARRIER CORP.	39999995	2718	544.3	16
	UNITED TECH. CARRIER CORP.	39999995	2718	509.6	8
	REXHAM CORP.	40500301	1819	161.2	24
	REXHAM CORP.	40500301	1819	170.9	24
	REXHAM CORP.	40500301	1819	97.7	24
	REXHAM CORP.	40500301	1819	219.8	24
	TENNESSEE VALLEY AUTHORITY	10100801	1819	130.8	24
	SHULTON INC.	30100902	2019	89.3	24

Table 3.1.1. (Cont.)

COUNTY	POINT SOURCE	SCC CODE	GRID NO	EMISSION (KG/DAY)	HOUR
SHELBY (Cont.)	SHULTON INC.	30100902	2019	18.6	24
	SHULTON INC.	30100902	2019	251.2	24
	DIXICO INC.	40500301	2019	247.0	24
	DIXICO INC.	40500301	2019	24.9	24
	DIXICO INC.	40500301	2019	32.4	24
	DIXICO INC.	40588801	2019	1246.2	24
	CLED DVSN OF GIBSON GREETINGS	40500501	2219	1729.7	24
	CLED DVSN OF GIBSON GREETINGS	40500501	2219	433.6	24
	CLED DVSN OF GIBSON GREETINGS	40500501	2219	899.7	24
	CLED DVSN OF GIBSON GREETINGS	40500501	2219	19.9	24
	BRYCE CORP.	40500301	2619	167.5	21
	BRYCE CORP.	40588801	2619	957.1	24
	BRYCE CORP.	40588801	2619	385.8	24
	BRYCE CORP.	40500301	2619	212.3	24
	BRYCE CORP.	40500301	2619	80.7	24

Table 3.1.1. (Cont.)

COUNTY	POINT SOURCE	SCC CODE	GRID NO	EMISSION (KG/DAY)	HOUR
SHELBY (Cont.)	BRYCE CORP.	40500301	2619	59.8	24
	CARGILL INC.	30201901	1920	777.6	24
	SONOCO PRODUCTS CO.	30902099	1920	756.0	24
	SONOCO PRODUCTS CO.	30901199	1920	37.8	8
	MAPCO PETROLEUM	30600701	1920	2831.3	10
	MAPCO PETROLEUM	40600132	1920	24.9	24
	MAPCO PETROLEUM	30699998	1920	52.3	24
	MAPCO PETROLEUM	40600242	1920	1919.1	24
	MAPCO PETROLEUM	30600401	1920	24.9	24
	MAPCO PETROLEUM	30699998	1920	4182.1	24
	TROPICANA ENERGY CO., INC.	40301009	1920	72.2	24
	GREAT DANE TRAILERS TN, INC.	40188801	2020	793.3	16
	THE DAVIS CHAIR CO.	30702098	2020	1291.8	8
	STERILIZATION SERVICES OF TN.	40100399	2020	161.9	24
	JEHLCCOPERAGE CO INC.	30902501	2121	97.7	8
	PLOUGH INC.	30299998	2221	13.9	8

Table 3.1.1. (Cont.)

COUNTY	POINT SOURCE	SCC CODE	GRID NO	EMISSION (KG/DAY)	HOUR
SHELBY (Cont.)	PLOUGH INC., PRINTING DVSN.	40500401	2221	230.30	16
	HUMCO CHEMICAL DVSN.	30103499	2222	248.84	24
	MANVILLE FOREST PRODUCTS	40588801	2222	331.49	24
	Q O CHEMICALS INC.	30183001	2222	97.20	24
	Q O CHEMICALS INC.	30199998	2222	62.32	24
	SOUTHERN COTTON OIL CO.	30201902	2222	1555.21	24
	VELSICOL CHEMICAL CORPORATION	30103311	2222	2400.08	24
	VELSICOL CHEMICAL CORPORATION	30103311	2222	7.48	24
	E. I. DUPONT DE NUMOURS	30199998	2124	436.13	24
	E. I. DUPONT NUMOURS	39999995	2124	84.73	24
	E. I. DUPONT DE NUMOURS	30188801	2124	67.31	24
	E. I. DUPONT DE NUMOURS	30199998	2124	4388.26	24
	E. I. DUPONT DE NUMOURS	30119013	2124	11045.52	24
	E. I. DUPONT DE NUMOURS	30199998	2124	44.04	24

Table 3.1.2. NO_x Emission Data for Point Sources by County.

COUNTY	POINT SOURCE	GRID NO	EMISSION (KG/DAY)	HOUR
TIPTON	RAYOVAC.	2730	22.5	24
	RAYOVAC.	2730	7.5	16
	COLONIAL FIBER	2830	39.3	24
	COLONIAL FIBER	2830	10.4	24
	COLONIAL FIBER	2830	12.0	24
	TEXAS GAS TR.	2829	3406.0	24
SHELBY	MAXWELL COMM.	2018	33.5	24
	SOUTHERN COTTON	2222	91.0	24
	CARGILL INC.	1920	125.0	24
	CARGILL INC.	1920	2004.0	24
	DIXICO INC.	2019	145.0	24
	DIXICO INC.	2019	277.0	24
	DIXICO INC.	2019	88.1	24
	DIXICO INC.	2019	1119.0	24
	DIXICO INC.	2019	2238.1	24
	MAPCO PETROLEUM	1920	969.5	24
	MAPCO PETROLEUM	1920	934.6	24

Table 3.1.2. (Cont.)

COUNTY	POINT SOURCE	GRID NO	EMISSION	HOUR
SHELBY (Cont.)	MAPCO PETROLEUM	1920	42.4	24
	MAPCO PETROLEUM	1920	1557.7	24
	HUMCO CHEMICAL	2222	34.2	24
	KIMBERLY-KLARK	2018	227.5	24
	Q O CHEMICALS	2222	26.4	24
	BRYCE CORP.	2619	12.5	24
	VELSICOL CHEMICAL	2222	89.0	24
	TENNESSEE VALLEY AUTHORITY	1819	68565.7	24
	MANVILLE FOREST	2222	18.2	24

discussed in Section 3.5.1.

3.2 Emissions from Area Sources

Area source emissions included the numerous small point, area and non-highway mobile source emissions. Area source emissions were calculated using the U.S. EPA emission estimating procedure (Davis et. al., 1990). The area source emission inventory for 1988 was done for VOCs, NO_x, and CO. The emissions were allocated to each grid using surrogate indicators of the relative emissions. Surrogate indicators included information such as population and rural versus urban land use patterns. Based on the surrogate indicators, total area source emissions in each county were subgrouped into two categories, population based emissions and source specific emissions. Again, the population based emissions were divided into 32 source categories for VOCs, 9 for NO_x and, 9 for CO including motorcycle emissions as shown in Table 3.2.1 through 3.2.3. The source specific emissions were divided into 4 subgroups such as railroad, recreational boat, rural, and aircraft emissions. Further, rural emissions were subdivided into two groups: pesticide application + farm equipment and forest fires. To estimate the area source emissions for a pollutant, county data such as population, harvested acres, and the number of registered boats were needed. Table 3.2.1 through 3.2.3 show the area

Table 3.2.1. Area Source VOC Emissions by Category and by County (tons/day).

CATEGORIES		SCC CODE	COUNTY			
			CRITTENDEN	DESOTO	SHELBY	TIPTON
POPULATION BASED	TANK TRUCK UNLOADING	1190	0.62	0.29	10.02	0.46
	UNDERGROUND TANK BREATHING	1190	0.05	0.03	0.87	0.04
	GAS TRUCKS IN TRANSIT	1190	0.02	0.01	0.24	0.01
	COMMERCIAL DRY CLEANING	1196	0.17	0.21	2.70	0.12
	DEGREASING COLD CLEANING	1195	0.25	0.37	3.97	0.18
	ARCHITECTURAL SURFACE COATING	9021	0.42	0.57	9.50	0.31
	AUTO REFINISHING	1194	0.19	0.24	3.02	0.14
	GRAPHICS ARTS	1191	0.08	0.00	1.27	0.06
	CUTBACK ASPHALT	0023	0.00	0.18	0.00	0.00
	COMMERCIAL/CONSUMER SOLVENT USE	0197	0.45	0.51	7.15	0.33
	MUNICIPAL SOLID WASTE LANDFILL	9022	0.00	0.00	0.15	0.00
	PUBLIC WATER TREATMENT WORKS	0000	0.04	0.00	2.47	0.03
	STATIONARY EXTERNAL COMBUSTION-COAL	1185	0.01	0.00	0.30	0.01
	STATIONARY EXT. COMBUSTION-FUEL OIL	0001	0.00	0.00	0.02	0.00
	STATIONARY EXT. COMBUSTION-NATURAL GAS	0003	0.00	0.00	0.10	0.00
	STATIONARY EXT. COMBUSTION-LPG	0002	0.00	0.00	0.00	0.00
	CONSTRUCTION EQUIPMENT	9002	0.00	0.00	0.84	0.00
	INDUSTRIAL EQUIPMENT	9002	0.02	0.00	0.86	0.02

Table 3.2.1. (Cont.)

CATEGORIES		SCC CODE	COUNTY			
			CRITTENDEN	DESOTO	SHELBY	TIPTON
POPULATION BASED (CONTD.)	LAWN AND GARDEN EQUIPMENT	9002	0.42	0.00	6.77	0.31
	ON SITE INCINERATION	0121	0.04	0.00	0.452	0.03
	OPEN-BURNING-RESIDENTIAL	0121	0.19	0.00	0.08	0.14
	OPEN-BURNING-COMMERCIAL	0121	0.00	0.00	0.08	0.00
	OPEN-BURNING-INDUSTRIAL	0121	0.00	0.00	0.00	0.00
	OPEN-BURNING-COMBUSTION	0121	0.00	0.00	0.54	0.04
	OTHERS	0000	0.00	0.00	7.03	0.00
	TOTAL		2.97	2.41	58.43	2.19
SOURCE SPECIFIC	RAILROAD	0008	0.38	0.18	1.44	0.22
	RECREATIONAL BOATS	1201	0.57	0.00	2.14	0.58
	MOTORCYCLES	9002	0.00	0.00	0.12	0.01
	PESTICIDE APPLICATION+FARM EQUIPMENT	1201	3.66	0.33	1.00	1.53
	AIRCRAFT	1099	0.01	0.00	2.75	0.01
	FOREST FIRES	0307	0.00	0.00	0.00	0.11
	TOTAL		4.62	0.51	7.45	2.46

Table 3.2.2. Area Source NO_x Emissions by Category and by County (tons/day).

CATEGORIES		COUNTY			
		CRITTENDEN	DESOTO	SHELBY	TIPTON
POPULATION BASED	EXTERNAL FUEL COMBUSTION; UTILITY BOILERS	0.00	0.00	0.00	0.00
	EXTERNAL FUEL COMBUSTION; INDUSTRIAL BOILERS	0.00	0.00	0.00	0.00
	EXTERNAL FUEL COMBUSTION; COMMERCIAL, INSTITUTIONAL, AND RESIDENTIAL	0.00	0.00	1.74	0.03
	COMBUSTION; WASTE DISPOSAL	0.01	0.00	0.16	0.01
	COMBUSTION; OPEN BURNING	0.04	0.00	0.66	0.03
	COMBUSTION; OTHERS	0.00	0.00	0.00	0.02
	CONSTRUCTION EQUIPMENT	0.00	0.00	3.36	0.00
	INDUSTRIAL EQUIPMENT	0.07	0.00	1.58	0.06
	LAWN AND GARDEN EQUIPMENT	0.04	0.00	0.29	0.03
	TOTAL	0.50	0.00	15.89	0.18
SOURCE SPECIFIC CATEGORIES	RAILROAD	1.49	0.72	5.67	0.87
	RECREATIONAL BOATS	0.02	0.00	11.96	0.02
	FARM EQUIPMENT	11.97	0.00	6.63	5.08
	AIRCRAFT	0.00	0.00	4.88	0.00
	TOTAL	13.48	0.72	29.14	5.97

Table 3.2.3. Area Source CO Emissions by Category and by County (tons/day).

CATEGORIES		COUNTY			
		CRITTENDEN	DESOTO	SHELBY	TIPTON
POPULATION BASED	EXTERNAL FUEL COMBUSTION; UTILITY BOILERS	0.00	0.00	0.00	0.00
	EXTERNAL FUEL COMBUSTION; INDUSTRIAL BOILERS	0.17	0.00	4.71	0.00
	EXTERNAL FUEL COMBUSTION; COMMERCIAL, INSTITUTIONAL & RESIDENTIAL	0.02	0.00	0.67	0.01
	COMBUSTION; WASTE DISPOSAL	0.69	0.00	1.89	0.51
	COMBUSTION; OTHERS	0.00	0.00	9.33	0.68
	CONSTRUCTION EQUIPMENT	0.00	0.00	27.1	0.00
	INDUSTRIAL EQUIPMENT	0.60	0.00	36.70	0.56
	LAWN AND GARDEN EQUIPMENT	3.92	0.00	48.4	2.87
	TOTAL	5.40	0.00	112.20	4.63
SOURCE SPECIFIC CATEGORIES	RAILROAD	0.52	0.255	1.99	0.30
	RECREATIONAL BOATS	1.80	0.00	4.30	1.80
	FARM EQUIPMENT	4.30	0.00	7.70	1.82
	AIRCRAFT	0.20	0.00	12.43	0.20
	MOTORCYCLES	0.013	0.00	0.00	0.024
	TOTAL	6.833	0.255	26.420	4.144

source emissions by category and by county in the modeling area for VOCs, NO_x, and CO. Figure 3.2.1 shows the population data for the counties where the inventory were done. Figure 3.2.2 through 3.2.5 show the allocation of area source emissions in the four counties according to the source specific category such as railroad, aircraft, recreational boat, and rural emissions. Appendix shows the gridded population data and other source specific area source emission distribution data by county.

The population based emissions of each county were allocated in each grid of that county with the help of gridded population data as given in Appendix using the following equation.

$$\text{Emissions in a Grid} = \frac{\text{(Total Emissions in the County)} * \text{(Population in that Grid)}}{\text{Total Population in the County}}$$

Other source specific emissions were allocated to those grids which contained that particular source. For example, for aircraft based emissions, the following equation was used.

$$\text{Aircraft Based Emissions in a Grid Containing Airports} = \frac{\text{(Total Emissions from the Aircraft in that County)} * \text{(No. of Airports in that Grid)}}{\text{Total Number of Airports in that County}}$$

3.3 Emissions from Mobile Sources

The emissions from automobiles and trucks travelling on different types of roads including interstate, major

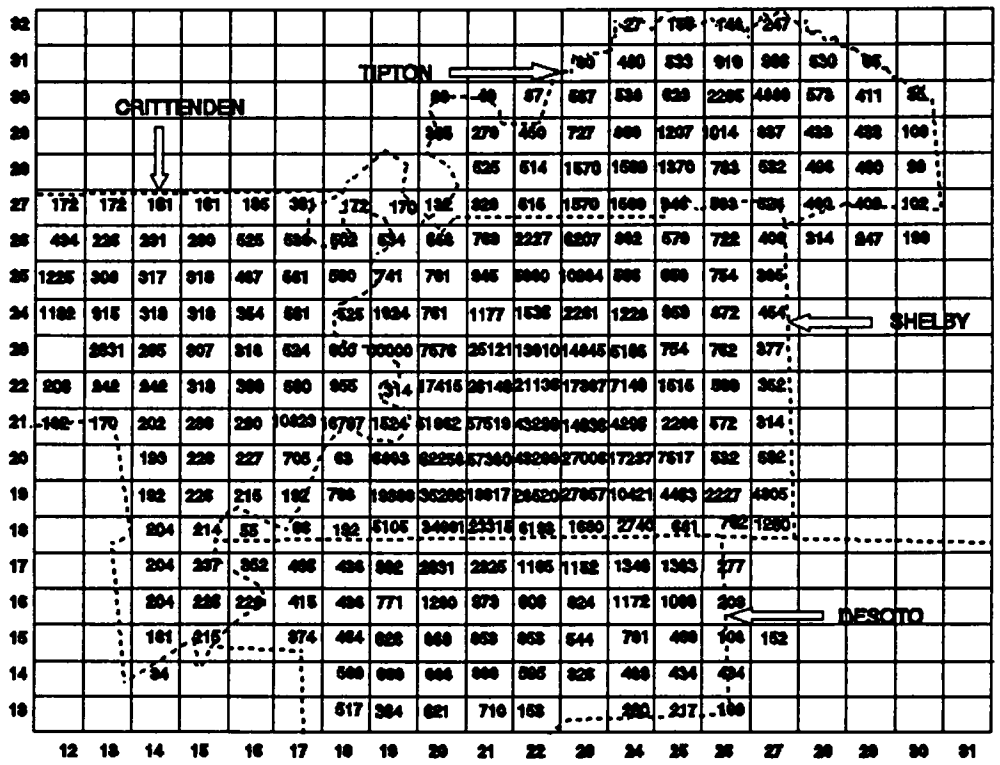


Figure 3.2.1. Population Data in Each Grid of the Counties that were Inventoried.

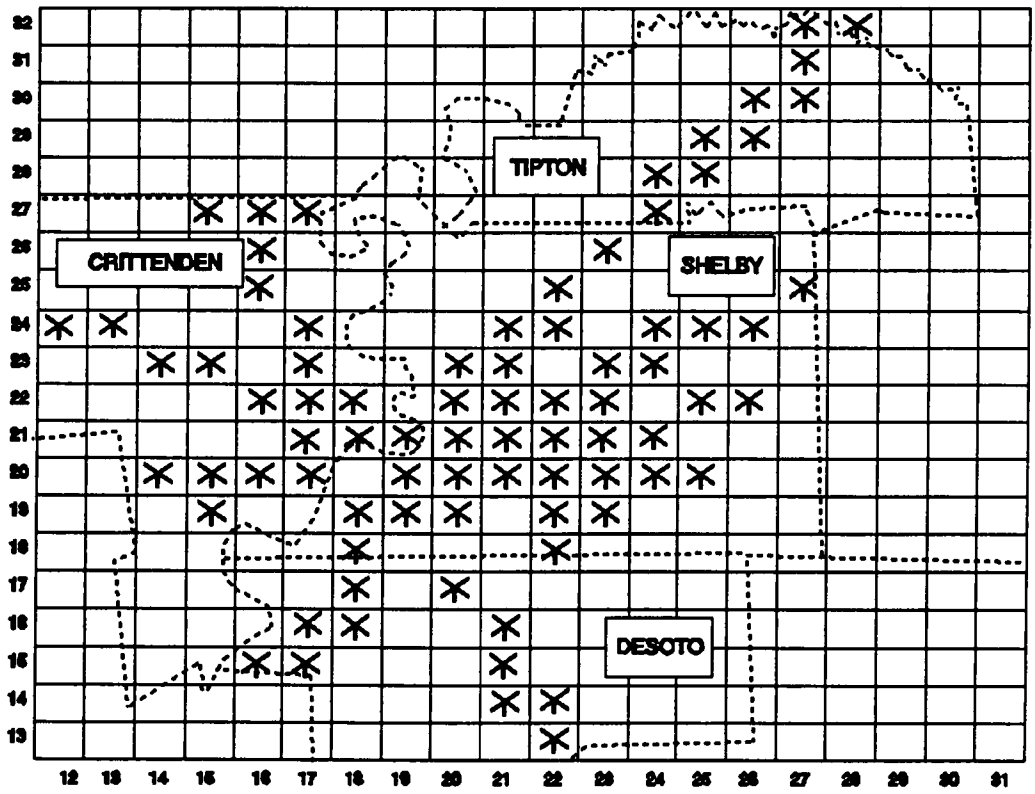


Figure 3.2.2. Allocation of Railroad Emissions in the Counties that were Inventoried.

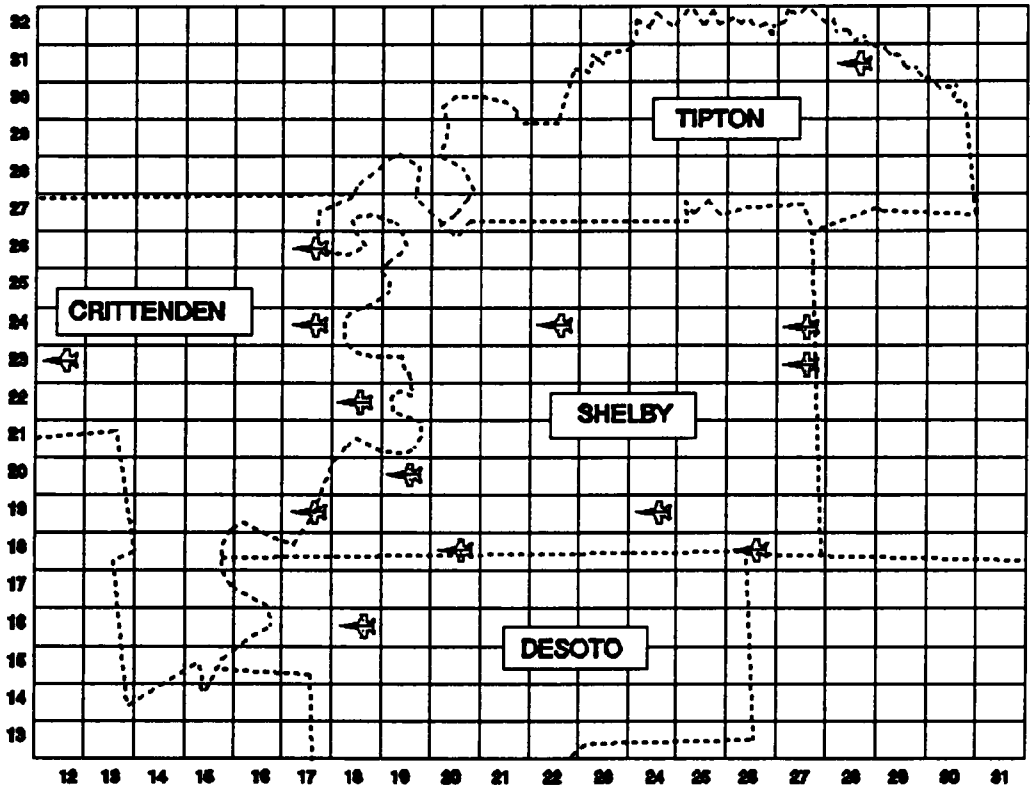


Figure 3.2.3. Allocation of Airport Emissions in the Counties that were Inventoried.

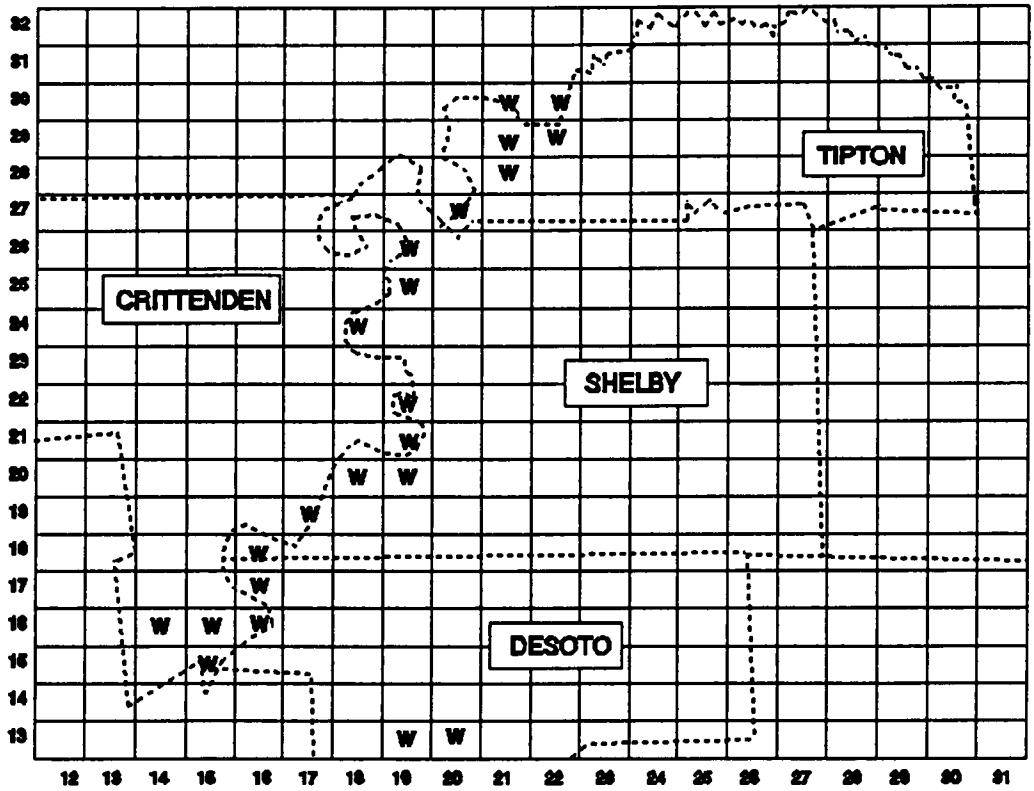


Figure 3.2.4. Allocation of Water Body Emissions in the Counties that were Inventoried.

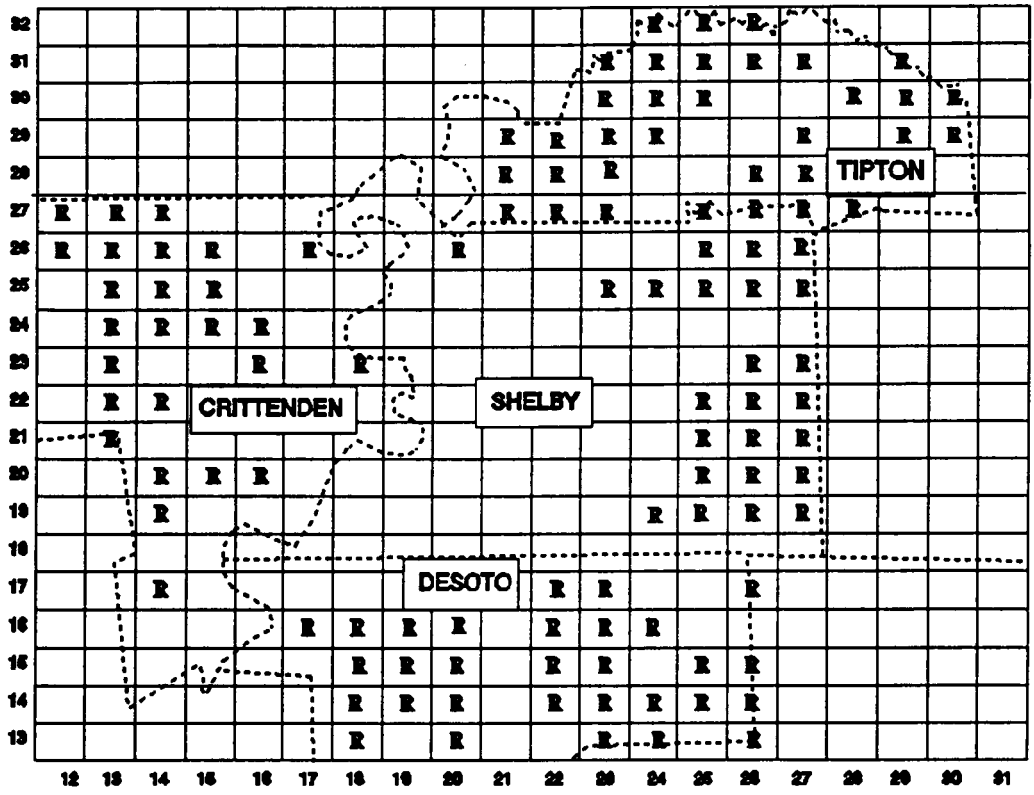


Figure 3.2.5. Allocation of Rural Emissions in the Counties that were Inventoried.

arterial, minor arterial, collector, and local roads (facility type) were considered as mobile source emissions. To calculate the mobile source emissions, the Vehicle Miles Traveled (VMT) were required for each county. For Shelby County, the gridded VMT data for 1988 were obtained from the Memphis and Shelby County Office of Planning and Development. For Tipton and Crittenden County, gridded VMT data were calculated by the University of Tennessee, Knoxville, Department of Civil Engineering based on the Average Daily Traffic (ADT), 1988. These ADT data were obtained from the Tennessee Department of Transportation and the Arkansas Department of Transportation (DOT). For Desoto County, the VMT data were obtained from the Mississippi Department of Transportation.

To calculate the emission factors for mobile sources, EPA's MOBILE 4.0 was used. The hourly average temperature profile used for the model is shown in Table 3.6.8.1. Hourly emission factors (g/vehicle mile/hr) for each species (VOCs, NO_x, and CO) were calculated for each facility type for urban and rural grids as shown in Table 3.3.1 through 3.3.6. Hourly gridded emissions in g/hr were calculated for each facility type for each pollutant as follows:

Hourly Emission (g/hr) = Gridded VMT * Hourly Emission Factors (g/VMT/hr)

Total hourly emissions of each pollutant were calculated by summing the hourly emissions for each facility type, i.e. major arterial, minor arterial etc.

Table 3.3.1. VOC Emission Factors for Urban Grids (g/vehicle mile/hr).

TIME	INTERSTATE	MAJOR ARTERIAL	MINOR ARTERIAL	COLLECTOR	LOCAL
1	0.0630	0.0601	0.0639	0.0502	0.0553
2	0.0462	0.0199	0.0212	0.0250	0.0276
3	0.0123	0.0200	0.0212	0.0250	0.0276
4	0.0121	0.0198	0.0211	0.0250	0.0278
5	0.0121	0.0396	0.0422	0.0250	0.0278
6	0.0292	0.0748	0.0813	0.0952	0.1110
7	0.1957	0.2576	0.2779	0.2840	0.3234
8	0.3938	0.2928	0.3170	0.3508	0.4011
9	0.2532	0.2019	0.2206	0.2488	0.2778
10	0.2091	0.1956	0.2138	0.2377	0.2692
11	0.1946	0.2076	0.2145	0.2717	0.3180
12	0.2004	0.2515	0.2621	0.3277	0.3630
13	0.2104	0.2873	0.2977	0.3669	0.4136
14	0.2111	0.2896	0.3101	0.3814	0.4145
15	0.2320	0.3456	0.3776	0.4215	0.4425
16	0.4126	0.4330	0.4598	0.5366	0.5823
17	0.5244	0.4807	0.5078	0.5572	0.5971
18	0.4488	0.4677	0.4930	0.5260	0.5407
19	0.2487	0.3356	0.3539	0.4042	0.4142
20	0.1849	0.2640	0.2790	0.3209	0.3288
21	0.1317	0.2015	0.2138	0.2472	0.2539
22	0.1055	0.1696	0.1801	0.1832	0.1883
23	0.0831	0.1231	0.1945	0.1844	0.1309
24	0.0653	0.0829	0.0881	0.1036	0.1130
TOTAL	4.4802	5.1218	5.5122	6.1992	6.6494

Table 3.3.2. VOC Emission Factors for Rural Grids (g/vehicle mile/hr).

TIME	INTERSTATE	MAJOR ARTERIAL	MINOR ARTERIAL	COLLECTOR	LOCAL
1	0.0552	0.0583	0.0630	0.0494	0.0505
2	0.0445	0.0193	0.0209	0.0247	0.0252
3	0.0408	0.0193	0.0209	0.0247	0.0252
4	0.0368	0.0191	0.0208	0.0247	0.0252
5	0.0416	0.0383	0.0416	0.0247	0.0252
6	0.0601	0.0710	0.0789	0.0972	0.1008
7	0.0868	0.2465	0.2713	0.2872	0.2961
8	0.1080	0.2851	0.3081	0.3588	0.3715
9	0.1757	0.1911	0.2100	0.2571	0.2756
10	0.2528	0.1845	0.2030	0.2491	0.2671
11	0.2923	0.1963	0.2150	0.2959	0.3154
12	0.3054	0.2410	0.2597	0.3411	0.3598
13	0.3113	0.2750	0.2968	0.3878	0.4098
14	0.3116	0.2776	0.2990	0.3895	0.4104
15	0.3119	0.3334	0.3566	0.4167	0.4386
16	0.3285	0.4214	0.4510	0.5423	0.5557
17	0.2890	0.3953	0.5010	0.5560	0.5674
18	0.2517	0.4583	0.4833	0.5152	0.5362
19	0.2228	0.3288	0.3468	0.3942	0.4107
20	0.1684	0.2577	0.2731	0.3124	0.3263
21	0.1275	0.1964	0.2090	0.2402	0.2519
22	0.1062	0.1650	0.1759	0.1778	0.1872
23	0.0886	0.1197	0.1279	0.1236	0.1301
24	0.0719	0.0806	0.0871	0.1020	0.1041
TOTAL	4.0894	4.8790	5.3207	6.1923	6.4660

Table 3.3.3. NO_x Emission Factors for Urban Grids (g/vehicle mile/hr).

TIME	INTERSTATE	MAJOR ARTERIAL	MINOR ARTERIAL	COLLECTOR	LOCAL
1	0.1007	0.0325	0.0321	0.0212	0.0225
2	0.0831	0.0111	0.0108	0.0108	0.0112
3	0.0593	0.0111	0.0108	0.0108	0.0112
4	0.0594	0.0111	0.0109	0.0109	0.0113
5	0.0594	0.0219	0.0216	0.0109	0.0113
6	0.0688	0.0732	0.0621	0.0728	0.0451
7	0.1465	0.1759	0.1614	0.1764	0.1213
8	0.2185	0.2129	0.1895	0.2287	0.1386
9	0.1673	0.1817	0.1503	0.1931	0.0876
10	0.1447	0.1691	0.1377	0.1803	0.0762
11	0.1456	0.1641	0.1350	0.1850	0.0848
12	0.1485	0.1444	0.1247	0.1621	0.0934
13	0.1411	0.1693	0.1445	0.1892	0.1019
14	0.1394	0.1634	0.1397	0.1819	0.1016
15	0.1547	0.1752	0.1534	0.1834	0.1118
16	0.1863	0.1775	0.1643	0.1974	0.1488
17	0.2249	0.1711	0.1662	0.1780	0.1607
18	0.2280	0.1673	0.1653	0.1575	0.1505
19	0.1772	0.1236	0.1239	0.1224	0.1238
20	0.1665	0.1063	0.1066	0.1054	0.1064
21	0.1452	0.0889	0.0892	0.0881	0.0889
22	0.1339	0.0803	0.0806	0.0697	0.0702
23	0.1287	0.0610	0.0594	0.0494	0.0507
24	0.1048	0.0418	0.0414	0.0408	0.0435
TOTAL	3.3325	2.7347	2.4814	2.8262	1.9733

Table 3.3.4. NO_x Emission Factors for Rural Grids (g/vehicle mile/hr).

TIME	INTERSTATE	MAJOR ARTERIAL	MINOR ARTERIAL	COLLECTOR	LOCAL
1	0.2135	0.0308	0.0312	0.0203	0.0203
2	0.1837	0.0106	0.0107	0.0103	0.0102
3	0.1672	0.0106	0.0106	0.0103	0.0101
4	0.1655	0.0106	0.0107	0.0103	0.0102
5	0.1681	0.0208	0.0211	0.0103	0.0102
6	0.1782	0.0802	0.0693	0.0498	0.0409
7	0.1886	0.1865	0.1747	0.1280	0.1095
8	0.1891	0.2530	0.2117	0.1546	0.1258
9	0.2546	0.2060	0.1719	0.1121	0.0857
10	0.2873	0.1938	0.1600	0.1012	0.0745
11	0.3232	0.1877	0.1554	0.1078	0.0829
12	0.3335	0.1579	0.1368	0.1068	0.0916
13	0.3107	0.1878	0.1603	0.1197	0.0996
14	0.3058	0.1801	0.1548	0.1178	0.0996
15	0.3283	0.1885	0.1661	0.1248	0.1093
16	0.2919	0.2048	0.1763	0.1519	0.1351
17	0.2782	0.2012	0.1694	0.1536	0.1457
18	0.3070	0.1577	0.1580	0.1412	0.1472
19	0.3234	0.1143	0.1163	0.1148	0.1211
20	0.3245	0.0979	0.1002	0.0983	0.1042
21	0.2982	0.0821	0.0836	0.0818	0.0870
22	0.2825	0.0742	0.0756	0.0648	0.0688
23	0.2857	0.0561	0.0574	0.0468	0.0494
24	0.2346	0.0396	0.0403	0.0395	0.0395
TOTAL	6.2233	2.9328	2.6224	2.0768	1.8784

Table 3.3.5. CO Emission Factors for Urban Grids (g/vehicle mile/hr).

TIME	INTERSTATE	MAJOR ARTERIAL	MINOR ARTERIAL	COLLECTOR	LOCAL
1	0.1851	0.2472	0.2950	0.2983	0.3666
2	0.1374	0.0829	0.0990	0.1501	0.1854
3	0.0408	0.0823	0.0983	0.1490	0.1838
4	0.0412	0.0852	0.1018	0.1544	0.1915
5	0.0412	0.1707	0.2038	0.1544	0.1915
6	0.0903	0.3208	0.3896	0.5769	0.7629
7	0.6106	1.2189	1.4583	1.7520	2.2054
8	1.2569	1.3419	1.6137	2.1078	2.6250
9	0.7718	0.8000	0.9698	1.4023	1.6360
10	0.6265	0.7423	0.9021	1.2972	1.5320
11	0.5804	0.7711	0.9052	1.4862	1.7799
12	0.5986	0.9235	1.0819	1.7724	2.0183
13	0.6315	1.0498	1.2194	1.9710	2.2891
14	0.6342	1.0577	1.2625	2.0434	2.2935
15	0.6932	1.2647	1.5356	2.2589	2.4543
16	1.3001	1.7122	2.0359	2.8839	3.2183
17	1.6377	1.9332	2.2867	3.0389	3.3778
18	1.3267	1.5884	1.8981	2.7054	2.8699
19	0.7504	1.1735	1.4030	2.1288	2.2506
20	0.5693	0.9542	1.1425	1.7339	1.8356
21	0.4064	0.7452	0.8947	1.3575	1.4393
22	0.3269	0.6408	0.7703	1.0223	1.0859
23	0.2603	0.4718	0.7408	0.9353	0.7629
24	0.2018	0.3385	0.4035	0.6122	0.7342
TOTAL	13.7193	19.7168	23.7115	33.9925	38.2897

Table 3.3.6. CO Emission Factors for Rural Grids (g/vehicle mile/hr).

TIME	INTERSTATE	MAJOR ARTERIAL	MINOR ARTERIAL	COLLECTOR	LOCAL
1	0.1774	0.2243	0.2856	0.2892	0.3043
2	0.1447	0.0751	0.0958	0.1457	0.1533
3	0.1320	0.0745	0.0951	0.1446	0.1522
4	0.1235	0.0769	0.0984	0.1497	0.1576
5	0.1373	0.1541	0.1971	0.1497	0.1576
6	0.1903	0.2857	0.3704	0.5860	0.6281
7	0.2832	1.1069	1.4001	1.7611	1.8693
8	0.3570	1.4685	1.5474	2.1542	2.2959
9	0.5506	0.7390	0.9094	1.4535	1.6274
10	0.7698	0.6908	0.8479	1.3682	1.5220
11	0.8836	0.7230	0.8830	1.6053	1.7670
12	0.9243	0.8806	1.0586	1.8452	2.0031
13	0.9457	1.0040	1.2069	2.0972	2.2713
14	0.9473	1.0138	1.2159	2.1046	2.2757
15	0.9455	1.2141	1.4512	2.2530	2.4355
16	1.0490	1.7311	1.9931	2.9234	3.0865
17	0.9179	1.9432	2.2460	3.0302	3.1821
18	0.7641	1.5339	1.8439	2.6419	2.8498
19	0.6904	1.1256	1.3585	2.0624	2.2364
20	0.5370	0.9068	1.1010	1.6715	1.8260
21	0.4107	0.7008	0.8568	1.3008	1.4343
22	0.3452	0.5972	0.7343	0.9758	1.0836
23	0.2937	0.4379	0.5399	0.6832	0.7618
24	0.2355	0.3119	0.3922	0.5955	0.6262
TOTAL	12.7557	19.0197	22.7285	33.9919	36.7070

3.4 Emissions from Biogenic Sources

Emissions of VOCs from trees and other vegetation have a significant effect on ozone formation, thus requiring an estimation of biogenic emissions. These VOCs are highly reactive and shortlived (National Research Council, 1991).

The personal computer program PC-BEIS was used to estimate the hourly biogenic emissions. The site information data and the hourly meteorological data were required by the program for each county of interest. The site information data are shown in Table 3.4.1. The procedure for selection of the day of interest is discussed in this section. The meteorological data of this particular day were used as input to PCBEIS.

Selection of meteorological data were done as follows (EPA, 1991a). First the top ten days with the highest hourly ozone readings between 1986 to 1988 were selected. Then the daily maximum temperature data for each of the ten days were obtained as shown in Table 3.4.2. The daily maximum temperatures were ranked from highest to lowest as shown in Table 3.4.3. The fourth highest day was selected based upon the daily maximum temperature as shown in Table 3.4.3. The meteorological data for this day were used as the input to the program PC-BEIS as shown in Table 3.4.4. This is the procedure currently recommended by the U.S.EPA (EPA, 1991b).

The emission data obtained from the PCBEIS program for

Table 3.4.1. Site Information by County for PCBEIS Program.

COUNTY	FIPS CODE	LATITUDE	LONGITUDE	TIME ZONE	BEGIN HR	END HR
SHELBY	47157	35.10	89.50	5	1	24
TIPTON	47167	35.30	89.45	5	1	24
CRITTENDEN	5035	35.15	90.15	5	1	24
DESOTO	28033	34.90	89.50	5	1	24

Table 3.4.2. Daily Maximum Temperature of Ten Highest Ozone Days.

DATE	OZONE (ppm)	MAXIMUM TEMPERATURE (^{0}F)
07/24/86	0.165	98
08/05/86	0.159	90
06/24/87	0.146	91
06/15/88	0.144	94
06/23/88	0.140	98
06/21/88	0.140	97
07/30/87	0.134	96
05/13/86	0.130	87
06/09/87	0.127	92
06/22/88	0.125	99

Table 3.4.3. Ranking of Days by Temperature.

DATE	OZONE (ppm)	MAXIMUM TEMPERATURE (^{0}F)	
06/22/88	0.125	99	
07/24/86	0.165	98	
06/23/88	0.140	98	
06/21/88	**0.140**	**97**	**4th Highest Selected**
07/30/87	0.134	96	
06/15/88	0.144	94	
06/09/87	0.127	92	
06/24/87	0.146	91	
08/05/86	0.159	90	
05/13/86	0.130	87	

Table 3.4.4. Meteorological Data of 06/21/88 used for PCBEIS Program.

TIME	SURFACE WIND (M/S)	AMBIENT TEMPERATURE (^{0}C)	RELATIVE HUMIDITY	OPAQUE SKY COVER
0100	2.60	25.00	0.642	0.0
0200	0.00	25.00	0.642	0.0
0300	2.60	25.00	0.642	0.0
0400	2.60	24.44	0.664	0.0
0500	2.60	23.89	0.711	0.1
0600	2.08	23.89	0.711	0.0
0700	0.00	27.22	0.604	0.0
0800	2.08	30.00	0.514	0.0
0900	1.56	32.78	0.409	0.0
1000	1.56	33.89	0.359	0.0
1100	3.12	39.37	0.349	0.0
1200	3.64	33.33	0.370	0.1
1300	2.60	36.11	0.328	0.2
1400	2.60	35.55	0.339	0.2
1500	2.60	35.55	0.327	0.2
1600	2.08	35.55	0.315	0.4
1700	2.60	34.44	0.336	0.4
1800	2.60	33.89	0.346	0.2
1900	2.08	36.87	0.409	0.1
2000	1.56	32.22	0.408	0.0
2100	2.08	29.44	0.513	0.0
2200	2.08	28.33	0.566	0.0
2300	1.56	27.78	0.585	0.0
2400	2.08	26.11	0.645	0.0

each county are shown in Table 3.4.5 through 3.4.8.

3.5 Speciation and Allocation

Ozone precursors are emitted from different types of sources including point, area, mobile and biogenic sources. Each source has a different temporal and spatial distribution with specific chemical composition. Therefore, it was necessary to speciate and distribute the emissions of each source separately.

3.5.1 Speciation of VOC

VOC emission data were speciated according to SCC code and distributed spatially and temporally. Zhou (1991) described the procedure to speciate the VOCs according to the SCC code. He developed a data file called VOCSPEC.DBF containing speciation coefficient of each of the ten VOC species according to the SCC code. This data file was used as a source of speciation data. This data file contained the speciation coefficients of olefins (OLEMOLE), paraffins (PARMOLE), Toluenes (TOLMOLE), Xylenes (XYLMOLE), Formaldehydes (FORMMOLE), Higher Aldehydes (ALD2MOLE), Ethane (ETHMOLE), Isoprene (ISOPMOLE), Ethanole (ETOHMOLE), and Methanol (MEOHMOLE).

For point sources, the grid number for each source was obtained from the exact location (longitude and latitude)

Table 3.4.5. Output of PCBEIS Program for Shelby County.

HR	CLD frac	RELH frac	WIND m/s	TMPSRF C	ISOPRENE kg/h	ISO FLUX kg/km2-h	ALPHA-P kg/h	APH FLUX kg/km2-h	MONOTERP kg/h	MON FLUX kg/km2-h	UNKNWN kg/h	UNK FLUX kg/km2-h
1	.00	.64	2.60	25.00	.00	.000	151.11	.075	156.77	.078	316.17	.158
2	.00	.64	.00	25.00	.00	.000	143.52	.072	147.86	.074	295.18	.147
3	.00	.64	2.60	25.00	.00	.000	151.11	.075	156.77	.078	316.17	.158
4	.00	.66	2.60	24.44	.00	.000	145.80	.073	150.71	.075	303.92	.152
5	.10	.71	2.60	23.89	.00	.000	140.75	.070	144.96	.072	292.25	.146
6	.00	.71	2.08	23.89	.73	.000	136.85	.068	140.48	.070	284.04	.142
7	.00	.60	.00	27.22	146.92	.073	182.46	.091	193.24	.096	387.45	.193
8	.00	.51	2.08	30.00	438.17	.218	232.73	.116	252.88	.126	508.66	.254
9	.00	.41	1.56	32.78	834.68	.416	289.12	.144	321.50	.160	646.14	.322
10	.00	.36	1.56	33.89	1062.62	.530	321.26	.160	361.42	.180	725.42	.362
11	.00	.35	3.12	39.37	1406.71	.701	447.66	.223	520.58	.260	1046.86	.522
12	.10	.37	3.64	33.33	1121.09	.559	325.07	.162	366.43	.183	733.80	.366
13	.20	.33	2.60	36.11	1336.61	.666	381.08	.190	436.46	.218	875.66	.437
14	.20	.34	2.60	35.55	1288.25	.642	367.68	.183	419.57	.209	841.80	.420
15	.20	.33	2.60	35.55	1232.90	.615	359.40	.179	408.95	.204	820.94	.409
16	.40	.31	2.08	35.55	1146.08	.571	344.72	.172	390.22	.195	784.97	.391
17	.40	.34	2.60	34.44	932.48	.465	311.30	.155	348.48	.174	701.56	.350
18	.20	.35	2.60	33.89	739.32	.369	287.83	.143	319.37	.159	644.43	.321
19	.10	.41	2.08	36.87	389.84	.194	328.99	.164	369.78	.184	748.45	.373
20	.00	.41	1.56	32.22	.81	.000	231.93	.116	251.35	.125	508.81	.254
21	.00	.51	2.08	29.44	.00	.000	200.02	.100	213.56	.106	430.90	.215
22	.00	.57	2.08	28.33	.00	.000	186.35	.093	197.51	.098	398.37	.199
23	.00	.58	1.56	27.78	.00	.000	178.78	.089	188.65	.094	379.86	.189
24	.00	.64	2.08	26.11	.00	.000	161.76	.081	168.97	.084	340.46	.170
Total Species				:	12077.21	6.021	6007.28	2.995	6626.50	3.303	13332.28	6.646

Table 3.4.6. Output of PCBEIS Program for Tipton County.

HR	CLD frac	RELH frac	WIND m/s	TMPSRF C	ISOPRENE kg/h	ISO FLUX kg/km2-h	ALPHA-P kg/h	APH FLUX kg/km2-h	MONOTERP kg/h	MON FLUX kg/km2-h	UNKNWN kg/h	UNK FLUX kg/km2-h
1	.00	.64	2.60	25.00	.00	.000	56.77	.051	58.82	.053	152.96	.137
2	.00	.64	.00	25.00	.00	.000	53.15	.047	54.60	.049	139.99	.125
3	.00	.64	2.60	25.00	.00	.000	56.77	.051	58.82	.053	152.96	.137
4	.00	.66	2.60	24.44	.00	.000	54.80	.049	56.56	.051	147.07	.131
5	.10	.71	2.60	23.89	.00	.000	52.91	.047	54.42	.049	141.43	.126
6	.00	.71	2.08	23.89	.43	.000	51.18	.046	52.45	.047	137.03	.122
7	.00	.60	.00	27.22	64.77	.058	69.05	.062	73.09	.065	188.21	.168
8	.00	.51	2.08	30.00	196.21	.175	89.12	.080	96.88	.086	250.18	.223
9	.00	.41	1.56	32.78	397.11	.355	111.33	.099	123.91	.111	319.26	.285
10	.00	.36	1.56	33.89	535.93	.479	124.25	.111	139.96	.125	359.94	.321
11	.00	.35	3.12	39.37	722.68	.645	172.12	.154	200.30	.179	516.84	.461
12	.10	.37	3.64	33.33	588.54	.525	126.66	.113	143.03	.128	366.05	.327
13	.20	.33	2.60	36.11	694.11	.620	147.89	.132	169.64	.151	435.60	.389
14	.20	.34	2.60	35.55	666.43	.595	142.74	.127	163.13	.146	418.89	.374
15	.20	.33	2.60	35.55	626.68	.560	138.92	.124	158.25	.141	407.05	.363
16	.40	.31	2.08	35.55	565.58	.505	132.41	.118	149.99	.134	387.22	.346
17	.40	.34	2.60	34.44	428.45	.383	118.99	.106	133.23	.119	344.67	.308
18	.20	.35	2.60	33.89	300.54	.268	109.23	.098	121.15	.108	314.84	.281
19	.10	.41	2.08	36.87	161.98	.145	123.29	.110	138.35	.124	361.97	.323
20	.00	.41	1.56	32.22	.39	.000	86.25	.077	93.24	.083	244.25	.218
21	.00	.51	2.08	29.44	.00	.000	74.89	.067	79.82	.071	207.83	.186
22	.00	.57	2.08	28.33	.00	.000	69.81	.062	73.87	.066	192.21	.172
23	.00	.58	1.56	27.78	.00	.000	66.88	.060	70.44	.063	182.85	.163
24	.00	.64	2.08	26.11	.00	.000	60.67	.054	63.28	.057	164.36	.147
Total Species				:	5949.83	5.312	2290.10	2.045	2527.21	2.256	6533.64	5.834

Table 3.4.7. Output of PCBEIS Program for Desoto County.

HR	CLD frac	RELH frac	WIND m/s	TMPSRF C	ISOPRENE kg/h	ISO FLUX kg/km2-h	ALPHA-P kg/h	APH FLUX kg/km2-h	MONOTERP kg/h	MON FLUX kg/km2-h	UNKNWN kg/h	UNK FLUX kg/km2-h
1	.00	.64	2.60	25.00	.00	.000	71.22	.056	73.14	.058	219.90	.173
2	.00	.64	.00	25.00	.00	.000	67.37	.053	68.70	.054	201.56	.159
3	.00	.64	2.60	25.00	.00	.000	71.22	.056	73.14	.058	219.90	.173
4	.00	.66	2.60	24.44	.00	.000	68.71	.054	70.30	.055	211.39	.167
5	.10	.71	2.60	23.89	.00	.000	66.31	.052	67.60	.053	203.22	.160
6	.00	.71	2.08	23.89	.43	.000	64.68	.051	65.73	.052	197.77	.156
7	.00	.60	.00	27.22	110.46	.087	85.43	.067	89.48	.071	268.14	.211
8	.00	.51	2.08	30.00	337.60	.266	108.97	.086	117.09	.092	355.07	.280
9	.00	.41	1.56	32.78	678.08	.535	135.15	.107	148.58	.117	451.95	.356
10	.00	.36	1.56	33.89	906.76	.715	149.85	.118	166.62	.131	507.70	.400
11	.00	.35	3.12	39.37	1220.23	.962	209.41	.165	240.77	.190	732.76	.578
12	.10	.37	3.64	33.33	986.65	.778	151.07	.119	168.25	.133	513.81	.405
13	.20	.33	2.60	36.11	1168.65	.921	177.64	.140	201.08	.159	614.01	.484
14	.20	.34	2.60	35.55	1122.21	.885	171.28	.135	193.15	.152	589.83	.465
15	.20	.33	2.60	35.55	1058.98	.835	167.64	.132	188.54	.149	574.69	.453
16	.40	.31	2.08	35.55	964.11	.760	161.31	.127	180.55	.142	549.31	.433
17	.40	.34	2.60	34.44	739.24	.583	145.92	.115	161.55	.127	490.39	.387
18	.20	.35	2.60	33.89	532.29	.420	135.36	.107	148.60	.117	450.29	.355
19	.10	.41	2.08	36.87	283.69	.224	155.53	.123	173.06	.136	521.78	.411
20	.00	.41	1.56	32.22	.44	.000	109.90	.087	117.95	.093	353.89	.279
21	.00	.51	2.08	29.44	.00	.000	94.39	.074	99.76	.079	299.43	.236
22	.00	.57	2.08	28.33	.00	.000	87.90	.069	92.22	.073	276.77	.218
23	.00	.58	1.56	27.78	.00	.000	84.26	.066	88.00	.069	263.23	.208
24	.00	.64	2.08	26.11	.00	.000	76.22	.060	78.81	.062	236.37	.186
Total Species				:	10109.82	7.970	2816.75	2.221	3072.66	2.422	9303.13	7.334

Table 3.4.8. Output of PCBEIS Program for Crittenden County.

HR	CLD frac	RELH frac	WIND m/s	TMPSRF C	ISOPRENE kg/h	ISO FLUX kg/km2-h	ALPHA-P kg/h	APH FLUX kg/km2-h	MONOTERP kg/h	MON FLUX kg/km2-h	UNKNWN kg/h	UNK FLUX kg/km2-h
1	.00	.64	2.60	25.00	.00	.000	24.41	.015	25.27	.016	39.78	.024
2	.00	.64	.00	25.00	.00	.000	23.30	.014	23.95	.015	37.98	.023
3	.00	.64	2.60	25.00	.00	.000	24.41	.015	25.27	.016	39.78	.024
4	.00	.66	2.60	24.44	.00	.000	23.55	.014	24.29	.015	38.23	.023
5	.10	.71	2.60	23.89	.00	.000	22.74	.014	23.36	.014	36.77	.023
6	.00	.71	2.08	23.89	.03	.000	22.10	.014	22.63	.014	35.76	.022
7	.00	.60	.00	27.22	21.14	.013	29.33	.018	30.98	.019	48.52	.030
8	.00	.51	2.08	30.00	64.20	.039	37.40	.023	40.55	.025	63.00	.039
9	.00	.41	1.56	32.78	113.31	.070	46.53	.029	51.65	.032	79.90	.049
10	.00	.36	1.56	33.89	132.59	.081	51.63	.032	57.98	.036	89.33	.055
11	.00	.35	3.12	39.37	170.11	.105	72.03	.044	83.61	.051	129.41	.080
12	.10	.37	3.64	33.33	130.80	.080	52.31	.032	58.89	.036	90.16	.055
13	.20	.33	2.60	36.11	158.87	.098	61.36	.038	70.19	.043	107.81	.066
14	.20	.34	2.60	35.55	154.16	.095	59.20	.036	67.47	.041	103.62	.064
15	.20	.33	2.60	35.55	151.92	.093	57.93	.036	65.82	.040	101.37	.062
16	.40	.31	2.08	35.55	147.72	.091	55.64	.034	62.90	.039	97.38	.060
17	.40	.34	2.60	34.44	132.75	.082	50.32	.031	56.24	.035	87.40	.054
18	.20	.35	2.60	33.89	120.69	.074	46.56	.029	51.58	.032	80.61	.050
19	.10	.41	2.08	36.87	64.67	.040	53.25	.033	59.72	.037	94.24	.058
20	.00	.41	1.56	32.22	.40	.000	37.51	.023	40.54	.025	64.36	.040
21	.00	.51	2.08	29.44	.00	.000	32.32	.020	34.43	.021	54.34	.033
22	.00	.57	2.08	28.33	.00	.000	30.12	.019	31.84	.020	50.23	.031
23	.00	.58	1.56	27.78	.00	.000	28.91	.018	30.43	.019	48.04	.030
24	.00	.64	2.08	26.11	.00	.000	26.14	.016	27.25	.017	42.94	.026
Total Species				:	1563.37	.960	969.02	.595	1066.81	.655	1660.96	1.020

of the plant, and the temporal distribution was done according to the operating hours of each point source. Table 3.1.1 in Section 3.1 shows the data for the point sources with VOC emissions in Memphis area in 1988. Speciation data for point source VOC emissions by county are shown in Table 3.5.1.1 through 3.5.1.4.

The UAM used the point source emission data through an input file called PTSOURCE. Development of this file for point source emissions is shown in Figure 3.5.1.1. One computer program called PTSPEC.FOR was developed to calculate the data for speciated and temporally distributed VOC emissions for each point source. There were 96 VOC sources in the modeling area. The UAM preprocessor program PTSRCE was used to generate the point source emissions file PTSOURCE for UAM. Again, the input file for this preprocessor program PTSRCE called INPTSR.OUT was developed as shown in Figure 3.5.1.1. The computer program called INPTSR.FOR was used to develop this input file. The program INPTSR.FOR used the longitude, latitude, flow rate, and temperature data and the hourly speciated VOC emissions datafrom the output of the program PTSPEC.FOR for each point source as input.

For area sources, countywide VOC emissions data were obtained for population based categories and source specific categories. The SCC code was available for each source type

Table 3.5.1.1. Speciation Coefficients for Point Sources for Shelby County.

SCC CODE	OLEMOLE	PARMOLE	TOLMOLE	XYLMOLE	FORMMOLE	ALD2MOLE	ETHMOLE	ISOPMOLE	ETOHMOLE	MEOHMOLE
10100801	.00007129	.00147100	.00000000	.00000000	.00000000	.00000000	.00417100	.00000000	.00000000	.00000000
30100902	.00006672	.00997200	.00107000	.00009443	.00000000	.00001176	.00065830	.00222800	.00046450	.00000000
30103311	.00000000	.03877000	.00054270	.00141300	.00000000	.00131600	.00000000	.00000000	.00000000	.00000000
30103499	.00000000	.05163000	.00000000	.00000000	.00000000	.00000000	.00000000	.00000000	.00000000	.00000000
30119013	.00276000	.01123000	.00000000	.00000000	.00000000	.00000000	.00000000	.01848000	.00000000	.00000000
30183001	.00222600	.01758000	.00063200	.00004792	.00032930	.00056060	.00321300	.00091140	.00003907	.00000000
30188801	.00222600	.01758000	.00063200	.00004792	.00032930	.00056060	.00321300	.00091140	.00003907	.00000000
30199998	.00222600	.01758000	.00063200	.00004792	.00032930	.00056060	.00321300	.00091140	.00003907	.00000000
30201901	.00000000	.00017620	.00000000	.00000000	.00000000	.00000000	.00000000	.00000000	.02161000	.00000000
30201902	.00000000	.00017620	.00000000	.00000000	.00000000	.00000000	.00000000	.00000000	.02161000	.00000000
30299998	.00000000	.00017620	.00000000	.00000000	.00000000	.00000000	.00000000	.00000000	.02161000	.00000000
30600401	.00044260	.04248000	.00004775	.00001790	.00295700	.00000000	.00000000	.00000000	.00000000	.00000000
30600701	.00000000	.06930000	.00000000	.00000000	.00000000	.00000000	.00000000	.00000000	.00000000	.00000000
30699998	.00044260	.04248000	.00004775	.00001790	.00295700	.00000000	.00000000	.00000000	.00000000	.00000000
30701399	.00580200	.04783000	.00000000	.00000000	.00000000	.00697600	.00000000	.00000000	.00000000	.00000000

Table 3.5.1.1. (Cont.)

SCC CODE	OLEMOLE	PARMOLE	TOLMOLE	XYLMOLE	FORMMOLE	ALD2MOLE	ETHMOLE	ISOPMOLE	ETOHMOLE	MEOHMOLE
30702098	.00580200	.04783000	.00000000	.00000000	.00000000	.00697600	.00000000	.00000000	.00000000	.00000000
30901199	.00191600	.02266000	.00050980	.00007699	.00082010	.00047820	.00228900	.00060860	.00024310	.00000000
30902099	.00003848	.01028000	.00102200	.00056830	.00014690	.00167800	.00000000	.00000000	.00000000	.00000000
30902501	.00191600	.02266000	.00050980	.00007699	.00082010	.00047820	.00228900	.00060860	.00024310	.00000000
39999995	.00191600	.02266000	.00050980	.00007699	.00082010	.00047820	.00228900	.00060860	.00024310	.00000000
40100399	.00009725	.01803000	.00096610	.00038750	.00000000	.00011120	.00160500	.00000000	.00000000	.00000000
40188801	.00006672	.00997200	.00107000	.00009443	.00000000	.00001176	.00065830	.00222800	.00046450	.00000000
40201301	.00001337	.03069000	.00416100	.00079530	.00000000	.00054820	.00000000	.00000000	.00000000	.00000000
40301009	.00061260	.06279000	.00007614	.00003467	.00027700	.00176900	.00000000	.00000000	.00000000	.00000000
40500301	.00000000	.05160000	.00070330	.00000000	.00000000	.00000000	.00000000	.00000000	.00000000	.00000000
40500401	.01211000	.01803000	.00000000	.00000000	.00725900	.00000000	.00071300	.00000000	.00000000	.00000000
40500501	.00000000	.04376000	.00056510	.00052150	.00000000	.00447400	.00000000	.00187300	.00000000	.00000000
40500513	.00000000	.04368000	.00141100	.00037680	.00000000	.00728100	.00000000	.00000000	.00000000	.00000000
40588801	.00003198	.04318000	.00001916	.00000000	.00000000	.00005689	.00000000	.00000000	.00000000	.00000000
40600132	.00000000	.05367000	.00015190	.00000000	.00000000	.00000000	.00000000	.00000000	.00000000	.00000000
40600242	.00086100	.02636000	.00257400	.00310600	.00000000	.00023920	.00000000	.00000000	.00000000	.00000000

Table 3.5.1.2. Speciation Coefficients for Point Sources for Crittenden County.

SCC CODE	OLEMOLE	PARMOLE	TOLMOLE	XYLMOLE	FORMMOLE	ALD2MOLE	ETHMOLE	ISOPMOLE	ETOHMOLE	MEOHMOLE
40300115	.00000000	.06930000	.00000000	.00000000	.00000000	.00000000	.00000000	.00000000	.00000000	.00000000
40301119	.00000000	.07042000	.00000000	.00000000	.00000000	.00000000	.00000000	.00000000	.00000000	.00000000
40400108	.00061260	.06279000	.00007614	.00003467	.00027700	.00176900	.00000000	.00000000	.00000000	.00000000
40400111	.00061260	.06279000	.00007614	.00003467	.00027700	.00176900	.00000000	.00000000	.00000000	.00000000
40600141	.00086100	.02636000	.00257400	.00310600	.00000000	.00023920	.00000000	.00000000	.00000000	.00000000

Table 3.5.1.3. Speciation Coefficients for Point Sources for Tipton County.

SCC CODE	OLEMOLE	PARMOLE	TOLMOLE	XYLMOLE	FORMMOLE	ALD2MOLE	ETHMOLE	ISOPMOLE	ETOHMOLE	MEOHMOLE
10200603	.00000000	.02022000	.00021710	.00000000	.00266400	.00000000	.00000000	.00000000	.00000000	.00000000
30500205	.00191000	.02552000	.00058710	.00032590	.00066200	.00119100	.00112000	.00043700	.00029520	.00005872
40200601	.00000000	.03064000	.00480900	.00034660	.00000000	.00085700	.00000000	.00000000	.00000000	.00000000
40200902	.00000000	.05165000	.00000000	.00000000	.00000000	.00000000	.00000000	.00000000	.00000000	.00000000
49099999	.00255000	.01132000	.00000000	.00096010	.00000000	.00130100	.00000000	.00000000	.00000000	.00000000

Table 3.5.1.4. Speciation Coefficients for Point Sources for Desoto County.

SCC CODE	OLEMOLE	PARMOLE	TOLMOLE	XYLMOLE	FORMMOLE	ALD2MOLE	ETHMOLE	ISOPMOLE	ETOHMOLE	MEOHMOLE
30101401	.00000000	.01073000	.00875300	.00000000	.00000000	.00000000	.00000000	.00000000	.00000000	.00000000
30101801	.00000000	.00000000	.00000000	.00000000	.00000000	.00000000	.01600000	.00000000	.00000000	.00000000
30500201	.00000000	.02022000	.00021710	.00000000	.00266400	.00000000	.00000000	.00000000	.00000000	.00000000
30501402	.00090720	.04321000	.00008465	.00054700	.00053280	.00000000	.00030660	.00000000	.00000000	.00000000
40201702	.00191000	.02552000	.00058710	.00032590	.00066200	.00119100	.00112000	.00043700	.00029520	.00005872
40500301	.00000000	.05160000	.00070330	.00000000	.00000000	.00000000	.00000000	.00000000	.00000000	.00000000

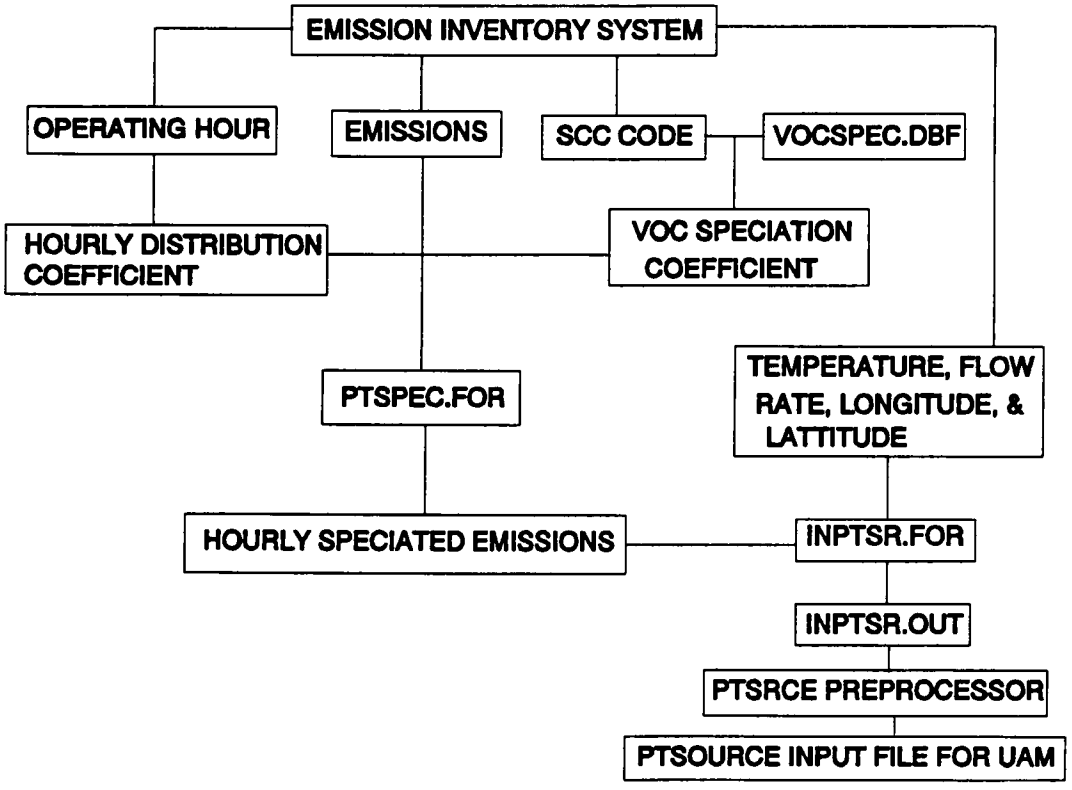


Figure 3.5.1.1. Flow Chart for Point Source VOC Emissions Speciation and Preparation of Input for UAM Preprocessor PTSRCE.

as shown in Table 3.2.1 in Section 3.2. Speciation data for area source VOC emissions are shown in Table 3.5.1.5. Area source population based emissions were spatially distributed by the gridded population data in each county as shown in Figure 3.2.1 and Table 3.2.4 in section 3.2. Temporal distribution was made considering an 8-hr emission (8 a.m. - 4 p.m.) for each source, except for railroads and forest fires, which were distributed over 24 hours. A computer program called ARVOCSPC.FOR was used to speciate the area source VOC emissions data and to distribute them spatially and temporally as shown in Figure 3.5.1.2.

For mobile sources, hourly VOC emissions were allocated into the categories of gasoline exhaust (SCC code : 1203), gasoline evaporative emissions (SCC code : 1204) and diesel exhaust (SCC code : 1186) as shown in Table 3.5.1.6. Each category was speciated according to its SCC code. Table 3.5.1.7 shows the speciation factors for the mobile source emissions. The speciated VOC data were calculated using the data in these two tables.

3.5.2 Speciation of NO_x

The NO_x emission data were initially expressed in terms of Nitrogen Dioxide (NO_2). The NO_x data were speciated into Nitric Oxide (NO) (90%) and NO_2 (10%). Temporal and spatial distributions were done in the same way as for VOCs.

Table 3.5.1.5. Data for Area Source VOC Emissions Speciation.

SCC CODE	OLEMOLE	PARMOLE	TOLMOLE	XYLMOLE	FORMMOLE	ALD2MOLE	ETHMOLE	ISOPMOLE	ETOHMOLE	MEOHMOLE
1190	0.00086100	0.02636000	0.00257400	0.00310600	0.00000000	0.00023920	0.00000000	0.00000000	0.00000000	0.00000000
1196	0.00006455	0.00905300	0.00008688	0.00009422	0.00000000	0.00000527	0.00000000	0.00000000	0.00000000	0.00000000
1195	0.00009725	0.01803000	0.00096610	0.00038750	0.00000000	0.00011120	0.00160500	0.00000000	0.00000000	0.00000000
9021	0.00004757	0.03644000	0.00077220	0.00057940	0.00000000	0.00120600	0.00000000	0.00000000	0.00072280	0.00103900
1194	0.00078640	0.03472000	0.00213800	0.00208400	0.00000000	0.00059410	0.00000000	0.00000000	0.00000000	0.00000000
1191	0.00003198	0.04318000	0.00001916	0.00000000	0.00000000	0.00005689	0.00000000	0.00000000	0.00000000	0.00000000
23	0.00000000	0.06284000	0.00000000	0.00000000	0.00000000	0.00000000	0.00071300	0.00000000	0.00000000	0.00000000
197	0.00000000	0.01895000	0.00000000	0.00000000	0.00019980	0.00000000	0.00000000	0.00000000	0.00801000	0.00000000
9022	0.00151400	0.01653000	0.00000326	0.00000283	0.00000000	0.00000000	0.00334000	0.00000000	0.00000000	0.00000000
0	0.00191000	0.02552000	0.00058710	0.00032590	0.00066200	0.00119100	0.00112000	0.00005872	0.00029520	0.00043700
1185	0.00126800	0.02906000	0.00144500	0.00135300	0.00000000	0.00000000	0.00000000	0.00000000	0.00000000	0.00000000
1	0.00000000	0.02765000	0.00000000	0.00000000	0.01399000	0.00000000	0.00000000	0.00000000	0.00000000	0.00000000
3	0.00000000	0.02022000	0.00021710	0.00000000	0.00266400	0.00000000	0.00000000	0.00000000	0.00000000	0.00000000
2	0.00000000	0.03515000	0.00000000	0.00000000	0.01622000	0.00000000	0.00000000	0.00000000	0.00000000	0.00000000
9002	0.00465900	0.00884100	0.00000109	0.00000177	0.00256500	0.00001791	0.00517300	0.00000000	0.00000000	0.00000000
121	0.00441700	0.04656000	0.00000000	0.00000000	0.00000000	0.00000000	0.00691600	0.00000000	0.00000000	0.00000000
8	0.00908800	0.01468000	0.00000000	0.00000000	0.00000000	0.00000000	0.01023000	0.00000000	0.00000000	0.00000000
1201	0.00152800	0.02685000	0.00169700	0.00013660	0.00286700	0.00133800	0.00079700	0.00000000	0.00000000	0.00000000
1099	0.00279300	0.01626000	0.00013070	0.00011220	0.00576300	0.00178200	0.00551900	0.00000000	0.00000000	0.00000000
307	0.00145900	0.03802000	0.00000000	0.00000000	0.00000000	0.00000000	0.00681300	0.00000000	0.00000000	0.00000000

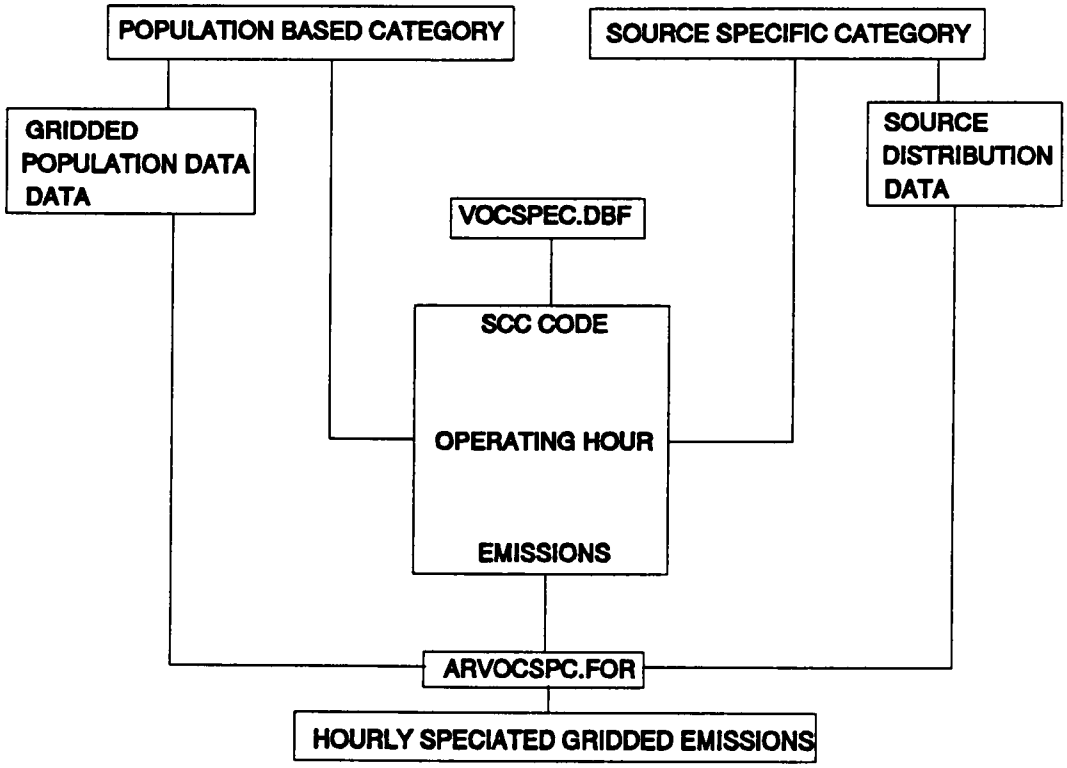


Figure 3.5.1.2. Flow Chart for Area Source VOC Emissions Speciation and Distribution.

Table 3.5.1.6. Table for Mass Ratio of VOC Emissions.

TIME HOUR	GASOLINE EXHAUST 1203	GASOLINE EVAPORATION 1204	DIESEL EXHAUST 1186
1	0.481000	0.497024	0.022457
2	0.489617	0.486893	0.022593
3	0.494951	0.481968	0.022730
4	0.498348	0.478551	0.022776
5	0.501758	0.475847	0.022823
6	0.492322	0.483909	0.022684
7	0.459032	0.517840	0.022190
8	0.455234	0.523151	0.021104
9	0.430902	0.548646	0.019188
10	0.405527	0.576977	0.017374
11	0.387798	0.595705	0.016194
12	0.377947	0.606705	0.015499
13	0.374659	0.609915	0.015205
14	0.375289	0.608249	0.015330
15	0.373334	0.610978	0.015143
16	0.377947	0.606705	0.015499
17	0.387260	0.596110	0.016170
18	0.403097	0.579246	0.017214
19	0.425121	0.554802	0.018771
20	0.436454	0.541918	0.019660
21	0.449636	0.530132	0.020599
22	0.456275	0.521371	0.021426
23	0.458397	0.520469	0.021802
24	0.459913	0.517442	0.022234

Table 3.5.1.7. Speciation Factors for Mobile Sources.

SCC CODE / SPECIES	1203	1204	1186
OLEFINE	0.0014920	0.0006930	0.001530
PARAFFINE	0.0325000	0.0539800	0.026850
TOLUENE	0.0009970	0.0010600	0.001700
XYLENE	0.0012590	0.0005780	0.000137
FORMALDEHYDE	0.0004990	0.0000000	0.002870
ALDEHEDYDE	0.0616200	0.0010400	0.001340
ETHANE	0.0029980	0.0000107	0.000797
ISOPRENE	0.0000248	0.0000000	0.000000

Table 3.1.2 shows the data for the point sources with NO_x emissions in the Memphis area in 1988. There were 26 NO_x sources in modeling the domain. Table 3.2.2 shows the data for the area sources with NO_x emissions in the Memphis area in 1988.

3.5.3 Speciation of Biogenic Emissions

Biogenic emissions data were obtained from the PCBEIS-program. The personal computer program PC-BEIS was used to estimate the hourly emissions of isoprene, alpha-pinene, monoterpene, and undefined hydrocarbons for the counties in the modeling domain. These VOCs were speciated (Causley, 1990) as shown in Table 3.5.3.1, where ISOP, OLE, PAR, ALD2 are the chemical species used in Carbon Bond-IV Mechanism and refer to Isoprene, Olefins, Paraffins, and higher Aldehydes.

3.6 Preparation of Inputs for Model

3.6.1 AIRQUALITY

The AIRQUALITY file was used to initialize the concentration of every species at the beginning of the simulation. The initial condition developed an air mass with the initial concentration of every species at the beginning of the simulation. For a one day simulation, the

Table 3.5.3.1. Speciation Factors for Biogenic Emissions

VOCs	ISOP	OLE	PAR	ALD2	Non Reactive
Isoprene	1.0	-	-	-	-
Monoterpene	-	0.5	6.0	1.5	-
Alpha-pinene	-	0.5	6.0	1.5	-
Unknown	-	0.5	8.5	-	0.5

Source : Causley, 1990.

prediction is highly sensitive to the initial concentration. The AIRQUALITY file contained a three-dimensional matrix of concentration data for each species over the modeling domain. The concentration of each species representing the initial condition was obtained from EPA's recommended default value (EPA, 1991a) except for the concentration of ozone. The monitoring station data were analyzed to obtain the initial concentration of ozone. Table 3.6.1.1 shows the concentration data (EPA, 1991a) for each species.

3.6.2 BOUNDARY

The BOUNDARY file defined the boundaries of the modeling domain and also hourly pollutant concentrations in each of the external boundary cell. The model used the boundary concentration data to represent the pollutant concentration passing over the boundary region into the modeling domain at each hour of the simulation time. The concentration data in the BOUNDARY file had more influence on the cells closed to the boundary. Figure 3.6.2.1 shows a 20 X 20 cell domain along with the boundaries. The concentration of each species representing the boundary condition was obtained from EPA's recommended default value (EPA, 1991a) except for the concentration of ozone. The monitoring station data were analyzed to obtain the boundary

Table 3.6.1.1. Initial Concentration of each Species used in the AIRQUALITY File.

SPECIES	SPECIES NAME	CONCENTRATION, ppm
NO	NITRIC OXIDE	00.0001
NO2	NITROGEN DIOXIDE	00.0020
O3	OZONE	00.08667
OLE	OLEFINES	00.0003
PAR	PARAFFINES	00.01494
TOL	TOLUENE	00.00018
XYL	XYLENE	00.0000975
FORM	FORMALDEHYDE	00.0021
ALD2	HIGHER ALDEHYDES	00.000555
ETH	ETHANE	00.00051
MEOH	METHANOL	00.100
ETOH	ETHANOL	00.100
ISOP	ISOPRENE	00.100
CO	CARBON MONOXIDE	00.350

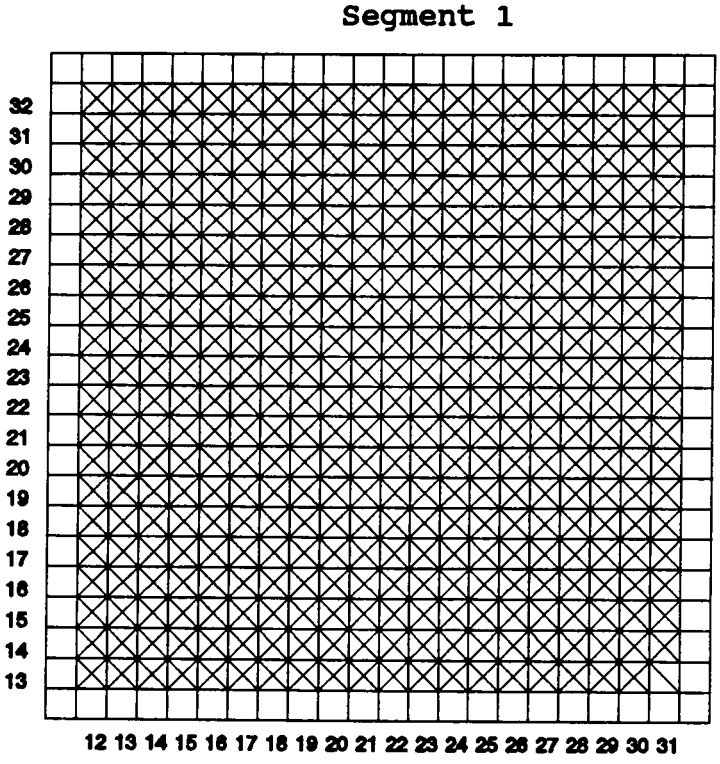


Figure 3.6.2.1. Definition of Boundaries of the Modeling Domain.

concentration of ozone. Table 3.6.2.1 shows the boundary concentration (EPA, 1991a) of the pollutants except for ozone for each of the vertical layers. The boundary concentration for species did not vary spatially in this analysis. The boundary ozone concentration was obtained by analyzing the actual monitoring station data. Table 3.6.2.2 shows the boundary ozone data obtained by analyzing the Braden monitoring station data on 06/15/88. The actual ozone concentration data of the Braden monitoring station on June 15, 1988 were analyzed in order to find the boundary ozone concentration. On that day, the predominant wind direction was from the south to the north. The Braden monitoring station whose location is shown in Figure 3.1 was not under the influence of any major emission sources due to the predominant wind direction and the observed ozone concentration was considered as the background ozone concentration.

3.6.3 DIFFBREAK

The DIFFBREAK file defined the diffusion break heights for the modeling domain at each hour of the simulation period. Diffusion break heights were used to define the heights of the cells in the vertical direction at each hour. The diffusion break heights are usually the same as the mixing heights. Hourly mixing height data were very

Table 3.6.2.1. Boundary Concentrations for Pollutants (ppm).

TIME	PAR
NO	0.0001
NO2	0.002
OLE	0.0003
PAR	0.01494
TOL	0.00018
XYL	0.0000975
FORM	0.0021
ALD2	0.000555
ETH	0.00051
ISOP	0.10
ETOH	0.10
MEOH	0.10
CO	0.35

Table 3.6.2.2. Boundary Concentrations for Ozone (ppb).

TIME	FIRST LAYER	SECOND LAYER	THIRD LAYER
0000	40.00	86.67	86.67
0001	40.00	87.50	87.50
0002	40.00	88.33	88.33
0003	40.00	89.16	89.16
0004	40.00	90.00	90.00
0005	40.00	90.83	90.83
0006	40.00	91.66	91.66
0007	40.00	92.50	92.50
0008	40.00	93.33	93.33
0009	50.00	94.16	94.16
0010	60.00	95.00	95.00
0011	70.00	95.83	95.83
0012	80.00	96.66	96.66
0013	90.00	97.50	97.50
0014	100.00	100.00	98.33
0015	100.00	100.00	99.16
0016	100.00	100.00	100.00
0017	100.00	100.00	99.16
0018	100.00	100.00	98.33
0019	100.00	100.00	97.50
0020	85.00	96.66	96.66
0021	70.00	95.83	95.83
0022	55.00	95.00	95.00
0023	40.00	94.16	94.16

important in order to predict the ozone concentration as the dilution of ozone precursors in the atmosphere depends on the mixing height. The mixing height started growing in the morning and reached a maximum in the afternoon because of the increasing solar heating of the ground level. The morning and the afternoon mixing heights for the Memphis area were 400 m and 1500 m respectively based on the mean annual morning and afternoon mixing height data for the Memphis area (Holzworth, 1972). Table 3.6.3.1 and Figure 3.6.3.1 show the mixing height data.

3.6.4 EMISSIONS

The EMISSIONS file defined the total ground level gridded emissions from different source types including area, mobile, and biogenic sources. The speciation and distribution of hourly emissions from each source are described in section 3.2 through 3.5. One computer program called COMBINE.FOR was developed to combine the emissions of each source in EMISSIONS file.

3.6.5 METSCALARS

The METSCALARS file defines time-varying meteorological data for the modeling domain. These data do not vary spatially. Different data needed are as follows :

- temperature gradient below the diffusion break

Table 3.6.3.1. Mixing Height Data Used for Modeling.

TIME	MIXING HEIGHT (m)
0000	400
0001	400
0002	400
0003	400
0004	400
0005	400
0006	400
0007	400
0008	400
0009	416
0010	633
0011	850
0012	1067
0013	1283
0014	1500
0015	1500
0016	1500
0017	1500
0018	1500
0019	1000
0020	800
0021	600
0022	400
0023	400

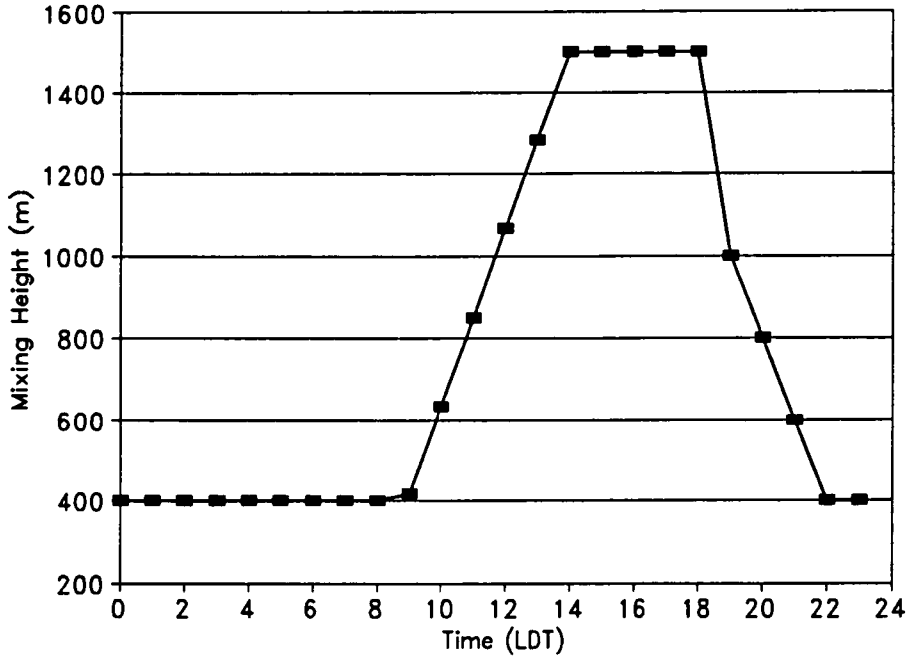


Figure 3.6.3.1. Mixing Height Profile Used for Modeling.

(TGRADBELOW)

- temperature gradient above the diffusion break (TGRADABOVE)
- exposure class (EXPCLASS)
- radiation factor (RADFACTOR)
- average concentration of water (CONCWATER)
- atmospheric pressure (ATMOSPRESS)

Table 3.6.5.1 shows the meteorological data used for modeling. Temperature gradient below the diffusion break was calculated based on the solar intensity, cloud cover and wind speed using the method discusses by Zannetti, 1990. Temperature above the diffusion break was chosen by assuming the stability class of 'F' (Stable) for above the diffusion break. The average atmospheric pressure and the average concentration of water were obtained by averaging the data for ten highest ozone days.

3.6.6 PTSOURCE

The PTSOURCE file defined the location of the point sources in the modeling domain and calculated and allocated the time-varying emission data from point sources into specific vertical cells. There were 120 point sources for VOC and NO_x emissions as discussed in section 3.5.1. The UAM preprocessor PTSRCE was used to develop PTSOURCE file, which calculated plume rise from the given flow rate and

Table 3.6.5.1. Meteorological Data Used for Modeling.

TIME LDT	RAD. FACTOR MIN^{-1}	ATMOS PRESS ATM	WATER CONC. PPM	TEMP GRAD BELOW °K/M	TEMP GRAD ABOVE °K/M	EXPO-SURE CLASS
0100	0.00	0.99	20723	0.0275	0.005	-2.0
0200	0.00	0.99	21071	0.0275	0.005	-2.0
0300	0.00	0.99	21155	0.0275	0.005	-2.0
0400	0.00	0.99	19574	0.0275	0.005	-2.0
0500	0.00	0.99	21406	0.0275	0.005	-2.0
0600	0.03896	0.99	21985	-0.01	0.005	1.0
0700	0.2016	0.99	22655	-0.016	0.005	1.0
0800	0.3545	0.99	22920	-0.018	0.005	1.0
0900	0.4535	0.99	22354	-0.018	0.005	2.0
1000	0.5180	0.99	22338	-0.018	0.005	2.0
1100	0.5570	0.99	21399	-0.019	0.005	3.0
1200	0.5772	0.99	20786	-0.018	0.005	3.0
1300	0.5815	0.99	20814	-0.019	0.005	3.0
1400	0.5701	0.99	20708	-0.018	0.005	3.0
1500	0.5422	0.99	20151	-0.019	0.005	2.0
1600	0.4927	0.99	19571	-0.018	0.005	2.0
1700	0.4140	0.99	20696	-0.018	0.005	2.0
1800	0.2944	0.99	20548	-0.016	0.005	1.0
1900	0.1225	0.99	21477	-0.01	0.005	1.0
2000	0.00	0.99	21491	-0.01	0.005	-2.0
2100	0.00	0.99	22203	0.005	0.005	-2.0
2200	0.00	0.99	22498	0.005	0.005	-2.0
2300	0.00	0.99	22159	0.005	0.005	-2.0
2400	0.00	0.99	22264	0.005	0.005	-2.0

temperature data for each source and allocated the emissions into specific vertical cells.

3.6.7 REGIONTOP

The REGIONTOP file defined the region top heights for the modeling domain. The regiontop height is defined as the height of the the top of the modeling domain above the ground. For Memphis modeling, the regiontop height was chosen to be 3000 m and kept constant during the total period of the simulation.

3.6.8 TEMPERATUR

The TEMPERATUR file defined the temperature data for the modeling domain. The hourly averages of temperatures for the 10 highest ozone days were used in the modeling. Table 3.6.8.1 gives the temperature data for the ten highest ozone violation days in the Memphis area. The hourly average temperatures were calculated from this table. Figure 3.6.8.1 shows the average temperature profile used in modeling. The maximum average temperature was 93.6 ^{o}F which occurred at 1400 hrs.

3.6.9 TERRAIN

The TERRAIN file defined the surface roughness and vegetation factors for the modeling domain to calculate the

Table 3.6.8.1. Temperature Data Associated with the Highest Ozone Violation.

TIME	TEMPERATURE (^{o}F) OZONE CONCENTRATION (ppb)										
	130	165	159	127	146	134	144	140	125	140	AVG.
0100	69	79	72	74	72	78	72	81	78	77	75.2
0200	68	79	70	74	71	78	71	80	77	77	74.5
0300	67	80	69	74	72	79	72	80	79	77	74.9
0400	66	78	66	72	71	77	69	78	75	76	72.8
0500	65	77	66	72	71	77	70	77	76	75	72.6
0600	66	78	66	71	72	78	71	78	77	75	73.2
0700	72	82	71	77	77	83	78	80	80	81	78.1
0800	77	86	76	81	81	86	82	84	83	86	82.2
0900	79	90	82	84	84	88	86	88	87	91	85.9
1000	84	93	84	85	86	91	90	93	91	93	89.0
1100	85	94	86	88	87	93	92	95	93	95	90.8
1200	85	95	88	90	89	95	92	97	96	92	91.9
1300	86	97	88	91	90	96	93	98	99	97	93.5
1400	87	98	90	91	91	92	94	98	99	96	93.6
1500	87	98	90	92	89	86	94	96	98	96	92.6
1600	86	97	90	91	91	94	94	98	97	96	93.4
1700	86	96	88	90	91	94	93	85	96	94	91.3
1800	84	95	87	88	85	93	91	92	95	93	90.3
1900	82	93	84	85	87	90	88	91	92	91	88.3
2000	76	92	81	85	86	88	86	88	89	90	86.1
2100	76	87	80	80	84	87	80	86	89	85	83.4
2200	76	86	77	78	83	85	78	84	83	83	81.3
2300	74	83	74	78	81	84	78	84	83	82	80.1
2400	73	83	74	76	79	83	75	83	82	79	78.7

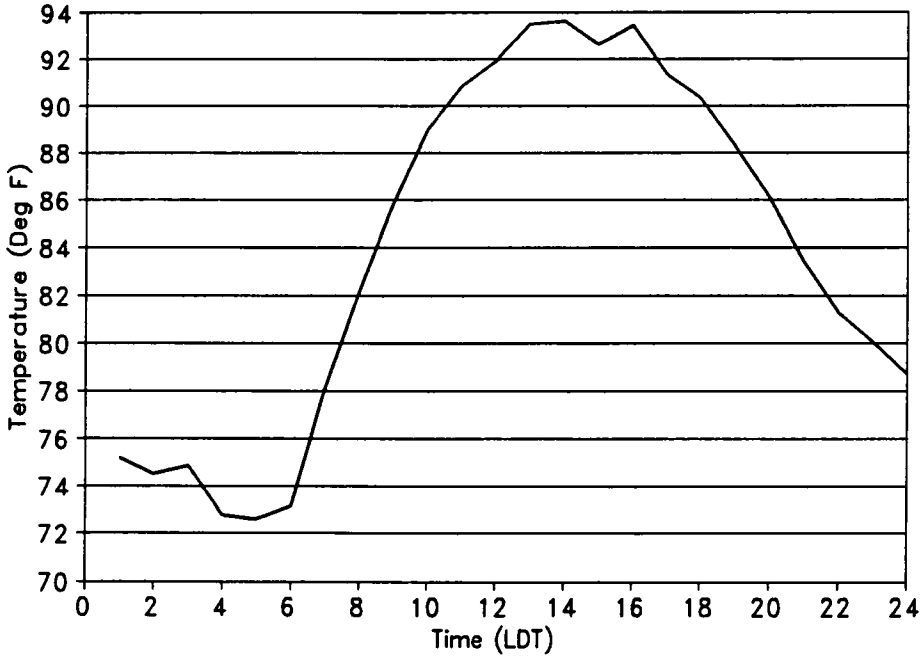


Figure 3.6.8.1. Average Temperature Profile Used in Modeling.

vertical diffusivity and surface deposition. The surface roughness factor was considered as 1.0 m and the vegetation factor was considered as 0.3 throughout the modeling domain.

3.6.10 TOPCONC

The TOPCONC file defined the pollutant concentration at the top of the region during the period of simulation. The model showed very small impact of high stratospheric ozone concentration. The concentration of each species representing the concentration at the top of the region was obtained from EPA's recommended value (EPA, 1991a) except for the concentration of ozone. The Braden monitoring station data for the day 06/15/88 as discussed in Section 3.6.2 were analyzed to obtain the concentration of ozone at the top of the region. The afternoon ozone concentration data were obtained for 3 days from 06/14/88 to 06/16/88. The ground level ozone concentration were considered as the same as the concentration at the top of the region because of the maximum vertical mixing in the afternoon. The ozone concentration for the top of the region were obtained by interpolating the 3 days ozone concentrations as mentioned above. Table 3.6.10.1 shows the temporal concentration of ozone at the top of the region. The concentration of other pollutants at the top of the region were the same as in the AIRQUALITY file.

Table 3.6.10.1. Concentration of Ozone at top of the Region.

TIME	OZONE CONCENTRATION (ppb)
0000	86.67
0001	87.50
0002	88.33
0003	89.16
0004	90.00
0005	90.83
0006	91.66
0007	92.50
0008	93.33
0009	94.16
0010	95.00
0011	95.83
0012	96.66
0013	97.50
0014	98.33
0015	99.16
0016	100.00
0017	99.16
0018	98.33
0019	97.50
0020	96.66
0021	95.83
0022	95.00
0023	94.16

3.6.11 WIND

The WIND file defined the horizontal wind vector values in the modeling domain and overall maximum and average values at the boundaries. For modeling, a constant wind speed of 3.5 km/hr was chosen with a calm period of 6 - 9 A.M.

4.0 ANALYSIS OF RESULTS

The CAAA (1990) requires a demonstration of attainment of the NAAQS of ozone through photochemical grid modeling. The UAM was run for a base case condition after which a sensitivity analyses was conducted in order to determine the effect of various emissions sources on ozone formation.

4.1 Base Case Evaluation

In order to evaluate the validity of the model, the model was run for a base case condition and compared to the actual observations at a monitoring station in the Memphis area. The base case was defined as the scenario which included emissions from all sources.

The model was run with the input data as described in sections 3.5 and 3.6. Figure 4.1.1 shows the predicted ozone concentration isopleth in ppm for the base case simulation over the modeling domain for the simulation period of 10:00 to 21:00. From 10:00 to 12:00, ozone formation was low and an ozone depletion was observed in the immediate vicinity downwind of the TVA power plant which was located in grid (18,19). At 14:00, an ozone plume having a maximum concentration of 130 ppb was observed in the vicinity of the north-east corner of the modeling domain which was downwind of the urban area; ozone depletion was observed in immediately downwind of the power plant. From 16:00 to

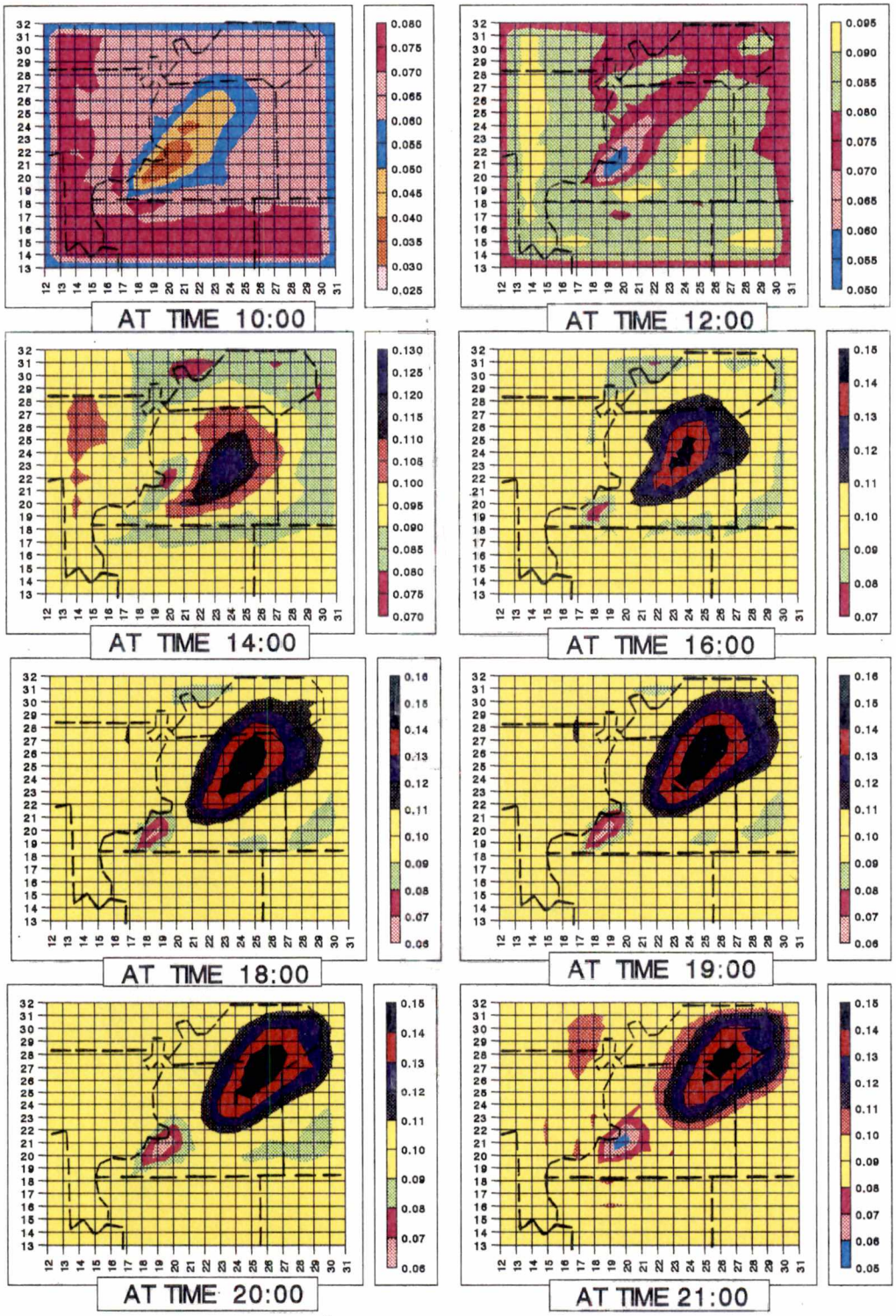


Figure 4.1.1. Ozone Concentration Isopleth: Base Case Simulation.

21:00, the urban plume containing high ozone concentration, was moving slowly to the north-east and was growing in size, and the ozone depletion was still observed in the immediate downwind direction from the power plant.

A comparison of the actual observed peak ozone at the Mudville monitoring station located in grid (25,26) northeast of the urban area and that predicted by the model is shown in the Figure 4.1.2. The highest observed ozone concentration profile in Figure 4.1.2 was obtained by plotting the highest ozone concentration at each hour for the ten highest ozone days. Similarly, the second highest ozone concentration profile was obtained by plotting the second highest ozone concentration at each hour for the ten highest ozone days. The ozone concentration profile from the model output shows a peak of 152.2 ppb at 19:00, whereas the observed peak was 165.0 ppb at 14:00 as shown in Figure 4.1.2. The model predicted the peak concentration within 7% of the observed peak. This is in agreement with previous UAM studies. Seinfield (1988) showed that the grid-based photochemical models generally predict the peak to within 15 - 20% of the measured value. He also stated that the measured ozone concentrations contain some uncertainty including measurement errors and the naturally random character of the atmosphere. Again, the model predicts volume average concentrations over the grid, whereas

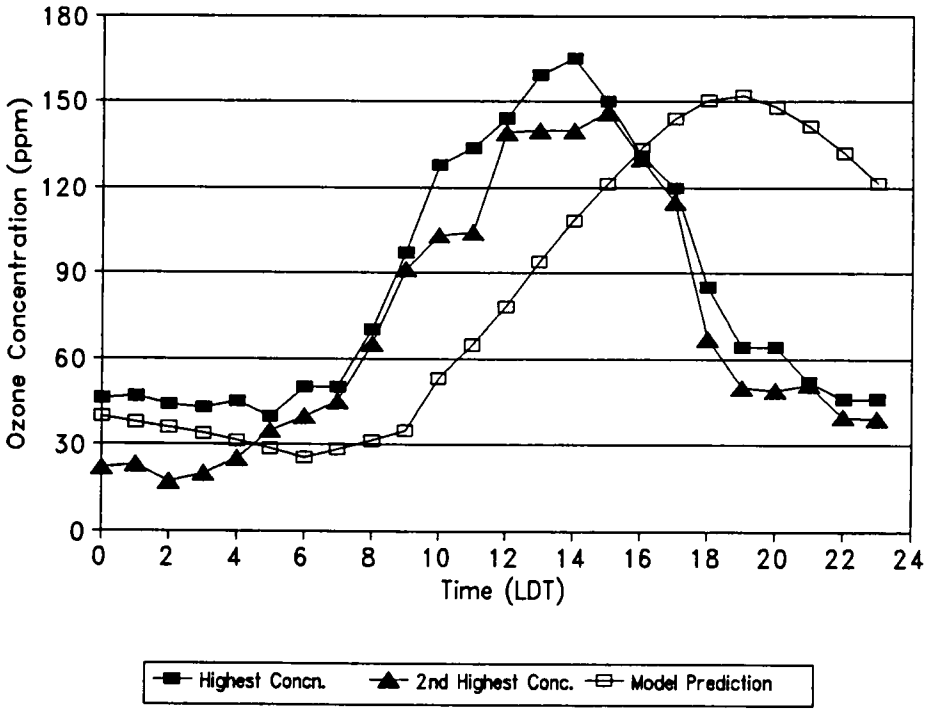


Figure 4.1.2. Comparison of Observed and Predicted Ozone Peak: Base Case Evaluation.

observations represent point measurements at the station. While the model predicted the peak concentration within an acceptable error, it should be noted that the model predicted peak occurred at 18:00 - 20:00 compared to the observed peaks which occurred in the 13:00 - 15:00 period. Preliminary evaluations of this discrepancies have not identified the reason for this shift. It should be noted that Zhou (1991) found a similar shift in the modeling of the Middle Tennessee area.

4.2 Sensitivity Analysis

In order to determine the effect of different categories of emissions on formation of ozone, the UAM was run with a variety of combinations of emission sources which are discussed in this section. The relative contribution to the ozone formation of various source categories is shown in Table 4.2.1.

4.2.1 Effect of a Large NO_x Point Source

The Memphis area has a large NO_x source (TVA power plant) within the modeling region in the grid (18,19). This source accounted for 28.6% of total NO_x emissions in the modeling domain.

To understand the contribution of the TVA power plant to the ozone formation in the overall modeling domain, a

Table 4.2.1. The Relative Contribution of Each Source and the Location.

Location (1)		Without Source Category			
		TVA Power Plant (2)	Mobile (3)	Area (4)	Biogenic (5)
Mudville at 19:00 (25,26) (2)	Base case (ppb)	152.2	152.2	152.2	152.2
	Without Source (ppb)	142.8	128.0	129.5	149.3
	% Reduction (%)	6.2 (9.4 ppb)	15.9 (24.2 ppb)	14.9 (22.7 ppb)	1.9 (2.9 ppb)
At Location of Peak (Without Source Category) (3)	Base Case (ppb)	152.2	152.2	152.2	152.2
	Without Source (ppb)	142.8	128.0	129.5	149.3
	% Reduction (%)	6.2 (9.4 ppb)	15.9 (24.2 ppb)	14.9 (22.7 ppb)	1.9 (2.9 ppb)
	Time (hr)	19:00	19.00	19.00	19.00
	Grid Number	25,26	25,26	25,26	25,26
At Location of Maximum Effect (Without Source Category) (4)	Base Case (ppb)	130.9	136.5	121.6	118.9
	Without Source (ppb)	118.8	105.3	96.5	107.5
	% Reduction (%)	9.2 (12.1 ppb)	22.85 (31.2 ppb)	20.64 (25.1 ppb)	9.6 (11.4ppb)
	Time (hr)	20:00	20:00	19:00	17:00
	Grid Number	27,30	27,27	29,26	22,24

modeling scenario was conducted in which the TVA power plant emissions was removed (Scenario PAMB). This Scenario was then compared to the base case Scenario to determine the relative impact of the TVA power plant on ozone formation. The results for Scenario PAMB are presented in column (2) of Table 4.2.1. For this Scenario, the peak ozone concentration was predicted to occur at the Mudville monitoring station (25,26) at 19:00 as shown in row (3) of Table 4.2.1. At this grid (25,26), the ozone concentration decreased from 152.2 ppb with the plant emissions down to 142.8 ppb without the plant emissions at 19:00. The predicted contribution of the plant was 6.2% (9.4 ppb) of the total ozone concentration. However, the maximum contribution of the power plant was predicted to occur in another grid (27,30) directly downwind from the Mudville monitoring station as shown in Table 4.2.1 (Column (2) and row (4)). At this grid (27,30), the predicted contribution of the plant was 9.2% (12.1 ppb) of the base case concentration of 130.9 ppb.

Figure 4.2.1.1 compares the ozone concentration profiles with and without the power plant emissions at grids (25,26) and (27,30). It was observed that at the Mudville monitoring station (25,26), the ozone concentration profile did not show any apparent change up to 6:00 with or without the power plant emissions, and after that the ozone concentration profile was lower (ozone scavenging) up to

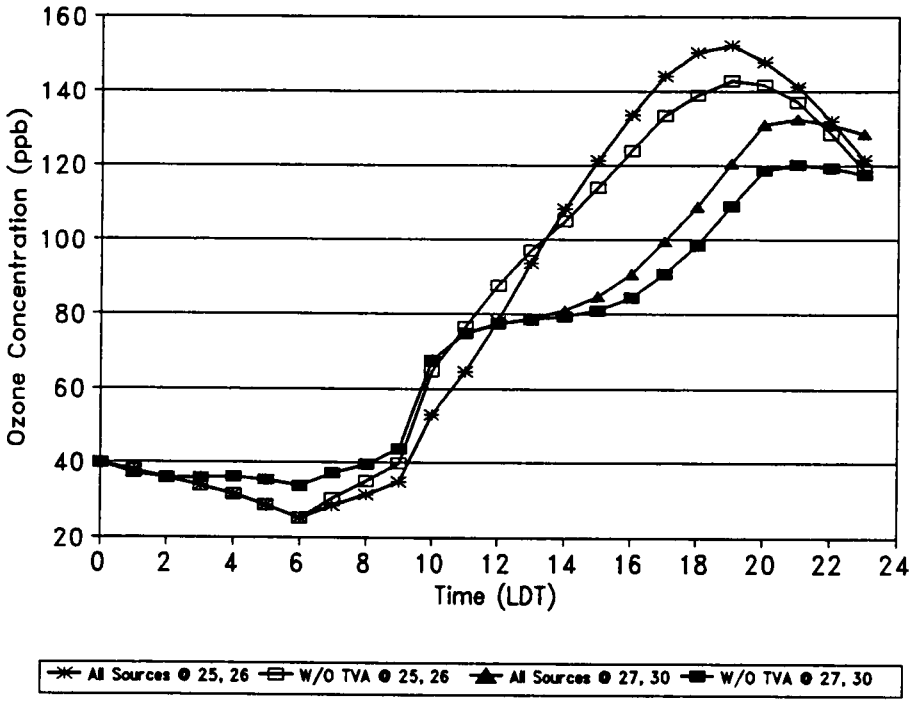


Figure 4.2.1.1. Comparison of Ozone Concentration Profiles at Grids (25,26) and (27,30): with and without the TVA Power Plant Emissions.

13:00 in the scenario containing all the sources as compared to the Scenario PAMB without the power plant emissions. After 13:00, an incremental increase in ozone concentration up to the end of the simulation period was observed at the Mudville monitoring station with the addition of the power plant emissions in the modeling domain. On the other hand, at the location of the maximum effect (27,30), the ozone concentration profile did not show any apparent change up to 13:00 with or without the power plant emissions. After that, there was an incremental increase in ozone concentration up to the end of the simulation period with the addition of the power plant.

This large NO_x point source resulted in ozone scavenging in the immediate downwind direction from the power plant as shown in Figure 4.1.1. Figure 4.2.1.2 shows the comparison of the predicted ozone profiles at the TVA power plant location (18,19) with or without the TVA power plant emissions. The maximum ozone concentration at grid 18,19 with the TVA power plant emissions was 65.9 ppb at 19:00, whereas the maximum ozone concentration without the power plant emissions was 93.6 ppb at 19:00. The presence of the power plant caused a reduction of ozone concentration by 27.7 ppb at 19:00.

Figure 4.2.1.3 shows the differential ozone concentration isopleth in ppm over the modeling domain for

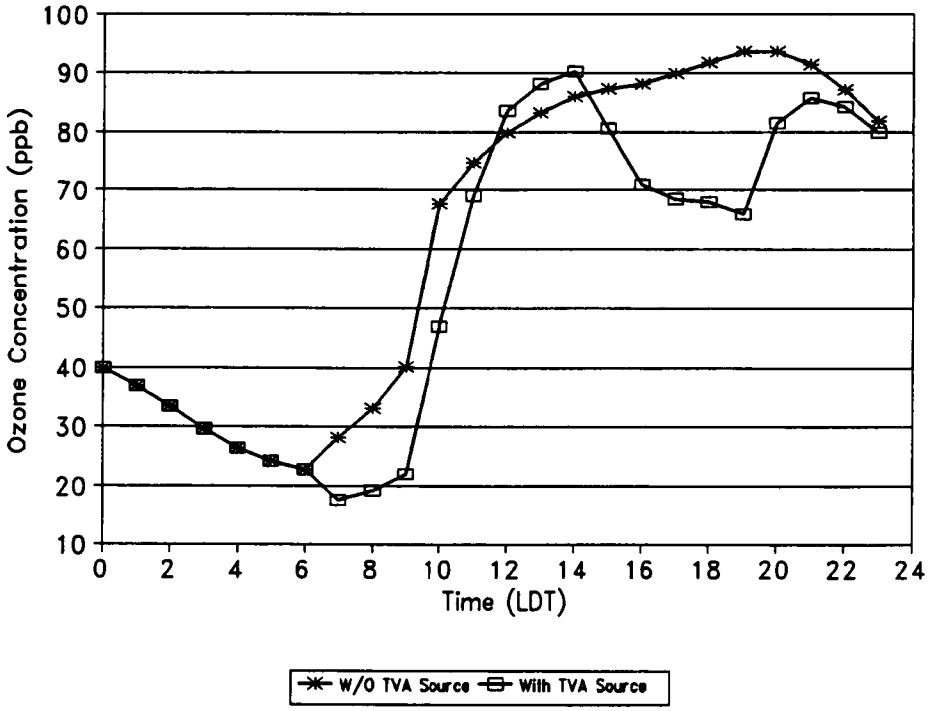


Figure 4.2.1.2. Comparison of Ozone Concentration Profiles at the TVA Power Plant Location (18,19) - with and without the TVA Plant Emissions.

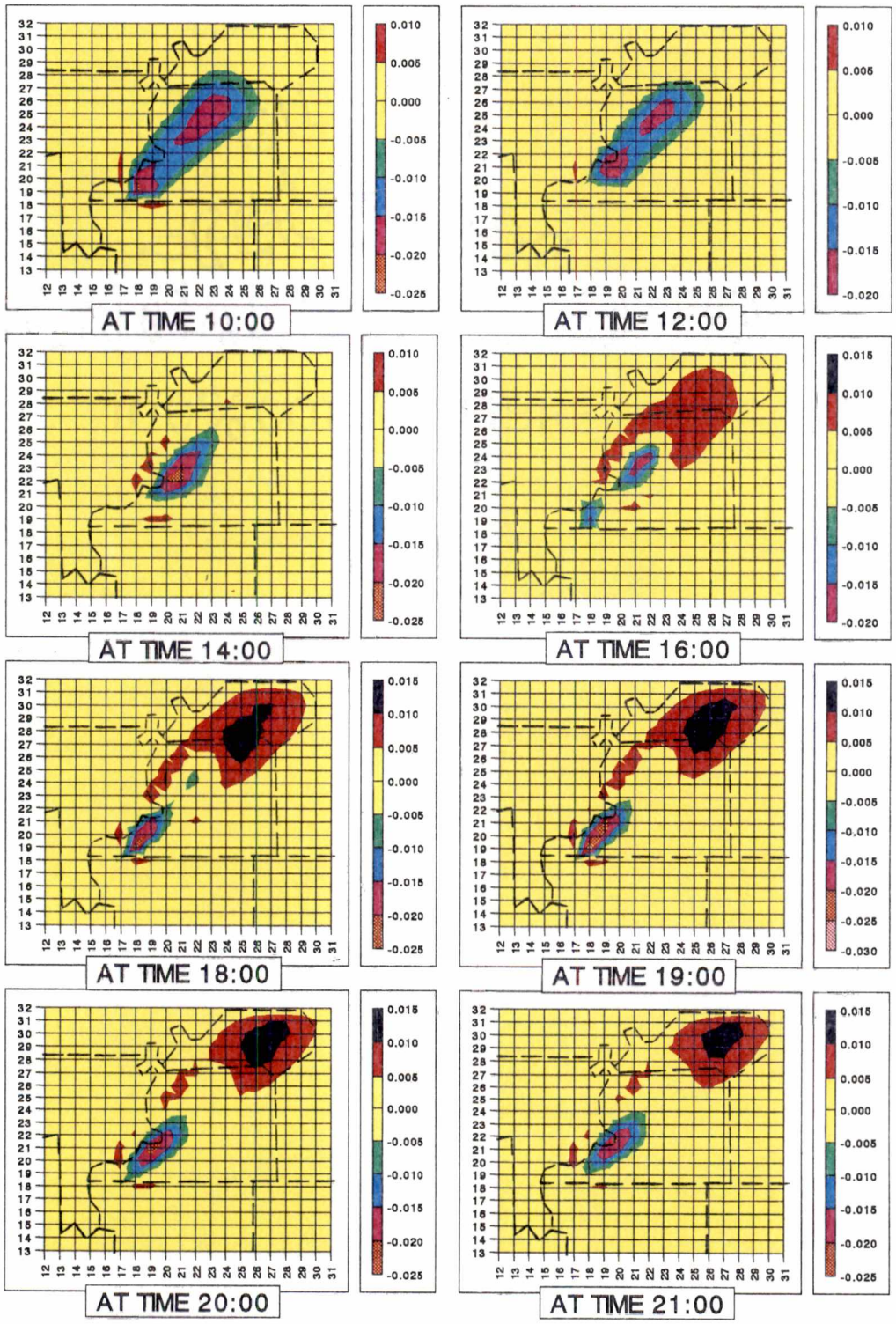


Figure 4.2.1.3. Differential Ozone Concentration Isopleth for TVA Power Plant Emissions (Scenario PTAMB - Scenario PAMB)

the simulation period of 10:00 to 21:00. This isopleth was obtained by taking the difference between the ozone concentrations obtained in the base case and those obtained in Scenario PAMB (without the power plant). No apparent ozone formation was observed in the modeling domain up to 12:00 as shown in Figure 4.2.1.3. At that time, a plume of ozone depletion extended from grid (18,19) up to grid (25,27) a distance of 53 km. The ozone concentration was reduced by 20 - 25 ppb in these grids. At 14:00, ozone formation was predicted in some scattered areas and the depleted ozone plume was only observed in the immediate downwind location of the TVA power plant. After 16:00, a significant amount of ozone formation was observed and an ozone plume having a positive differential ozone concentration of up to 12.1 ppb was observed in the downwind direction from the TVA power plant. The ozone plume was predicted to move toward the north-east corner of the modeling domain with time, indicating that the power plant contributed more to the far downwind direction in the late afternoon.

4.2.2 Effect of Biogenic Sources

Biogenic sources accounted for about 33% of the total VOC emissions in the modeling domain. To understand the contribution of the biogenic source emissions to the ozone

formation in the overall modeling domain, a modeling scenario was conducted in which biogenic source emissions were removed (Scenario PTAM). The result for this Scenario is presented in column (5) of Table 4.2.1. In this Scenario, the peak ozone concentration occurred at the Mudville monitoring station (25,26). At this grid (25,26), ozone concentrations decreased from a base case peak concentration of 152.2 ppb to 149.3 ppb at 19:00, which was a reduction of 1.9%. However, the maximum reduction in ozone concentration occurred in another grid (22,24) upwind from the Mudville monitoring station as shown in row (4) and column (5) of Table 4.2.1. In this grid (22,24) the ozone concentration was reduced from a base case value of 118.9 ppb to 107.5 ppb at 17:00, which is a reduction of 9.6%.

Figure 4.2.2.1 compares the ozone concentration profiles with and without biogenic source emissions at the grids (25,26) and (22,24). The ozone concentration profile at the Mudville monitoring station (25,26) did not show any apparent change, up to 11:00 with or without biogenic source emissions. After that, an incremental increase in ozone concentration was observed at the Mudville monitoring station with the addition of the biogenic source emissions in the modeling domain. On the other hand, at the location of maximum effect (22,24), the ozone concentration profile did not show any apparent change up to 10:00 with

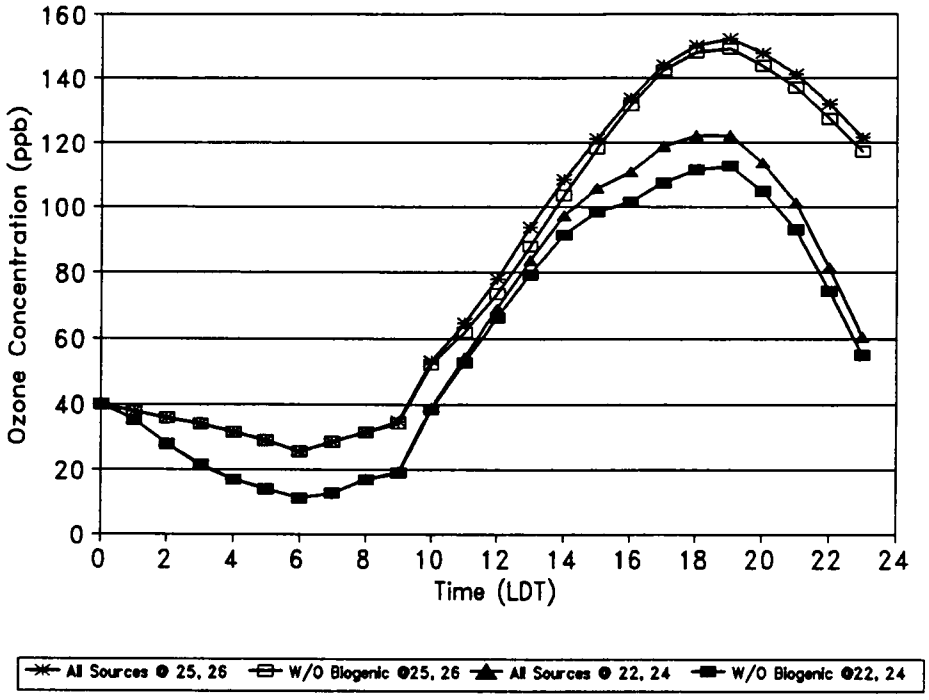


Figure 4.2.2.1. Comparison of Ozone Concentration Profiles at Grids (25,26) and (22,24): with and without the Biogenic Source Emissions.

and without the biogenic source emissions. After that, there was an incremental increase in ozone concentration up to the end of the simulation period with the addition of the biogenic source emissions.

Figure 4.2.2.2 shows the differential ozone concentration isopleth for biogenic emissions over the modeling domain for the simulation period of 10:00 to 21:00. No apparent ozone formation was predicted in the modeling domain up to 10:00 as shown in Figure 4.2.2.2. After 12:00, ozone formation was predicted and an ozone formation of a maximum of 11 ppb was predicted at 18:00. After 18:00, the differential ozone concentration started decreasing up to the end of the simulation period. The biogenic source VOCs were emitted mostly during the daytime, which was the reason for the reduction in ozone formation in the late afternoon.

4.2.3 Effect of Area Sources

The area source emissions accounted for about 20% of total VOC and 32% of the total NO_x emissions in the modeling domain. To understand the contribution of the area source emissions to the ozone formation in the overall modeling domain, a modeling scenario was conducted in which area source was removed (Scenario PTMB). The result for this Scenario is presented in column (4) of Table 4.2.1. In this

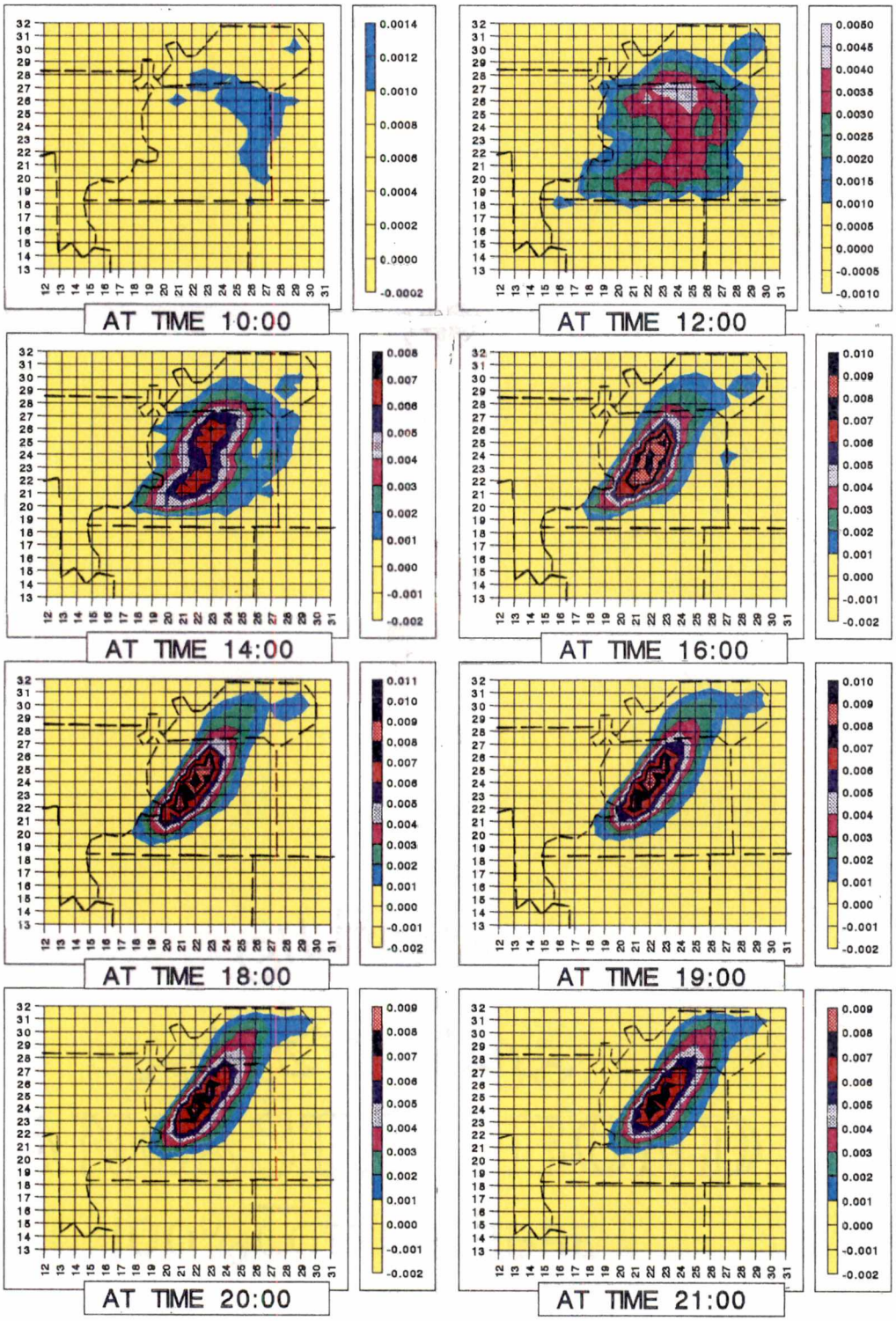


Figure 4.2.2.2. Differential Ozone Concentration Isopleth for Biogenic Source Emissions (Scenario PTAMB - Scenario PTAM)

Scenario, the peak ozone concentration again occurred at the Mudville monitoring station (25,26). At this grid (25,26), ozone concentrations decreased from the base case peak concentration of 152.2 ppb to 129.5 ppb at 19:00, which was a reduction of 14.9% (22.7 ppb). However, the maximum reduction in the ozone concentration occurred in another grid (29,26) east of the Mudville monitoring station as shown in column (4) and row (4) of Table 4.2.1. In this grid (29,26) the ozone concentration reduced from a base case value of 121.6 ppb to 96.5 ppb at 19:00, which is a reduction of 20.6% (25.1 ppb).

Figure 4.2.3.1 compares ozone concentration profiles with and without the area source emissions at grids (25,26) and (29,26). It was observed that at the Mudville monitoring station (25,26), the ozone concentration profile was lower (ozone scavenging) up to 13:00 in the Scenario containing all the sources (PTAMB) than the Scenario without the area source emissions (PTMB). After 13:00, an incremental increase in ozone concentration was observed at the Mudville monitoring station with the addition of the area source emissions in the modeling domain. On the other hand, at the location of maximum effect (29,26), the ozone concentration profile did not show any apparent change up to 10:00 with or without the area source emissions. After that, there was an incremental increase in ozone

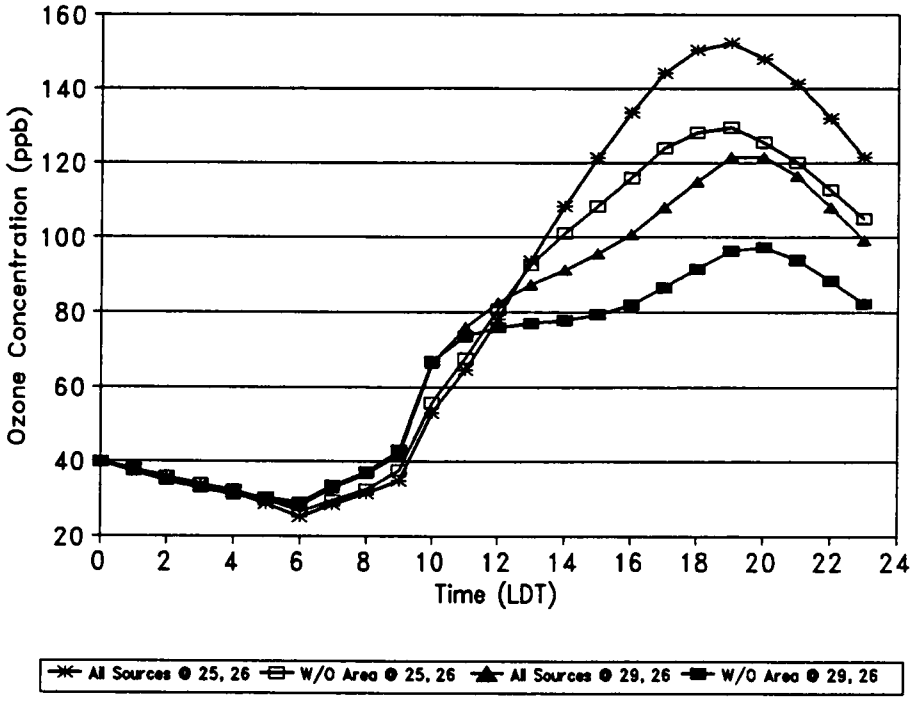


Figure 4.2.3.1. Comparison of Ozone Concentration Profiles at Grids (25,26) and (29,26): with and without the Area Source Emissions.

concentration up to the end of the simulation period with the addition of the area source emissions.

Figure 4.2.3.2 shows the differential ozone concentration isopleth for the area source emissions over the modeling domain for the simulation period of 10:00 to 21:00. There were no apparent ozone formation was observed in the modeling domain up to 10:00 as shown in Figure 4.2.3.2. At that time (10:00), a plume of ozone depletion was predicted in urban grids. The ozone concentration was reduced by up to 9.0 ppb in these grids. At 12:00, ozone formation was in some scattered areas downwind from the urban grids and the depleted plume up to 15 ppb was only observed in the close vicinity of the urban grids. After 14:00, a significant amount of ozone formation was observed and an ozone plume having a positive differential ozone concentration of up to 25.1 ppb was predicted in the downwind direction of the urban area. It was observed that the differential ozone concentration plume spread over a large area from 14:00 to 19:00. After that, the plume started reducing up to the end of the simulation period. The majority of the area source emissions were distributed over 8 hours from 9:00 to 16:00, which reduced the ozone formation after 19:00. As a result of that the differential ozone concentration plume reduced in size after 19:00 as shown in Figure 4.2.3.2.

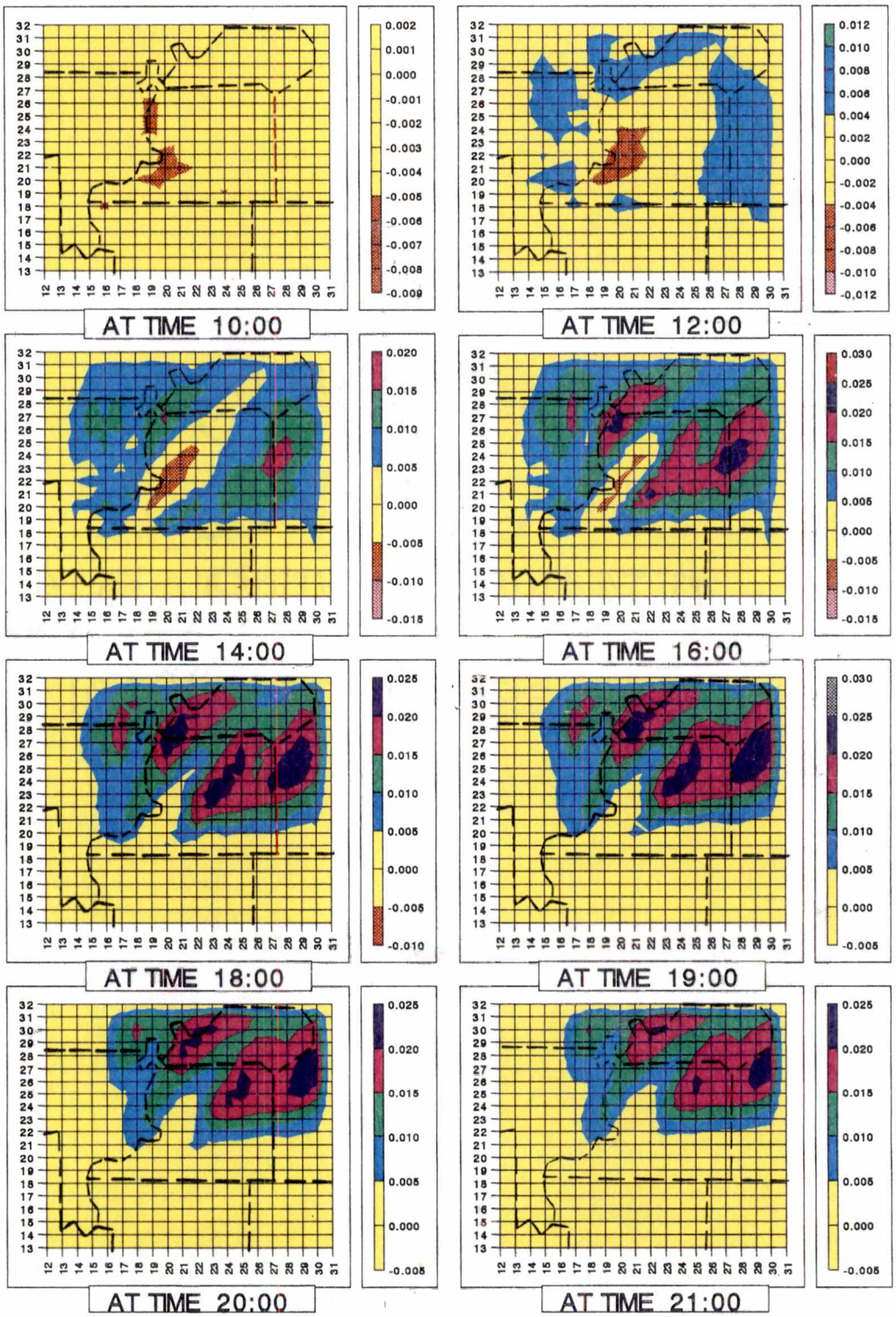


Figure 4.2.3.2. Differential Ozone Concentration Isopleth for Area Source Emissions (Scenario PTAMB - Scenario PTMB)

4.2.4 Effect of Mobile Sources

The Mobile source emissions accounted for about 36% of total VOC and 34% of the total NO_x emissions in the modeling domain.

To understand the contribution of the mobile source emissions to the ozone formation in the overall modeling domain, a modeling scenario was conducted in which mobile source emissions were removed (Scenario PTAB). The result for this scenario is presented in column (3) of Table 4.2.1. In this scenario, the peak ozone concentration occurred at the Mudville monitoring station (25,26). At this grid (25,26), ozone concentrations decreased from 152.2 ppb with the mobile source emissions down to 128.0 ppb without the mobile source emissions at 19:00. The contribution of the mobile source emissions was 15.9% (24.2 ppb) of the total ozone concentration. However, the maximum contribution of the mobile source emissions was predicted to occur in another grid (27,27) further downwind from the Mudville monitoring station as shown in column (3) and row (4) of Table 4.2.1. At this grid (27,27) predicted contribution of the mobile source emissions was 22.9% (31.2 ppb) of the base case concentration of 136.5 ppb.

Figure 4.2.4.1 compares the ozone concentration profiles with and without mobile source emissions at the grid (25,26) and (27,27). It was observed that at the

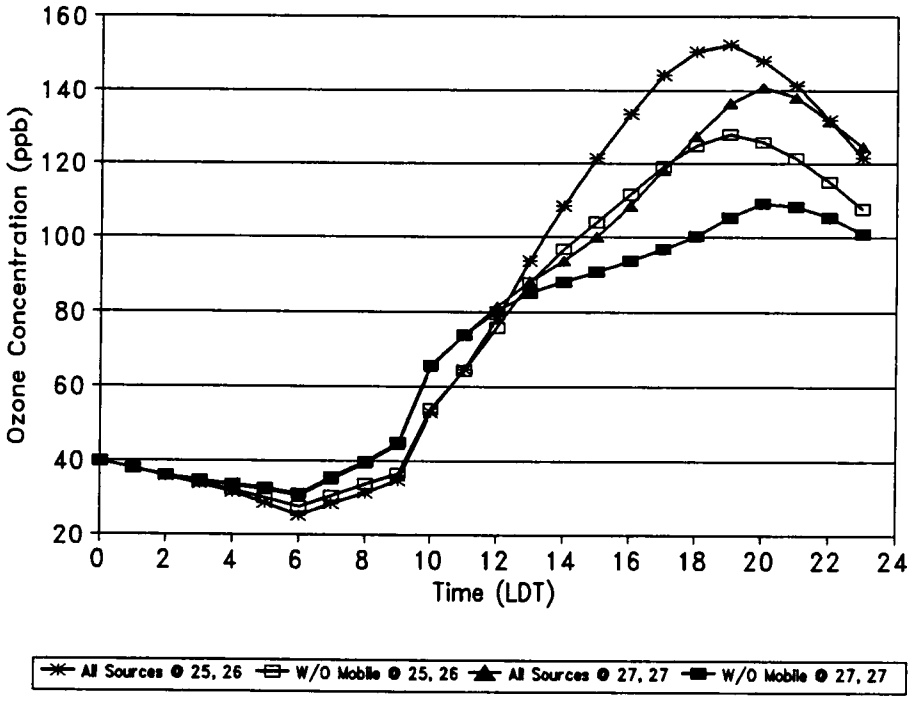


Figure 4.2.4.1. Comparison of Ozone Concentration Profiles at Grids (25,26) and (27,27): with and without the Mobile Source Emissions.

Mudville monitoring station (25,26), the ozone concentration profile was lower (ozone scavenging) up to 10:00 in the Scenario containing all sources (PTAMB) than the Scenario without mobile source emissions (PTAB). After 11:00, an incremental increase in ozone concentration was observed at the Mudville monitoring station up to the end of the simulation period with the addition of the mobile source in the modeling domain. On the other hand, at the location of the maximum effect (27,27), the ozone concentration profile did not show any apparent change up to 11:00 with or without the mobile source emissions. After that, there was an incremental increase in ozone concentration up to the end of the simulation period with the addition of the mobile source emissions.

Figure 4.2.4.2 shows the differential ozone concentration isopleth for mobile source emissions over the modeling domain for the simulation period of 10:00 to 21:00. No apparent ozone formation was observed in the modeling domain up to 10:00 as shown in the Figure 4.2.4.2. At that time (10:00), a plume of ozone depletion was predicted in the urban area. The ozone concentration was reduced by up to 16 ppb in the urban area of the modeling domain. At 12:00, the depleted plume reduced in size and a slight ozone formation was observed in the downwind direction from the urban area. After 14:00, a significant amount of ozone

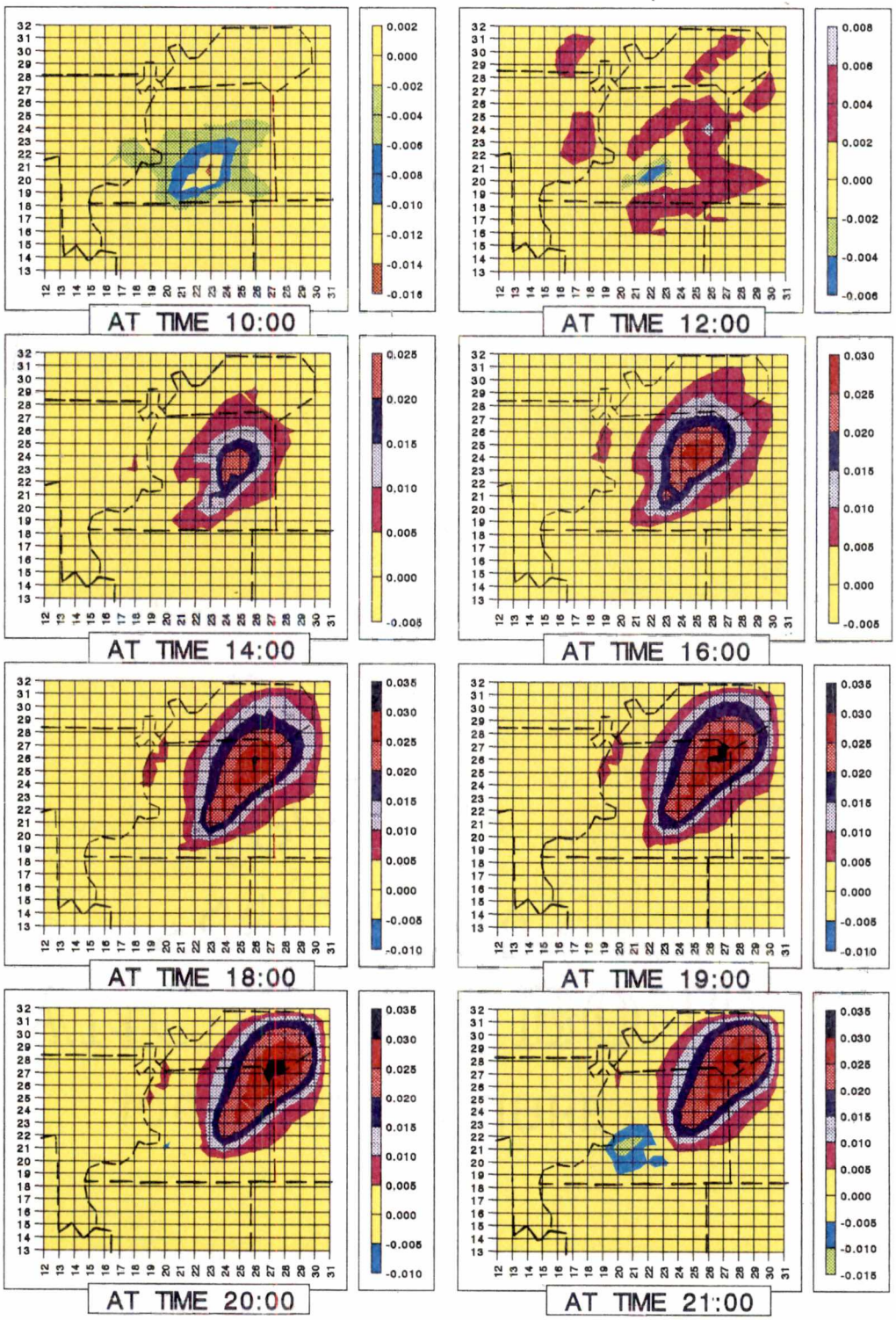


Figure 4.2.4.2. Differential Ozone Concentration Isopleth for Mobile Source Emissions (Scenario PTAMB - Scenario PTAB).

formation was observed and an ozone plume having a positive differential ozone concentration of up to of 31.2 ppb was observed in the downwind direction of the urban area. The ozone plume was predicted to move toward the north-east corner of the modeling domain with time, revealing the fact that the mobile sources contributed more to the far downwind direction in the late afternoon.

4.3 Discussion of Modeling Results

Mobile and area source emissions resulted in the greatest contribution to ozone formation as shown in Table 4.2.1. In other words, when mobile or area source emissions were added to the Scenarios containing all other sources except that source (mobile or area), the ozone formation was maximum. The NO_x emissions from mobile and area sources were of the same magnitude, and contributed to comparable amounts of ozone formation (14-16% at the Mudville monitoring station, and 22-23% at the point of maximum contribution). Although VOC emissions from mobile sources were much larger than that from area sources, addition of the higher VOC emissions by adding the mobile source did not show any further significant incremental increase in ozone concentration as compared to the addition of the lower VOC emissions by adding the area sources, indicating that ozone formation was not VOC limited but NO_x limited.

The NO_x emissions from the TVA power plant were also of the same magnitude as mobile and area sources, however, the contribution of this source to ozone formation was not as high (6.2% at Mudville at ground level). The ground level impact of this source was not as high as that for mobile and/or area sources due to the stack height of this source (120 m). Further analysis showed that this source had a higher impact in the higher vertical cells above the ground as shown in Table 4.3.1. It was observed that the TVA power plant had a maximum impact on the ozone formation in the third vertical cell of the modeling domain, contributing 11.4% to the ozone formation.

The contribution of biogenic emissions (VOC only) to ozone formation was less significant (1.9% at Mudville monitoring station, and 9.6% at the location of maximum effect). Further analysis showed that the maximum effect of biogenic emissions occurred upwind from the Mudville monitoring station, whereas, in most of the cases, the maximum effect of other sources occurred downwind from the Mudville monitoring station.

As a result of concerns expressed by various research groups that the mobile source VOC emissions may be underpredicted by the current U.S. EPA MOBILE emission factors model, a series of modeling scenarios were conducted by varying the amount of VOC emissions from mobile

Table 4.3.1. The Relative Contribution of the TVA Power Plant to the Ozone Formation at Different Vertical Cells.

Location		Ist Vertical Cell	Second Vertical Cell	Third Vertical Cell
At Mudville at 19:00	Base case	152.2	156.6	115.3
	Without TVA Power Plant	142.8	148.0	102.2
	Ozone Formation (ppb)	9.4	8.6	13.1
At Location of Maximum Effect (Without TVA Power Plant)	Base Case	130.9	137.0	104.7
	W/O TVA Power Plant	118.8	124.5	84.1
	Ozone Formation (ppb)	12.1	12.5	20.6
	Time	20:00	20:00	17:00
	Grid No.	27,30	27,30	24,26

sources as presented in Table 4.3.2 to determine the relative impact of VOC emissions from mobile sources. In these cases NO_x emissions were held constant and VOC emissions were varied by 200%, 300% and 50%. Column (2) of Table 4.3.2 presents the base case results. Column (3) through (5) show the results with various percentages of VOC emissions of mobile source. No significant changes in peak ozone concentrations were observed by changing the VOC emissions of mobile source. A series of modeling scenarios were also conducted by varying the amount of NO_x emissions from mobile sources as presented in Table 4.3.3. In these cases VOC emissions were kept constant and NO_x emissions were reduced by 50% and then to zero from mobile sources. Column (2) of Table 4.3.3 presents the base case results. Column (3) and (4) show the results with a 50% reduction and zero NO_x emissions, respectively, for mobile sources. The peak ozone concentration changed significantly when NO_x emissions from mobile source were reduced to 50% (10.3 ppb reduction) and 0% (20.1 ppb reduction).

From the above discussion and based on the modeling results, it can be stated that the ozone formation was NO_x limited rather than VOC limited. The data in Tables 4.3.3 and 4.3.4 clearly show that significant ozone reductions occurred where VOC emissions were held constant and NO_x emissions were reduced, whereas no significant ozone

Table 4.3.2. Contribution of Mobile Source VOC Emissions to the Ozone Formation.

Row No./ Column No. (1)	Scenario Containing all Other Sources (PTAB) and the Mobile Source Containing				
	100% NO_x 100% VOC (2)	100% NO_x 200% VOC (3)	100% NO_x 300% VOC (4)	100% NO_x 50% VOC (5)	
Peak Ozone Concen-tration (ppb) (2)	152.2	151.1	148.8	147.4	149.1
Time (3)	19:00	19:00	19:00	19:00	19:00
Grid No. (4)	25,26	25,26	25,26	25,26	25,25

Table 4.3.3. Contribution of Mobile Source NO_x Emissions to the Ozone Formation.

Row No./ Column No. (1)	Scenario Containing all Other Sources (PTAB) and the Mobile Source Containing			
	100% NO_x 100% VOC (2)	50% NO 100% VOC (3)	Zero NO_x 100% VOC (4)	
Peak Ozone Concentration (ppb) (2)	152.2	141.9	128.8	132.1
Time (3)	19:00	19:00	19:00	19:00
Grid No. (4)	25,26	25,26	25,26	25,27

Table 4.3.4. Comparisons of the Contribution of Mobile Source VOC and NO_x Emissions to the Ozone Formation.

Row No./ Column No.	100% NO_x		50% NO_x		100% VOC		50% VOC	
	100% VOC	50% VOC	100% VOC	50% VOC	100% NO_x	50% NO_x	100% NO_x	50% NO_x
Peak Ozone Concentration (ppb)	152.2	147.4	141.9	142.2	152.2	141.9	147.4	142.2
Differential Ozone Concentration (ppb)	4.8		-0.3		10.3		5.2	
Time	19:00	19:00	19:00	19:00	19:00	19:00	19:00	19:00
Grid NO.	25,26	25,26	25,26	25,26	25,26	25,26	25,26	25,26

reductions were observed when NO_x emissions were held constant and mobile source VOC emissions were reduced or increased by a factor of two.

5.0 CONCLUSIONS

The effects of various emission sources including point sources, mobile sources, area sources, and biogenic sources on ozone formation were evaluated by using the Urban Airshed Model. The Model predicted the peak ozone concentration within 7% of the observed peak ozone concentration.

A series of modeling runs were conducted by removing the emissions from one source or source category at a time. It was observed that the emissions from mobile sources had the single largest influence on the ozone formation. The VOC and NO_x emissions from mobile source were also greater than any other category. The contribution of the mobile source category to the ozone formation was found to be highest in the downwind direction in the late afternoon.

The emissions from the area sources in the modeling domain were also significant. The major portion of the emissions from area sources were distributed over 8 hours from 9:00 to 16:00. As a result, the contribution of the area sources to the ozone formation tended to occur in early afternoon and were predicted to start decreasing in the late afternoon.

The TVA power plant was predicted to contribute up to 6.2% of the ozone formation at the Mudville monitoring station at the ground level, while it showed a much higher impact on the higher vertical cells. However, The TVA power

plant was predicted to cause ozone depletion up to 12:00 in the immediate downwind direction from the plant. This depletion was a result of the low NMHC/NO_x ratio in the plume and also due to the ozone scavenging by nitric oxide emitted from the plant. The contribution of the TVA power plant to the ozone formation was found to be the highest in the downwind direction in the late afternoon.

While the biogenic source category was a significant contributor to the VOC emissions, it did not show a significant contribution to the ozone formation. The emissions from the biogenic sources were distributed primarily during daytime. As a result, the contribution of biogenic sources to the ozone formation started reducing in the late afternoon.

The overall study showed that the ozone formation was more dependent on the NO_x emissions than VOC emissions. In other words, in the scenario where NO_x emissions were reduced, ozone reductions were higher than in the scenario where VOC emissions were reduced, with the conclusion that the ozone formation was NO_x limited for those modeling scenarios and meteorological conditions studied.

Additional studies should be conducted in the following areas:

- This study used the U.S. EPA recommended default boundary concentrations for all emissions species

except for ozone. The study did not consider any change in these concentration data with the change in emissions in the modeling domain. However, the background also contains emissions from various sources and may, therefore, also be affected if emissions are changed. This study only looked at the effect of the urban area point/area/mobile/biogenic source emissions. Further work needs to be done to determine if there are changes in the concentrations of the species in the boundary when changes in emissions in the modeling domain are made.

- There was a shift in time of occurrence of the peak between the observed and the predicted ozone concentration. Further analyses and studies should be done to determine the cause of this shift, and to adjust the data base or model to correct for this problem.
- This study considered two vertical cells below the diffusion break and one vertical cell above the diffusion break. The Memphis area has a large point source with an effective release height well above the ground. The simulation may be improved by increasing the vertical resolution, since higher vertical resolution allows more accurate representation of the vertical layers at which elevated source emissions

interact with ground level emissions (EPA, 1991a), resulting in a more accurate estimation of the effect of the emission sources.

LIST OF REFERENCES

LIST OF REFERENCES

[1] Anderson, G. E., S. R. Hayes, M. J. Hillyer, J. P. Killus, and P. V. Mundkur. (1977) Air Quality in the Denver Metropolitan Region: 1974-2000. Systems Applications, Inc. San Rafael, CA (EPA-908/1-77-002)

[2] Causley, M. C., J. L. Fieber, M. Jimnez, and L. Gardner. (1990) United States Environmental Protection Agency. User's Guide for the Urban Airshed Model : Volume IV : User's Manual for the Emissions Preprocessor System. EPA-450/4-90-007D. Research Triangle Park. NC. (NTIS No. : PB91-131250).

[3] Chamedies W. L., Lindsay R. W., Richardson J. L. and Kiang C. S. (1988) Role of Biogenic Hydrocarbon in Urban Photochemical Smog. Science 241, 1473-1475.

[4] Chock, D. P., and J. M. Heuss. (1987) Urban Ozone and its Precursors. Environmental Science & Technology 21, No. 12, 1146-1153.

[5] Cirillo, M. C., and A. A. Poli. (1992) An Intercomparison of Semiemperical Diffusion Models Under Low Wind Speed, Stable Conditions. Atmospheric Environment 26, No. 5, 765-774.

[6] Clarke, J. F., and J. K. S. Ching. (1983) Aircraft Observations of Regional Transport of Ozone in the Northeastern United States. Atmospheric Environment 17, No. 9, 1703-1712.

[7] Decker, C. E., L. A. Ripperman, J. J. B. Worth, F. M. Vukovich, W. D. Bach, J. B. Tommerdahl, F. Smith, and D. E. Wagnor. (1976) Formation and transport of oxidants along Gulf Coast and in Northern U. S. EPA-450/3-76-003. U. S. Environmental Protection Agency, Research Triangle Park. N.C.

[8] Dennis, R. L., M.W. Downtown, and R.S. Keil. (1983) Evaluation of Performance Measures for an Urban Photochemical Model. EPA-450/4-83-021. U. S. Environmental Protection Agency, Office of Air Quality Planning and Standards, Research Triangle Park, NC.

[9] Dennis, R. L., and M. W. Downtown. (1984) Evaluation of urban photochemical models for regulatory use. Atmospheric Environment 18, No. 10, 2055-2069.

[10] Dodge, M. C. (1977) Combined Use of Modeling Techniques

and Smog Chamber Data to Derive Ozone-precursor Relationships. In International Conference on Photochemical Oxidant Pollution and its Control: Proceedings, II, B. Dimitriades, Ed. EPA/600/3-77-001b. U. S. Environmental Protection Agency, Environmental Sciences Research Laboratory, Research Triangle Park, N.C..

[11] EPA. (1991) National Air Quality and Emission Trends Report, 1989. EPA-450/4-91-003. U.S. Environmental Protection Agency,Office of Air Quality Planning and Standards, Research Triangle Park, NC.

[12] EPA. (1991a) Guideline for Regulatory Application of the Urban Airshed Model. EPA-450/4-91-013.

[13] Environmental Protection Agency. (1991b) User's Guide to the Personal Computer Version of the Biogenic Emissions Inventory System (PC-BEIS). EPA-450/4-91-017.

[14] Hess, G.D., F. Carnovale, M. E. Cope, and G. M. Johnson. (1992) The Evaluation of Some Photochemical Smog Reaction Mechanism-I. Temperature and Initial Composition Effects. Atmospheric Environment 26A, No. 4, 625-641.

[15] Hilzworth, G. C. (1972) Mixing Heights, Wind Speeds, and Potential for Urban Air Pollution Throughout the Contiguous United States. Environmental Protection Agency, Research Triangle Park, N.C., Publication Number AP-101.

[16] Japar, S. M., T. J. Wallington, S. J. Rudy, and T. Y. Chang. (1991) Ozone-Forming Potential of a Series of Oxygenated Organic Compounds. Environmental Science & Technology 25, No. 3, 415-420.

[17] Korsog, P. E., and G. T. Wolff. (1991) An Examination of Urban Ozone Trends in the Northeastern U.S. (1973-1983) Using a Robust Statistical Method. Environmental Science Department, General Motors Research Laboratories, Warren, MI - 48090, U.S.A. 0957-1272/91, 1991 Pergaman Press Pic.

[18] Lamb, B., A. Guenther, D. Gay and H. Westberg. (1987) A National Inventory of Biogenic Hydrocarbon Emissions. Atmospheric Environment 21, No. 8, 1695-1705.

[19] McKeen, S. A., E. Y. Hsie, R. Tallamraju, and S. C. Liu. (1991) A Regional Model Study of the Ozone Budget

in the Eastern United States. J. Geophy. Res. 96, 10809-10846.

[20] Paul J. A. (1991) Urban Air Quality : The Problem. EPA Journal 17, No. 1, 24-26.

[21] Roselle, J., S., T. E. Pierce, and K. L. Schere. (1991) The Sensitivity of Regional Ozone Modeling to Biogenic Hydrocarbons. J. Geophysics Res. 96 (D4), 7371-7394.

[22] Qin, H. (1992) The Role of Biogenic and Anhropogenic Air Pollution Emissions in the Production of Tropospheric Ozone in Middle Tennessee. A Thesis presented for the MS Degree. The University of Tennessee, Knoxville.

[23] Tesche, T. W. (1988) Accuracy of Ozon Air Quality Models. J. Environmental Eng. 114, 739-752.

[24] The Committee on Tropospheric Ozone Formation and Measurement of the National Researce Council (1991) Rethinking the Ozone Problem in Urban and Regional Air Pollution. National Academy Press.

[25] Schere, K. L. (1988) Modeling Ozone Concentrations. Environmental Science & Technology 22, No. 5, 488-495.

[26] Seinfield, J. H. (1988) Ozone Air Quality Models: A Critical Review. JAPCA 38, 616-645.

[27] Sexton, K., and H. Westberg. (1983) Photochemical Ozone Formation in Urban and Point Source Plumes. Environmental Science & Technology 17, 224-227.

[28] Sillman, S., J. A. Logan, and S. C. Wofsy (1990) The Sensitivity of Ozone to Nitrogen oxodes and Hydrocarbons in regional Ozone Episodes. J. Geophysics Res. 95, 1837-1851.

[29] Viezee, W., Johnson, W. B., and H. B. Singh. (1983) Stratospheric Ozone in the Lower Troposphere-II. Assessment of Downward Flux and Ground-Level Impact. Atmospheric Environment 17, No. 10, 1979-93.

[30] Wagner, K. K., and N. J. Wheeler. (1989) Variability of Photochemical Modeling Emission Sensitivity with Respect to Meteorology. Proceedings of the 6th Joint Conference on Applications of Air Pollution Meteorology. Boston : American Meteorology Society.

[31] Wakamatsu S., I. Uno, H. Ueda, K. Uehara, and H. Tateishi. (1989) Observational Study of Stratospheric Ozone Intrusions into the Lower Troposphere. Atmospheric Environment 23, No. 8, 1815-1826. Pergamon Press 1989.

[32] Zannetti, P. (1990) Air Pollution Modeling: Theroies, Computational Methods and Available Software, Van Nostrand Reinhold, NY.

[33] Zhou, N. (1992) Simulation of Ozone Formation in the Middle Tennessee Area. A Thesis presented for the MS Degree. The University of Tennessee, Knoxville.

APPENDIX

Area Source Allocation by County

COUNTY	GRID NO	POPULATION	RAIL ROAD	AIR PORT	WATER BODY	RURAL
SHELBY						
	1718	68				
	1818	500	YES			
	1918	5105				
	2018	34991		YES		
	2118	23315				
	2218	6193	YES			
	2318	1680				
	2418	2740				
	2518	681				
	2618	792		YES		
	2718	1260				
	1819	798	YES			
	1919	19388	YES			
	2019	35286	YES			
	2119	18817				
	2219	28520	YES			
	2319	27857	YES			
	2419	10421		YES		YES
	2519	4463				YES
	2619	2227				YES
	2719	4805				YES
	1820	63			YES	
	1920	6893	YES	YES	YES	
	2020	62258	YES			
	2120	57380	YES			
	2220	43299	YES			
	2320	27006	YES			
	2420	17237	YES			
	2520	7517	YES			YES

(Cont.)

COUNTY	GRID NO	POPULATION	RAIL ROAD	AIR PORT	WATER BODY	RURAL
SHELBY (CONTD.)						
	2720	592				YES
	2021	51962	YES		YES	
	2121	57519	YES			
	2221	43299	YES			
	2321	14936	YES			
	2421	4296	YES			
	2521	2288				YES
	2621	572				YES
	2721	314				YES
	2022	17415	YES		YES	
	2122	26148	YES			
	2222	21136	YES			
	2322	17367	YES			
	2422	7149				
	2522	1515	YES			YES
	2622	599	YES			YES
	2722	352				YES
	2023	7576	YES			
	2123	25121	YES			
	2223	13910				
	2323	14845	YES			
	2423	5195	YES			
	2523	754				
	2623	762				YES
	2723	377		YES		YES
	1924	761			YES	
	2024	761				
	2124	1177	YES			
	2224	1536	YES	YES		

(Cont.)

COUNTY	GRID NO	POPULATION	RAIL ROAD	AIR PORT	WATER BODY	RURAL
SHELBY (CONTD.)						
	2424	1228	YES			
	2524	959	YES			
	2624	872	YES			
	2724	454		YES		
	1925	741			YES	
	2025	761				
	2125	945				
	2225	5990	YES			
	2325	10984				YES
	2425	566				YES
	2525	659				YES
	2625	754				YES
	2725	385	YES			YES
	1926	534			YES	
	2026	658				YES
	2126	763				
	2226	2227				
	2326	6207	YES			
	2426	892				
	2526	579				YES
	2626	722				YES
	2726	409				YES
	1827	314				
	1927	247				
	1928	198				
CRITTENDEN	1414	34				
	1415	181				
	1515	215			YES	
	1416	204			YES	

(Cont.)

COUNTY	GRID NO	POPULATION	RAIL ROAD	AIR PORT	WATER BODY	RURAL
CRITTENDEN (CONTD.)	1516	226			YES	
	1616	226			YES	
	1417	204				YES
	1517	237				
	1418	204				
	1518	214				
	1618	55				
	1419	192				YES
	1519	226	YES			
	1619	215				
	1719	192		YES	YES	
	1420	193	YES			YES
	1520	226	YES			YES
	1620	227	YES			YES
	1720	705	YES			
	1221	182				
	1321	170				YES
	1421	202				
	1521	238				
	1621	290				
	1721	10823	YES			
	1821	16797	YES			
	1921	1524	YES			
	1222	206				
	1322	242				YES
	1422	242				YES

(Cont.)

COUNTY	GRID NO	POPULATION	RAIL ROAD	AIR PORT	WATER BODY	RURAL
CRITT-ENDEN (CONTD.)	1522	242				
	1622	318	YES			
	1722	369	YES			
	1822	560	YES	YES		
	1922	955		YES(2)		
	1323	2831				YES
	1423	265	YES			
	1523	307	YES			
	1623	318				YES
	1723	524	YES			
	1823	600				YES
	1224	1182	YES			
	1324	915	YES			YES
	1424	318				YES
	1524	318				YES
	1624	354				YES
	1724	561	YES	YES		
	1225	1082				
	1325	308				YES
	1425	317				YES
	1525	318				YES
	1625	487	YES			
	1725	561				
	1825	560				
	1226	434				YES
	1326	226				YES

(Cont.)

COUNTY	GRID NO	POPULATION	RAIL ROAD	AIR PORT	WATER BODY	RURAL
CRITTENDEN (CONTD.)	1426	231				YES
	1526	230				YES
	1626	525	YES			
	1726	538		YES		YES
	1826	502				
	1227	172				YES
	1327	172				YES
	1427	161				YES
	1527	161	YES			
	1627	185	YES			
	1727	381	YES			
DESOTO	1912	384			YES	
	2012	621			YES	YES
	2112	710	YES			
	2212	153				
	1813	517				YES
	1913	669			YES	
	2013	888			YES	YES
	2113	888				
	2213	595	YES			
	2313	326				YES
	2413	260				YES
	2513	217				
	2613	109				YES
	1814	569				YES
	1914	628				YES

(Cont.)

COUNTY	GRID NO	POPULATION	RAIL ROAD	AIR PORT	WATER BODY	RURAL
DESOTO (CONTD.)	2014	869				YES
	2114	853	YES			
	2214	544	YES			YES
	2314	489				YES
	2414	434				YES
	2514	434				YES
	2614	152				YES
	1615	286	YES			
	1715	374	YES			
	1815	464				YES
	1915	771				YES
	2015	1290				YES
	2115	973	YES			
	2215	606				YES
	2315	824				YES
	2415	791				
	2515	469				YES
	2615	108				YES
	1716	415	YES			YES
	1816	436	YES	YES		YES
	1916	992				YES
	2016	2831				YES
	2116	2325	YES			
	2216	1165				YES
	2316	1152				YES
	2416	1172				YES

(Cont.)

COUNTY	GRID NO	POPULATION	RAIL ROAD	AIR PORT	WATER BODY	RURAL
DESOTO (CONTD.)	2516	1099				
	2616	203				
	1617	352				
	1717	436				
	1817	436	YES		YES	
	1917	992				
	2017	9446	YES			
	2117	8141				
	2217	3759				YES
	2317	1433				YES
	2417	1348				
	2517	1383				
	2617	277				YES
TIPTON	2027	132			YES	
	2127	329				YES
	2227	515				YES
	2327	1570				YES
	2427	1569	YES			
	2527	946				YES
	2627	593				YES
	2727	524				YES
	2827	460				YES
	2927	409				
	3027	102				
	2128	525			YES	YES
	2228	514				YES

(Cont.)

COUNTY	GRID NO	POPULATION	RAIL ROAD	AIR PORT	WATER BODY	RURAL
TIPTON (CONTD.)	2328	1570				YES
	2428	1569	YES			
	2528	1370	YES			
	2628	783				YES
	2728	532				YES
	2828	496				
	2928	480				
	3028	99				
	2029	395				
	2129	279			YES	YES
	2229	450			YES	YES
	2329	727				YES
	2429	869				YES
	2529	1207	YES			
	2629	1014	YES			
	2729	837				YES
	2829	433				
	2929	433				YES
	3029	108				YES
	2030	99				
	2130	49			YES	
	2230	87			YES	
	2330	567				YES
	2430	538				YES
	2530	623				YES
	2630	2265	YES			

(Cont.)

COUNTY	GRID NO	POPULATION	RAIL ROAD	AIR PORT	WATER BODY	RURAL
TIPTON (CONTD.)	2730	4889	YES			
	2830	573				YES
	2930	411				YES
	3030	35				YES
	2331	80				YES
	2431	480				YES
	2531	533				YES
	2631	919				YES
	2731	986	YES			
	2831	530		YES		
	2931	65				YES
	2432	27				YES
	2532	159				YES
	2632	148				YES
	2732	247	YES			
	2832		YES			

VITA

The author was born on November 22, 1962, in Calcutta, India. She was brought up in Calcutta, India and received her primary and secondary education in the public school system and graduated high school from Vivekananda College, Calcutta, India in July 1980. She then studied chemical engineering at Jadavpur University, Calcutta, India and graduated with a B.S. in July 1984 and with a M.S. in March 1986.

The author was employed as Senior Software Engineer by Flakt India Limited, Calcutta, India from 1986 to 1990. The author's interest in environmental engineering started with work for Flakt India Limited. She enrolled in the graduate program in environmental engineering at the University of Tennessee in August 1990 to pursue her interests in the air pollution control field.

She is presently completing her thesis for the Master of Science degree in Environmental Engineering. Following the completion of her thesis she will join Georgia Institute of Technology as a Graduate Research Assistant and pursue her Ph.D in Environmental Engineering in January, 1993.